

A computational study of silicate oligomerization reactions

Citation for published version (APA):

Trinh, T. T. (2009). *A computational study of silicate oligomerization reactions*. [Phd Thesis 1 (Research TU/e / Graduation TU/e), Chemical Engineering and Chemistry]. Technische Universiteit Eindhoven.
<https://doi.org/10.6100/IR643387>

DOI:

[10.6100/IR643387](https://doi.org/10.6100/IR643387)

Document status and date:

Published: 01/01/2009

Document Version:

Publisher's PDF, also known as Version of Record (includes final page, issue and volume numbers)

Please check the document version of this publication:

- A submitted manuscript is the version of the article upon submission and before peer-review. There can be important differences between the submitted version and the official published version of record. People interested in the research are advised to contact the author for the final version of the publication, or visit the DOI to the publisher's website.
- The final author version and the galley proof are versions of the publication after peer review.
- The final published version features the final layout of the paper including the volume, issue and page numbers.

[Link to publication](#)

General rights

Copyright and moral rights for the publications made accessible in the public portal are retained by the authors and/or other copyright owners and it is a condition of accessing publications that users recognise and abide by the legal requirements associated with these rights.

- Users may download and print one copy of any publication from the public portal for the purpose of private study or research.
- You may not further distribute the material or use it for any profit-making activity or commercial gain
- You may freely distribute the URL identifying the publication in the public portal.

If the publication is distributed under the terms of Article 25fa of the Dutch Copyright Act, indicated by the "Taverne" license above, please follow below link for the End User Agreement:

www.tue.nl/taverne

Take down policy

If you believe that this document breaches copyright please contact us at:

openaccess@tue.nl

providing details and we will investigate your claim.

A Computational Study Of Silicate Oligomerization Reactions

PROEFSCHRIFT

ter verkrijging van de graad van doctor aan de
Technische Universiteit Eindhoven, op gezag van de
rector magnificus, prof.dr.ir. C.J. van Duijn, voor een
commissie aangewezen door het College voor
Promoties in het openbaar te verdedigen
op woensdag 1 juli 2009 om 16.00 uur

door

Trinh Thanh Thuat

geboren te Hanoi, Viëtnam

Dit proefschrift is goedgekeurd door de promotor:

prof.dr. R.A. van Santen

Copromotor:
dr. A.P.J. Jansen

Thuat T Trinh

A catalogue record is available from the Eindhoven University of Technology Library

ISBN: 978-90-386-1901-9

Copyright © 2009 by Thuat T. Trinh

The work described in this thesis has been carried out at the Schuit Institute of Catalysis within the Laboratory of Inorganic Chemistry and Catalysis, Eindhoven University of Technology, The Netherlands. Financial support has been supplied by National Research School Combination “Catalysis” (NRSCC).

Cover design: Paul Verspaget (Grafische Vormgeving-Communicatie) and Thuat T. Trinh

Printed at the Universiteitsdrukkerij, Eindhoven University of Technology.

Kính tặng bố mẹ,

CONTENTS

A Computational Study Of Silicate Oligomerization Reactions

Chapter 1	Introduction	1
Chapter 2	Mechanism of oligomerization reactions of silica	15
Chapter 3	The role of water in silicate oligomerization reaction.....	41
Chapter 4	Effect of counter ion on the silica oligomerization reaction.....	59
Chapter 5	Catalytic role of tetrapropylammonium in silica oligomerization reaction	79
Chapter 6	Silica condensation influenced by organic template	95
Summary	115
Tóm tắt	118
List of puclibcations	120
Acknowledgments	121
Curriculum vitae	123

CHAPTER 1

Introduction

1.1 Background

Zeolites were discovered in 1756 by the Swedish mineralogist Cronstedt, who named them from the Greek words *zein* and *lithos*, meaning “boiling stone” [1]. Nowadays, zeolites are widely applied to many important processes such as gas separation, softening of water, catalysis in petroleum processes and fine chemistry [2].

Zeolitic materials are crystalline silicates, formed by cornersharing TO_4 tetrahedra ($\text{T}=\text{Al}, \text{Si}$) with a regular array of microporous channels and/or cavities. This pore system, in combination with reactive intra- or extraframework species, is responsible for their unique properties. Many occur as natural minerals, but it is the synthetic varieties which are among the most widely used sorbents, catalysts and ion-exchange materials in the world.[1-3] Zeolite crystals are porous on a molecular scale, their structures revealing regular arrays of channels and cavities (ca. 3–15 Å), creating a nanoscale labyrinth which can be filled with water or other guest molecules. The resulting molecular sieving ability has enabled the creation of new types of selective separation processes (ion exchange, sorption), and in their acid form, zeolites are probably the most important heterogeneous acid catalysts used in industry.

The majority of the world's gasoline is produced by the fluidized catalytic cracking (FCC) of petroleum using zeolite catalysts. Their key properties are size and shape selectivity, together with the potential for strong acidity.

Figure 1.1 illustrates the relationship of a representative zeolite crystal to its micropore system, showing the existence of crystallographically defined channels and cavities and the cation-exchange centers resulting from the periodic replacement of $[\text{AlO}_4]^-$ for $[\text{SiO}_4]$.

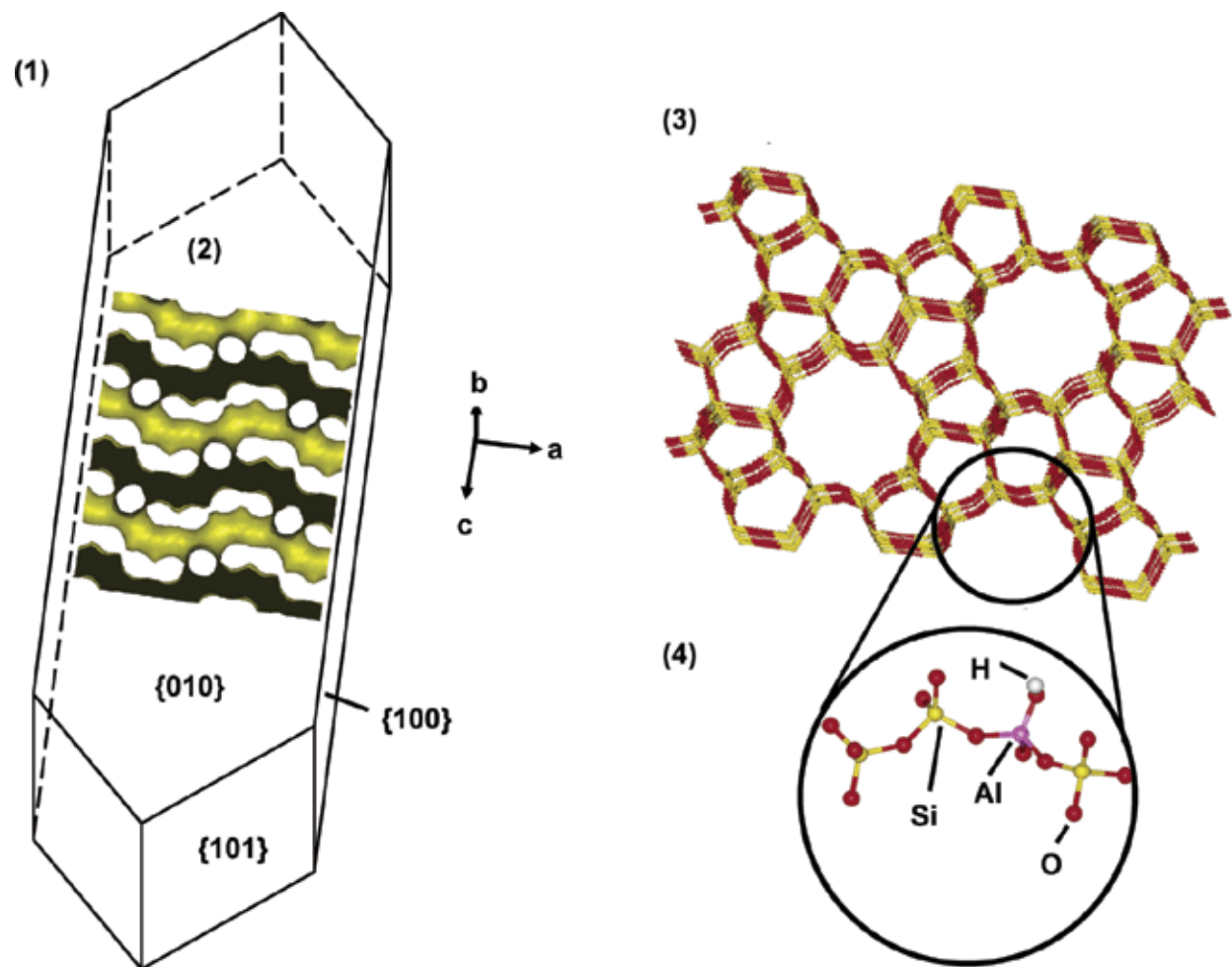


Figure 1.1 The key features of a representative zeolite, ZSM-5: (1) crystal morphology, showing the relationship to the major axes (a, b, c); (2) section of pore map, showing zigzag channels in the a-direction, intersecting with straight channels in the b-direction; (3) part of the crystal structure these sheets of 5- and 10-membered T-atom rings lie in the ac plane, giving the vertical straight channels shown in (2); (4) detail of the atomic structure, illustrating the linked TO4 tetrahedra. For ZSM-5, T = Si predominantly, but this insert shows an Al substituent (purple) with a hydrogen atom (white) occupying the associated cation exchange site.

In view of the industrial importance of zeolites and also because of the intrinsic scientific interest in their structural complexity and diverse chemistry, considerable effort has been directed into zeolite synthesis. It aimed for the synthesis of new materials and the building up of an understanding of the synthesis process. In recent years, many new zeolite-like materials

(zeotypes) containing elements other than silicon and aluminum have been synthesized [3,4] and related structures with much larger pore sizes (up to around 200 Å) have also been discovered [5,6]. These new materials have potential applications in (for example) fine chemicals synthesis, electronic arrays, and biomaterials.

1.2. Zeolite synthesis

Natural zeolites are found in volcanic or metamorphic rocks and their growth involves geological conditions (low temperature and pressure, low pH (8-9)) and time scale (thousands of years). Early efforts have been made by Saint Claire de Ville in 1862 to synthesize zeolites [7]. The absence of reliable characterization methods made it impossible to verify that zeolites were indeed fabricated. The first precise confirmation of zeolite synthesis can be traced on 1948 when Barrer reported the synthesis of an analogue of mordenite [8]. At the same time Milton and Beck succeeded in synthesizing other zeolite types using lower temperatures (≈ 100 °C) and a higher alkalinity [9]. It led to the discovery of one of the most commercially successful zeolites which has no natural counterpart, Linde A (LTA). Since then many new zeolite framework types have been attained thanks to important efforts by oil companies. In the early 1960s Barrer and Denny were the first to replace inorganic bases in the synthesis mixture with organic molecules [10]. The use of quaternary ammonium salts resulted in an increase in the Si/Al ratio and the discovery of ZSM-5, being the most important new structure [11]. The quest for higher Si/Al ratios ended in 1978 when Flanigen et al. reported the synthesis of silicalite-1 which is the all-silica counterpart of ZSM-5. This material shows remarkable properties because of its hydrophobic and organophilic character. A new class of materials analogous to zeolites was introduced in the 1980s: microporous aluminophosphates [12]. Nevertheless, poor thermal and hydrothermal stability of their metal substituted analogues hindered their commercial application. The most noteworthy advance in crystalline microporous solids has recently been the synthesis of extra large pore zeolites with more than 12-ring apertures [13].

Zeolite synthesis has been extensively reviewed in several books and literature on this subject is abundant [1-3,14]. The synthesis of zeolites is carried out under hydrothermal conditions. An aluminate solution and a silicate solution are mixed together in an alkaline medium to form a milky gel or in some instances, clear solutions. Various cations or anions can be added to the synthesis mixture. Synthesis proceeds at elevated temperatures (60-200 °C)

where crystals form through a nucleation step. The following sections give a general overview on the parameters governing zeolite synthesis. Emphasis will be given to structure direction by organic molecules. A schematic representation of the zeolite formation process is given in figure 1.2.

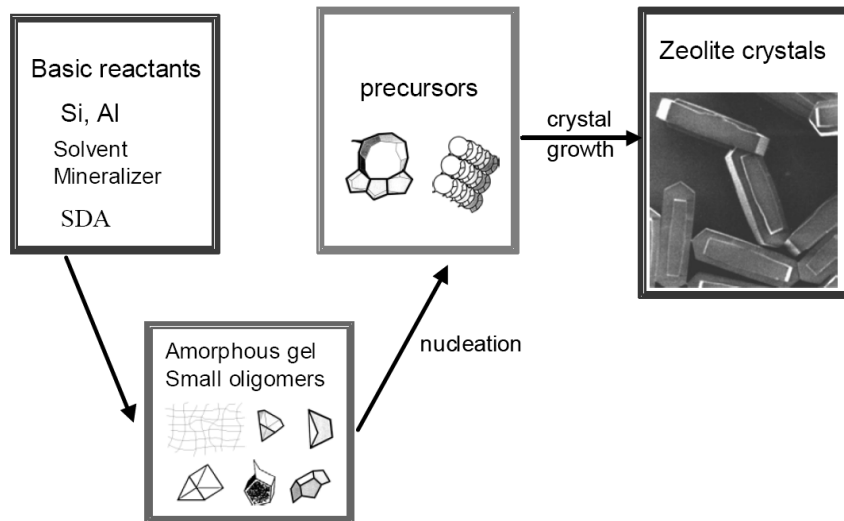


Figure 1.2: Simplified zeolite synthesis scheme. SDA stands for structure-directing agent.

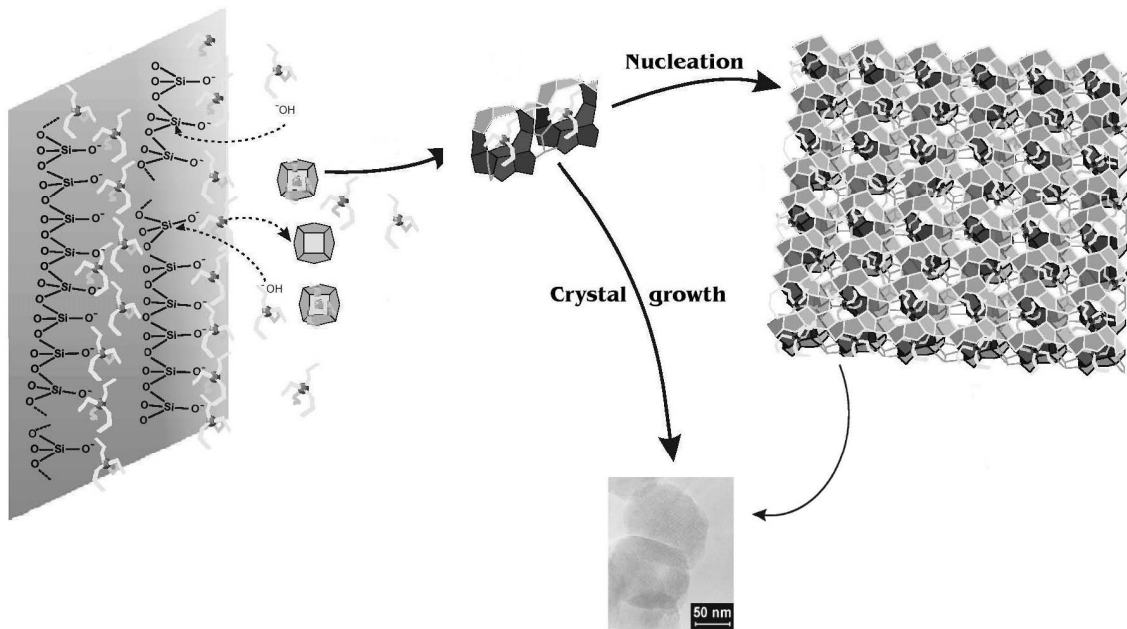


Figure 1.3: Formation of nanoparticle in zeolite synthesis [15]

The formation of zeolites from solution occurs through a complex sequence of several reactions that are partially running in parallel. During the early steps of the synthesis, the final structure of the zeolite can be already defined [16]. However, because of analytical limitations, little detail is known on the reactivity of intermediate oligomers. Various nucleation mechanisms have been proposed. There are major controversies on the actual mechanism in the literature [17].

1.3. Quantum chemical simulations

In less than 50 years, the field of computational chemistry has gone from being essentially non relevant to most of experimental chemistry and being an active counterpart of experimental investigations. High-performance computing, clever algorithmic implementations and information technology have dramatically influenced methods development and performance. This section briefly summarizes the computational chemistry techniques used in this thesis.

In order to calculate the electronic states of the system, quantum chemical methods attempt to solve Schrödinger equation, $\hat{H}\Psi = E\Psi$, where Ψ is the wave function and E is the energy of the N -particle (electrons and nuclei) system. \hat{H} is the Hamiltonian operator, which is comprised of the kinetic and potential energy operators acting on the overall wave function of the system. The exact solution for this equation can be found only for a very limited number of systems, and thus, a number of approximations are required to solve it for larger systems. More detailed discussion on the electronic structure calculations can be found in a number of very good references [18].

Traditional methods in electronic structure theory, in particular Hartree-Fock theory and its descendants, are based on the complicated many-electron wave-function. The main objective of density functional theory is to replace the many-body electronic wavefunction with the electronic density as the basic quantity. Whereas the many-body wavefunction is dependent on $3N$ variables, three spatial variables for each of the N electrons, the density is only a function of three spatial coordinates and is a simpler quantity to deal with both conceptually and practically. One of the deficiencies of the HF theory is that it does not treat dynamic electron correlation,

which refers to the fact that the motion of electrons is correlated so as to avoid one another. The neglect of this effect can cause very serious errors in the calculated energies, geometries, vibrational, and other properties. There are numerous so-called post-Hartree-Fock methods for treating correlated motion between electrons. One of the most widely used approaches is based on the definition of the correlation energy as a perturbation. In other words, the configurational interactions are treated as small perturbations to the Hamiltonian. Using this expansion the HF energy is equal to the sum of the zero and first order terms, whereas the correlation energy appears only as a second order term. The second order Møller-Plesset perturbation theory (MP2) typically recovers 80-90% of the correlation energy, while MP4 provides a reliably accurate solution to most system. Due to the extremely high computational costs, the application of the post-HF methods is commonly limited to the MP2 method.

Modern DFT is based on two theorems introduced by Hohenberg and Kohn [19]. The first theorem states that the external potential $v_{ext}(r)$ is uniquely determined by the ground state density φ_0 up to a constant

$$\varphi_0 \rightarrow v_{ext}(r) \quad (1.1)$$

Since the number of electrons (N_e) is uniquely defined by the electron density, $N_e = \int \varphi_0(r) dr$, φ_0 determines the full Hamiltonian and therefore implicitly all properties of the system. The first theorem allows us to write the total energy as a functional of the electron density in the following way:

$$E_0 = E_0(\varphi_0) \quad (1.2)$$

$$E_0(\varphi_0) = T(\varphi_0) + \int \rho(r)v_{ext}(r)dr + V_{ee}[\rho_0] \quad (1.3)$$

Where $T(\varphi_0)$ is the kinetic energy and $V_{ee}[\rho_0]$ is the electron-electron interaction energy. The exact form of the terms describing the kinetic energy and the electron interaction energy are not known. Thus, the energy cannot be determined.

The second theorem introduces the energy variational principle. It states that there exists a universal functional that yields the lowest energy if and only if the input density is the true ground state density, φ_0

$$E[\tilde{\rho}] \geq E[\varphi_0] \quad (1.4)$$

In 1965, Kohn and Sham suggested an avenue for how the unknown energy functional can be approximated [20]. They proposed to express the kinetic energy as the kinetic energy of a fictitious reference system s of n non-interacting electrons

$$T[\rho_s] = \sum_i^n \langle \phi_i^{KS} | -\frac{1}{2} \nabla^2 | \phi_i^{KS} \rangle \quad (1.5)$$

The connection of this artificial system to the one we are really interested in is established by choosing the effective potential v_{ext} such that the density resulting from the summation of the moduli of the squared orbitals exactly equals the ground state density of our real target system of interacting electrons

$$\rho_s(r) = \rho_0(r) = \sum_i^n |\phi_i^{KS}(r)|^2 \quad (1.6)$$

where $\phi_i^{KS}(r)$ are the orthonormal Kohn-Sham orbitals. The expression of the electron density and the kinetic energy is exact for a one determinant wave function of a system of non-interacting electrons. The difference in kinetic energy and in electronic interaction energy between the reference system and the real system is

$$\Delta T[\rho] = T[\rho] - T_s[\rho] \quad (1.7)$$

$$\Delta V_{ee}[\rho] = V_{ee}[\rho] - \frac{1}{2} \iint \frac{\rho(r_1) - \rho(r_2)}{|r_1 - r_2|} dr_1 dr_2 \quad (1.8)$$

Insertion in the Hohenberg-Kohn Eq. (1.3) yields

$$E^{KS}[\rho] = \int \rho(r) v_{ext}(r) dr + T_s[\rho] + \frac{1}{2} \iint \frac{\rho(r_1) - \rho(r_2)}{|r_1 - r_2|} dr_1 dr_2 + E_{xc}[\rho] \quad (1.9)$$

With

$$E_{xc}[\rho] = \Delta T[\rho] + \Delta V_{ee}[\rho] \quad (1.20)$$

The exchange-correlation functional $E_{xc}[\rho]$ represents the non-classical part of the electronic interaction energy and the difference in kinetic energy between the reference system and the real system. The Kohn-Sham orbitals are found by minimization of Eq. (1.9) under the constraint that $\langle \phi_i | \phi_j \rangle = \delta_{ij}$. This results into the Kohn-Sham equations

$$\left\{ -\frac{1}{2}\nabla^2 + v_{ext} + \int dr' \frac{\rho(r')}{|r-r'|} + v_{xc} \right\} \phi_i(r) = \varepsilon_i \phi_i(r) \quad (1.21)$$

which have to be solved self-consistently.

If only the correct expression for the exchange-correlation potential,

$v_{exc} = \frac{\delta E_{xc}[\rho(r)]}{\delta \rho(r)}$, was known, solving Eq. (1.21) would be equivalent to solving the exact electronic Schrödinger equation. Unfortunately, the exact exchange-correlation potential is unknown and much effort has been and is being devoted to find good approximations to v_{exc} . Therefore, the quality of the electronic structure calculation depends on the quality of the approximation used for v_{exc} .

Although DFT is in principle an exact approach, a number of assumptions and approximations have to be made usually due to the fact that the exact expression for the exchange correlation energy is not known. The most basic one is the local density approximation (LDA), which assumes that the exchange-correlation per electron is equivalent to that in a homogeneous electron gas, which has the same electron density at a specific point r . The LDA is obviously an oversimplification of the actual density distribution and usually leads to overestimation of calculated bond and binding energies.

One notes that the Hartree-Fock (HF) theory provides a more exact match of the exchange energy for single determinant systems. Thus, numerous hybrid functionals have been recently developed where the exchange functional is a linear combination of the HF exchange and the correlation (and exchange) calculated from LDA theory. The geometry and energetics calculated within this approach such as B3LYP [21] is usually in a good agreement with experimental results and those obtained by using post-HF methods. On the other hand, hybrid

functionals still fail in describing of chemical effects mainly associated with the electron-electron correlation such as dispersion and other weak interactions [22].

Ab-initio molecular dynamic

The growing need to understand complex phenomena on an atomistic level, taking into account the interactions between atoms and electrons, has recently stimulated the extension of the scope of molecular dynamics (MD) simulations. Having translated the problem to be investigated into a suitable atomistic model containing a limited number of atoms, the simulation can be used to study specific aspects, thus explaining observed phenomena or predicting unforeseen events. The starting point of any MD simulation is the definition of the molecular systems by an initial set of N particles within a volume V . The dynamics of particles is followed by integrating numerically classical Newton equations of motion, where the forces are computed as derivatives of a given potential. The resulting deterministic trajectories explore the available phase space under the assigned thermodynamic conditions. This means that long enough simulations will provide realistic descriptions of the thermodynamic equilibrium and of dynamical properties of the system. On top of that, the analysis of an atomistic trajectory allows the identification of individual events and complex mechanism of chemical reactions.

Classical force fields allows to routinely run simulations for a large systems ($> 100\ 000$ atoms) and for several nanoseconds. However, they are usually characterized by limited transferability and cannot account for strong variations in the structural and electronic properties, although more and more sophisticated models are being developed including polarization effects, charge transfer, non-additive many-body interactions. In chemically complex situations, the parameterization of reliable empirical potentials is not always possible. Since the electronic structure and chemical bonding change qualitatively in time.

These limitations are overcome by ab initio molecular dynamic (AIMD), where the forces are computed from electronic structure calculations. AIMD calculations are typically performed by using a plane-wave expansion of the DFT (Kohn-Sham) orbitals [23]. Formulation of AIMD in terms of a mixed approach based on Gaussians and plane waves has been proposed [24] and implemented in the CP2K code [25, 26]. The use of both localized and plane wave basis sets will potentially lead to linear scaling AIMD methodology in near future.

In Born-Oppenheimer Molecular Dynamics (BOMD), the static electronic structure problem is solved at every MD step given the set of fixed nuclear positions at that instant of time. Thus, the electronic structure part consists in solving the time-independent Schrödinger equation, while the nuclei are propagating via classical molecular dynamics. Thus, the time-dependence of the electronic structure is a consequence of nuclear motion. The BOMD method is defined by

$$M_i \ddot{R}_i = -\nabla_i \min_{\Psi_0} \{\langle \Psi_0 | H_e | \Psi_0 \rangle\} \quad (1.22)$$

$$E_0 \Psi_0 = H_e \Psi_0 \quad (1.23)$$

According to Eq. (1.22), the minimum of $\langle H_e \rangle$ has to be reached at each BOMD step. Since the accuracy of the forces depends linearly on the accuracy of the minimization of the Kohn-Sham energy, the wave function has to be tightly converged at each step.

Car-Parrinello Molecular Dynamics

The Car-Parrinello approach is closely related to BOMD since the motion of ions are also described classically. The fundamental difference is that the orbitals are no longer optimized at every time step but treated and propagated like classical objects, correspondingly being assigned a fictitious mass (μ) and temperature [27]. It could be shown that the adiabatic separation of the BO-approximation is also conserved for this approach [23]. In order to maintain this adiabaticity condition, it is necessary that the fictitious mass of the electrons is chosen small enough to avoid a significant energy transfer from the ionic to the electronic degrees of freedom. This small fictitious mass in turn requires that the equations of motion are integrated using a smaller time step (0.1-0.2 fs) than the ones commonly used in BOMD (0.5-1 fs). Hence, the computational bottleneck of BOMD, i.e the wavefunction optimization at each time step, can be circumvented within Car-Parrinello Molecular Dynamics (CPMD). More details on CPMD can be found in [23, 28]. The BO scheme will be mostly used in this thesis since a highly efficient wavefunction optimization procedure, namely the orbital transformation technique [29], has been implemented in the CP2K code. This method allows to use BOMD without any computational overhead with respect to CPMD. Indeed, our test calculations showed that the number of SCF-steps required for one BO-step is similar to the number of CP-steps required for the same time.

1.4. Scope of the thesis

This thesis deals with theoretical investigations of the silica condensation process, a key reaction to sol-gel chemistry and zeolite synthesis. The formation of zeolites from solution occurs through a complex sequence of numerous reactions that are partially running in parallel. During these early steps, the final structure of the zeolite can be strongly influenced.[16] However, because of analytical limitations, little is known about the species occurring during these steps. Thus, various nucleation mechanisms have been proposed and this topic is highly controversial.[17] The main goal of this thesis is to develop a deeper understanding of the structural, energetic and mechanistic aspect of the silicate oligomerization reaction. The effects of hydrogen bonding, water solvation, counter ion and organic template will also be focused.

The mechanism of the silica condensation reaction of small oligomer from dimer to pentamer with a continuum solvation model is studied in chapter 2. Based on the results of *ab initio* calculations (DFT), it discussed how the internal hydrogen bonding affects relative stabilities and activation barriers. Dependent on the pH of solution, there are two possible mechanisms for condensation, neutral and anionic. The anionic route that takes place in two steps is more kinetically and energetically favorable than the neutral one.

Chapter 3 reports a new insight in the mechanism of the silica condensation reaction in water environment using Car Parinello Molecular Dynamic simulations. The role of the hydrogen network created by the water molecules. Water molecules affect especially the proton transfer process and form stabilization hydrogen bond.

The *ab initio* molecular dynamic simulations of silica condensation in solution in the presence of counter ions such as Li^+ or NH_4^+ are studied in chapter 4. In this chapter an attempt is made to understand the importance of electrostatic interaction and of hydrogen bonding to the reactive event as well as the relative stabilities of oligomer. Based on obtained trajectories, an important information in the movement of cation ion and silicate molecule during the condensation reaction process is obtained.

We also did detailed studies of the reaction in the presence of organic basic compounds, such as tetrapropylammonium (TPA), such molecule act as templates in zeolite synthesis. Chapter 5 examines their effects on the kinetic and thermodynamic properties of small oligomer formation. It is shown that is essential to include the weak Van-der-Waals interactions to study the interaction between the silica and the template.

Chapter 6 reports an extensive investigation on the effect of the template on the stabilities of higher oligomers. Various silicate structure from dimer to double 4-ring, related to initial stage of zeolite synthesis, are computed and analyzed. The formation of linear, branched and ring oligomers depends on the use of templates is discussed.

References

- 1./Breck, D. W. *Zeolite Molecular Sieves*; Wiley: New York, 1974.
- 2./ Barrer, R. M. *Hydrothermal Chemistry of Zeolites*; Academic Press: London, 1982.
- 3./ Szostak, R. *Molecular Sieves – Principles of Synthesis and Identification* London, 1998.
- 4./ Flanigen, E. M.; Patton, R. L.; Wilson, S. T. *Stud. Surf. Sci. Catal* **1988**, 37, 13.
- 5./ Kresge, C. T.; Leonowicz, M. E.; Roth, W. J.; Vartuli, J. C.; Beck, J. S. *Nature* **1992**, 359, 710.
- 6./ Beck, J. S.; Vartuli, J. C.; Roth, W. J.; Leonowicz, M. E.; Kresge, C. T.; Schmitt, K. D.; Chu, C. T. W.; Olson, D. H.; Sheppard, E. W.; McCullen, S. B.; Higgins, J. B.; Schlenker, J. L. *J. Am. Chem. Soc* **1992**, 114, 10834.
- 7./ Sainte-Claire-Deville. *M. H. Compt. Rend* **1862**, 54, 324.
- 8./ Barrer, R. M. *J. Chem. Soc.* **1948**, 2158.
9. Milton, R. M. US Patent 2,882,243, 1959; Milton, R. M. US Patent 3,008,803, 1961. Barrer, R. M.; Denny, P. J. *J. Chem. Soc.* 1961, 971-982.
10. Argauer, R. J.; Landolt, G. R. US Patent 3,702,886 1972.
11. Grose, R. W.; Flanigen, E. M. US Patent 4,061,724 1977
12. Wilson, S. T.; Lok, B. M.; Flanigen, E. M. US Patent 4,310,440 1982.; Wilson, S. T.; Lok, B. M.; Flanigen, E. M. *J. Am. Chem. Soc* **1982**, 104, 1146.
- 13./ Zhou, Y.; Zhu, H.; Chen, Z.; Chen, M.; Xu, Y.; Zhang, H.; Zhao, D. *Angew. Chem. Int. Ed* **2001**, 40, 2166.; Lin, C. H.; Wang, S. L.; Lii, K. H. *J. Am. Chem. Soc* **2001**, 123, 4649.
- 14./ Jacobs, P. A.; Martens, J. A. *Synthesis of high-silica aluminosilicate zeolites*; Elsevier Science: New York, 1987; Vol. 33.
- 15./ C. Houssin, PhD thesis , Technique University of Eindhoven, 2003, ISBN 90-386-2874-9
- 16./ Snyder, M. A.; Tsapatsis, M. *Angew. Chem* **2007**, 119, 7704.
Snyder, M. A.; Tsapatsis, M. *Angew. Chem. Int. Ed.* **2007**, 46, 7560.
- 17./ Kirschhock, C. E. A.; Ravishankar, R.; Verspeurt, F.; Grobet, P. J.; Jacobs, P. A.; Martens, J. A. *J. Phys. Chem. B* **1999**, 103, 4965.
Knight, C. T. G.; Kinrade, S. D. *J. Phys. Chem. B* **2002**, 106, 3329.
Kragten, D. D.; Fedeyko, J. M.; Sawant, K. R.; Rimer, J. D.; Vlachos, D. G.; Lobo, R. F.; Tsapatsis, M. *J. Phys. Chem. B* **2003**, 107, 10006.
Tsapatsis, M.; Lovallo, M.; Davis, M. E. *Microporous Mater* **1996**, 5, 381.
Mintova, S.; H. Olson, N.; Valtchev, V.; Bein, T. *Science* **1999**, 283, 598.
L. Burkett, S.; Davis, M. E. *Chem. Mater* **1995**, 7, 920.
Dokter, W. H.; Garderen, H. F. v.; Beelen, T. P. M.; Santen, R. A. v.; Bras, W. *Angew. Chem. Int. Ed. Engl* **1995**, 34, 73.
Davis, M. E.; Lobo, R. F. *Chem. Mater* **1992**, 4, 756.
Schoeman, B. J. *Microporous Mesoporous Mater* **1998**, 22, 9.
Davis, T. M. *Nat. Mater* **2006**, 5, 400.
- 18./ Jensen, F. *Introduction to Computational Chemistry*, Wiley-Interscience, New York, **1999**; Leach, A.R. *Molecular Modeling: Principles and Applications*, Pearson Education, Harlow, **1996**; Foresman,

-
- J.B.;Frish, A. *Exploring Chemistry with Electronic Structure*, 2nd ed., Pittsburg, PA Gaussian, **1996**; Parr, R.G.;Yang, W. *Density Functional Theory of Atoms in Molecules*, Oxford University Press, New York, **1989**;Young, D.C. *Computational Chemistry: A Practical Guide for Applying Techniques to Real-World Problems*, Wiley-Interscience, New York, **2001**
- 19./ Hohenberg, P.; Kohn, W. *Phys. Rev. B* **1964**, *136*, 864.
- 20./ Kohn, W.; Sham., L. J. *Phys. Rev. A* **1965**, *140*, 1133.
- 21./ Becke, A. D. *J. Chem. Phys* **1993**, *98*, 5648.
- 22./ Fermi, E.; Pasta, J. G.; Ulam, S. M. *Los Alamos LASL Report* **1995**.
- 23./ Marx, D.; Hutter., J. *Ab initio Molecular Dynamics: Theory and Implementation, in Modern Methods and Algorithms of Quantum Chemistry*; Forschungszentrum Jülich, 2000; Vol. 1.
- 24./ Lippert, G.; Hutter, J.; Parrinello, M. *Theor. Chem. Acc* **1999**, *103*, 124.
- 25./ VandeVondele, J.; Krack, M.; Mohamed, F.; Parrinello, M.; Chassaing, T.; Hutter, J. *Comp. Phys. Comm* **2005**, *167*, 103.
- 26./ The CP2K developers group. Freely available at the URL.: <http://cp2k.berlios.de>, released under GPL license., 2009.
- 27./ Car, R.; Parrinello, M. *Phys. Rev. Lett* **1985**, *55*, 2471.
- 28./ CPMD, <http://www.cpmc.org/>, Copyright IBM Corp 1990-2008, Copyright MPI für Festkörperforschung Stuttgart 1997-2001.
- 29./ VandeVondele, J.; Hutter, J. *J. Chem. Phys* **2003**, *118*, 465.

CHAPTER 2

Mechanism Of Oligomerization

Reactions Of Silica

The mechanism of the oligomerization reaction of silica, the initial steps of silica formation, has been studied by quantum chemical techniques. The solvent effect is included using the COSMO model. The formation of various oligomers (from dimer to tetramer) was investigated. The calculations show that the anionic pathway is kinetically preferred over the neutral route. The first step in the anionic mechanism is the formation of the SiO-Si linkage between the reactants to form a five-coordinated silicon complex which is an essential intermediate in the condensation reaction. The rate-limiting step is water removal leading to the oligomer product. The activation energies for dimer and trimer formation (~80 kJ/mol) are significant higher than the subsequent oligomerization. The activation energies for the ring closure reaction (~100 kJ/mol) are even higher. The differences in activation energies can be related to the details in intra- and intermolecular hydrogen bonding of the oligomeric complexes.

2.1. INTRODUCTION

The silica condensation reaction is the essential elementary reaction step of sol-gel chemistry [1,2] and zeolite synthesis[3]. Understanding how zeolites nucleate and grow is of fundamental scientific and technological importance. Numerous experimental [4-11] and theoretical [12-19] studies have been devoted to investigate the silicate oligomers that occur in the prenucleation process of silicious zeolite.

Various experimental techniques can be used to reveal the structural information about species in solution and nucleation processes. During the first hours of sol-gel reactions, various silicate oligomers are formed in solution. They can be dimers, trimers, tetramers, 3-rings, 4-rings, double 3-rings, double 4-rings or other larger oligomer. The dominant species depends sensitively on reaction conditions, solvent used and presence or absence of structure directing agent (SDA) [10, 11].

Quantum chemical calculations of chains (dimer, trimer, tetramer, pentamer), rings (trimer, tetramer) and the cubic cage were reported by Pereira et al [12, 13]. Stabilities and structural conformations were reported. It was found that the strong hydrogen bonds formed by hydroxyl groups and the flexibility of the SiO-Si angle are the most important features for conformation of the silica cluster. Bond lengths and partial charges vary little when the conformation changes. Formation of silica rings was suggested to be due to the internal condensation reaction. Pereira et al.[14] also reported the mechanism of condensation reactions between two $\text{Si}(\text{OH})_4$ monomers in methanol environment using the conductor-like screening model (COSMO). The activation barrier was in the range 50-60 kJ/mol. Two different reaction mechanisms were found: one pathway is a SN^2 type reaction and the other one is a lateral attack route. Both of them require formation of intermediate containing five-coordinated silicon. The SN^2 mechanism is preferred over the lateral one.

Another study on the energies of the dimerization reaction of monosilic acid was reported by Tossel [15]. Using the COSMO solvent model, the author studied the free energy of reaction changes by varying temperature and dielectric constants of the solvent. The author found that the condensation reaction is more favorable at high temperature than at room temperature. Free energies of the silica condensation reaction have been recently presented by Mora-Fonz et al [16]. It was found that the formation of the small ring fragment is favorable in high pH media.

The mechanism of the quartz dissolution process was investigated by other authors [17-19]. Xiao et al used the dimer of silica as a model to study the hydrolyse pathway of quartz by OH⁻ in gas phase [17]. The authors proposed a hydrolysis mechanism with two steps: adsorption of H₂O on a SiO-Si⁻ site to form a five-fold silicon species (activation barrier as 79 kJ/mol) and breaking of the SiO-Si bond (activation barrier as 19 kJ/mol). The reverse process of his mechanism was formation of the dimer silica with two steps: formation of SiO-Si linkage (activation barrier as 69 kJ/mol) and cleavage of the H₂O (activation barrier as 79 kJ/mol). Other authors reported the mechanism of quartz dissolution on neutral silica surfaces and acid environment [18,19]. The healing reaction of neutral dimer on β -cristobalite surface, which is the SiO-Si bond formation, was found to have a barrier of 120 kJ/mol [18]. Silica dissolution in acid environment had an activation barrier about 120 kJ/mol. There was a five-coordinated silicon observed during the dissociation process [19].

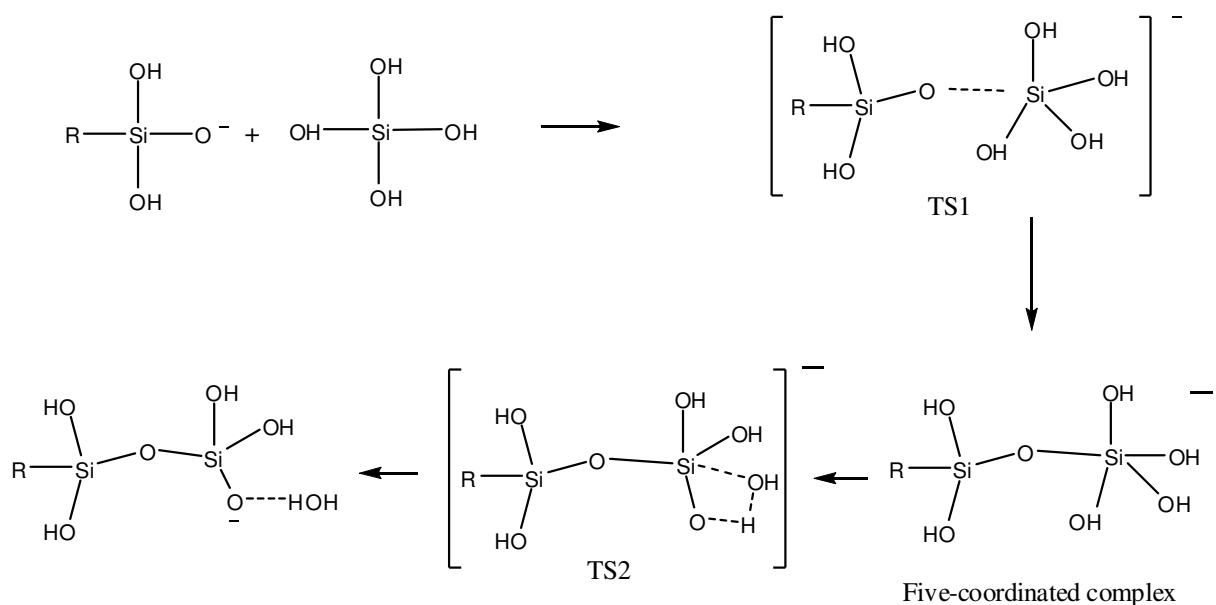
Most of the previous work has focused on the thermodynamic factors of silica condensation. Only the mechanism of the dimerization reaction was studied in methanol environment. Here we address the reaction pathway in alkaline media, which is the general condition for zeolite synthesis. The details of the mechanism of these reactions (especially the formation of the trimer, tetramer, pentamer and ring structure formation) are not fully elucidated. We have not only studied the formation of the dimer as in previous works but also larger clusters such as the trimer and tetramer. We propose a mechanism of ring formation which occurs via an internal condensation reaction.

2.2. COMPUTATIONAL DETAILS

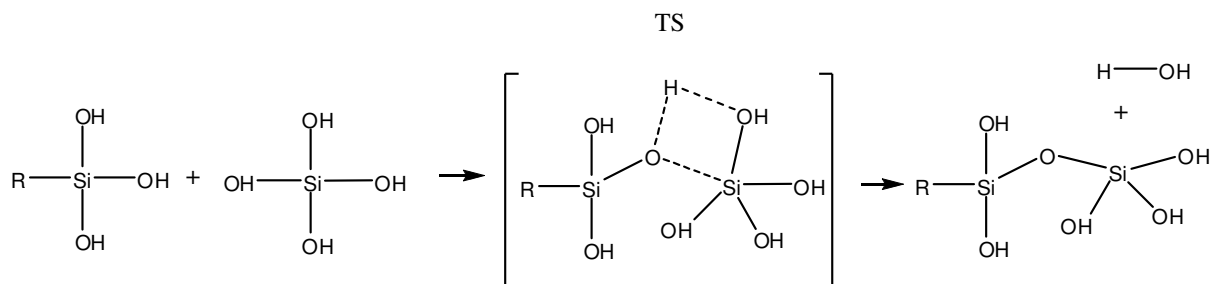
Density Functional Theory (DFT), with the B3LYP[20] hybrid exchange-correlation functional, was used to perform all of the calculations. The B3LYP method has been reported to provide excellent descriptions of various reaction profiles and particularly of geometries, heats of reaction, activation energies, and vibrational properties of various molecules [21]. Geometry optimization and saddle point searches were all performed using the Gaussian 03 program [22]. The basis set used to expand the molecular orbital were all electron type 6-31+G(d,p). For all the systems considered we have determined equilibrium geometries in gas-phase and have evaluated vibrational frequencies. The transition states were obtained by requiring that one and only one of

the eigenvalues of the Hessian matrix is negative. The solvation effect was included using the continuum solvation COSMO method implemented in GAUSSIAN03 package [22]. COSMO method has been reported to be an appropriate approach for studying the silica reaction in solution [16,22].

The calculations were performed on silica clusters with a focus on the two mechanisms concerning anion and neutral species sketched in scheme (2.1) and scheme (2.2).



Scheme 2.1: Anionic mechanism of the silica condensation reaction. R = H, $(\text{OH})_3\text{Si}-[\text{Si}(\text{OH})_2]_n-$ (n=0-2).



Scheme 2.2: Neutral mechanism of the silica condensation reaction. R = H, $(\text{OH})_3\text{Si}-[\text{Si}(\text{OH})_2]_n-$ (n=0-2).

Scheme (2.1) illustrates the anionic mechanism; the polymerization reaction is initiated by a silicate anion. The monomer $\text{Si}(\text{OH})_4$ is added step by step into the chain by condensation reactions. Scheme (2.2) represents the neutral mechanism in which all the reaction pieces are neutral.

For some species we calculated equilibrium geometries within the polarized continuum solvent model –COSMO. However, the change in bond distances in the COSMO optimization was always less than 0.01 Å. Therefore, we decided to use only the gas-phase equilibrium geometries in COSMO energy calculations, without reoptimizing the geometries.

We have tried to investigate the effect of water on the mechanism of this dimerization process by including water molecules explicitly in our calculations. Water molecules were added randomly around the dimer cluster. Up to ten water molecules were added. The influence of such water molecules is very small to the geometry of transition states and other intermediate. Their effect on activation barrier is also small. However, the time needed for the calculation of ten explicit water molecules for dimer is huge. Therefore, we decide to use continuum solvation model to evaluate the solvent effect of water. As will become apparent from our conclusions a more detailed analysis of explicit water interactions is necessary to use our results directly for reaction in water phase.

All the results in this study include the solvation effect using the COSMO model. The choice of cavities is important because the computed energies and properties depend on the cavity size. In this study, the PAULING cavity is used instead of the default model UA0 in GAUSSIAN03. The PAULING model has been reported to provide excellent solvation energies for anion species [25] and is acceptable for neutral species with reasonable computational time requirement.

We defined the overall-barrier as the difference in energy between the highest transition state and the initial complex formed that leads to the first transition state intermediate.

2.3. RESULTS

2.3.1 Two mechanisms: neutral vs. anion

2.3.1.1 Formation of the dimer.

Calculations concerning the thermodynamics of silica dimerization reaction have been reported before [14-17,19]. In this section we present studies representative of an alkaline environment that is generally used for zeolite synthesis. We will determine which under this condition is the

most suitable mechanism of SiO-Si bond formation. The two possible routes considered are via the anion and via the neutral species.

a. Anionic mechanisms:

Table 2.1: Selected distances (Å) of the intermediates and transition states along the anionic dimerization reaction.

Distance	O3-H1	O2-H1	O3-Si1	O1-Si1
I	1.015	1.616	3.609	1.691
TS1	1.563	1.016	2.61	1.702
II	2.177	0.965	1.775	1.794
TS2	2.515	0.965	1.691	2.556
III	3.405	0.963	1.682	3.346

In high pH environment, the dominant silicate species will be anionic. Thermodynamic calculations show that in solution the OH⁻ ion will deprotonate the monomeric species to form monocharged anion Si(OH)₃O⁻ [16]. The condensation reaction occurs through two reactions steps. The first step is the formation of the SiO-Si bond between two molecules, the second step is to remove water to form the dimer species. In the first step, the anion Si(OH)₃O⁻ will approach the monomer to a minimum distance to form a structure stabilised by three strong hydrogen bonds (Fig 2.1.I). The transition state corresponds to formation of the SiO-Si bond. In this step, a reaction intermediate is formed with a five-coordinated silicon (Fig 2.1.II). We notice the much elongated Si-O bond around the fivefold coordinated Si. The bond length of Si-O around fivefold coordinated Si is between 1.70 Å and 1.80 Å, whereas, the other Si-O bonds have a length of around 1.65 Å. The geometry of TS1 and the elongation of the bonds around the five-coordinated silicon were also reported by Xiao et al [17]. The presence of this five-fold complex has also been observed by Pereira et al. [14] when the dimerization reaction occurs in methanol environment and is acid catalysed. The activation barrier of this step in our study is 57 kJ/mol for the formation of dimer. This value is slightly smaller than the value obtained by Xiao et al (69 kJ/mol). This difference relate to differences in the details of calculations, as for instance type of

basis set used. Note that there is a hydrogen transfer step between two reactants in the first transition state. The variations of distances O3-H1 and O2-H1 show that one monomer deprotonates and transfers one H to the anion $\text{Si}(\text{OH})_3\text{O}^-$. The hydrogen bond of O3-H1 in structure (I) has to be broken to form the five-fold complex (II).

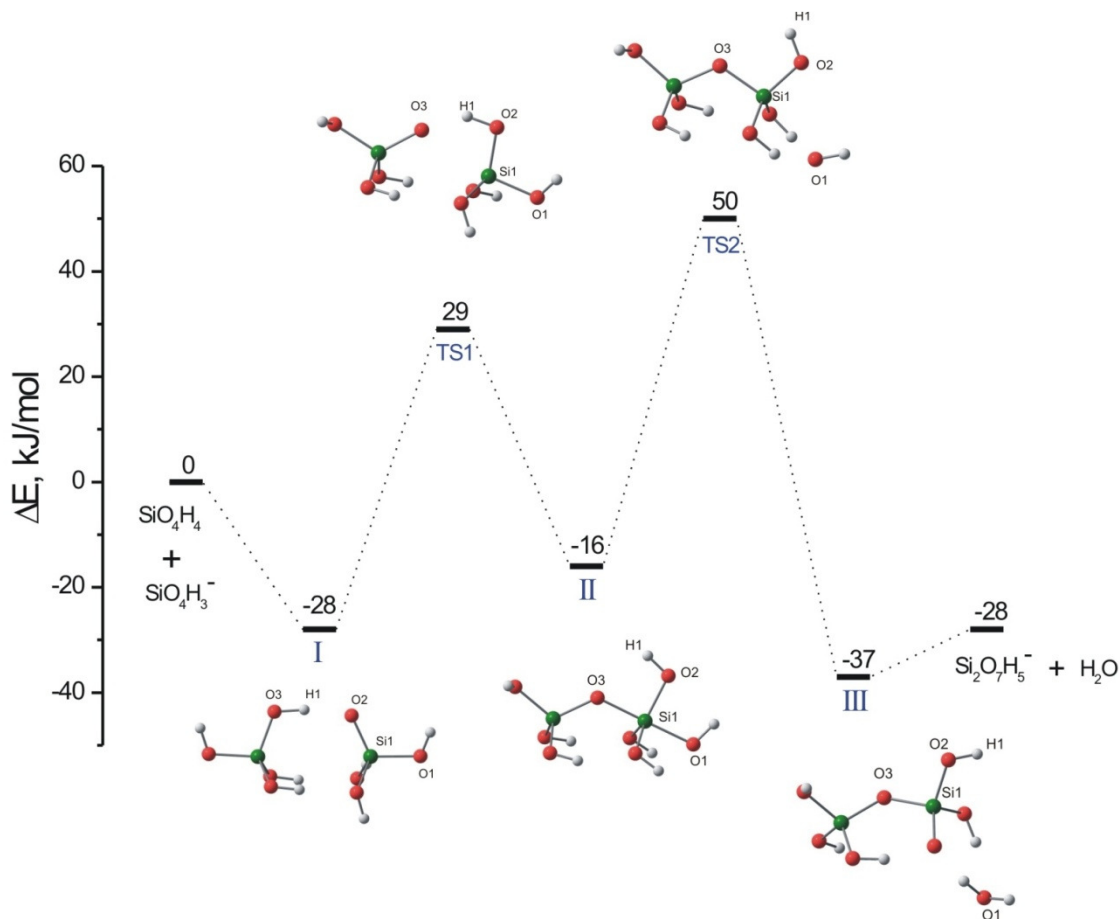


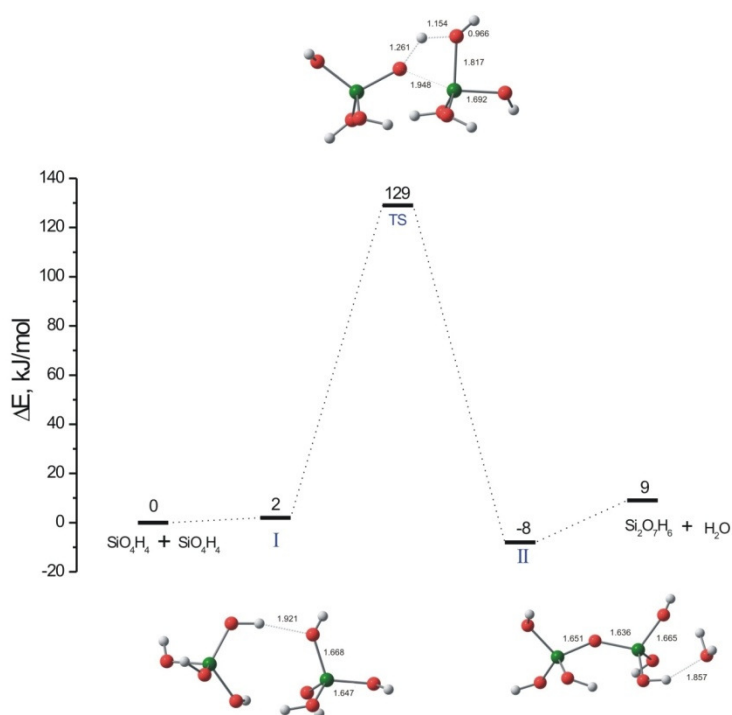
Fig 2.1. The anionic mechanism of dimerization reaction (B3LYP/6-31+G(d,p) – COSMO)

The most difficult reaction step is removal of water molecule to form the dimer silica. The activation energy of this step is 66 kJ/mol. Hydrogen is transferred at the same time that a hydroxyl group starts to leave. As a result, the water molecule will be the leaving group and the product is again an anion which can initiate another condensation reaction to form a trimer. One interesting note is that this product has an internal hydrogen bond. The overall barrier of this two step dimerization reaction is 78 kJ/mol. This second step is the reverse step of adsorption of water to anion dimer reported by Xiao et al. Our barrier (66 kJ/mol) is again comparable to that of Xiao's study (79 kJ/mol), but slightly lower.

b./ The neutral mechanism:

The dimerization reaction can also occur via neutral reactant species. Fig 2.2 shows the details of this reaction path. Two molecules approach through formation of hydrogen bonds to a minimum distance. This complex rearranges via a transition state with an intermolecular hydrogen transfer (TS). The 4 atoms Si, O, H and O are in the same plane. There is also an increase of the Si-O bond length (1.82 Å) towards which the H is transferred. This helps to cleave the Si-O bond. The activation energy of this step is very high: 127 kJ/mol due to strong interference of the hydroxyl proton. After H transfer, the water fragment leaves the molecule to form the dimer. The five-fold silicon complex is not observed in this neutral route with lateral attack. This is different from the proton catalysed mechanism reported by Pereira et al. [14]. They found that the five-silicon complex also is present in acid catalyzed dimerization in methanol environment.

In other theoretical studies of silica hydrolysis using B3LYP and a continuum solvent model (SCIPCM) calculations, Pelmenschikov et al. reported the mechanism of quartz dissolution on



neutral silica surfaces [18]. The healing reaction of neutral dimer on β -cristobalite surface, which was the SiO-Si bond formation, was reported to have a barrier of 120 kJ/mol. The values of the activation barrier in our model (127 kJ/mol) is comparable to that of Pelmenschikov et al.

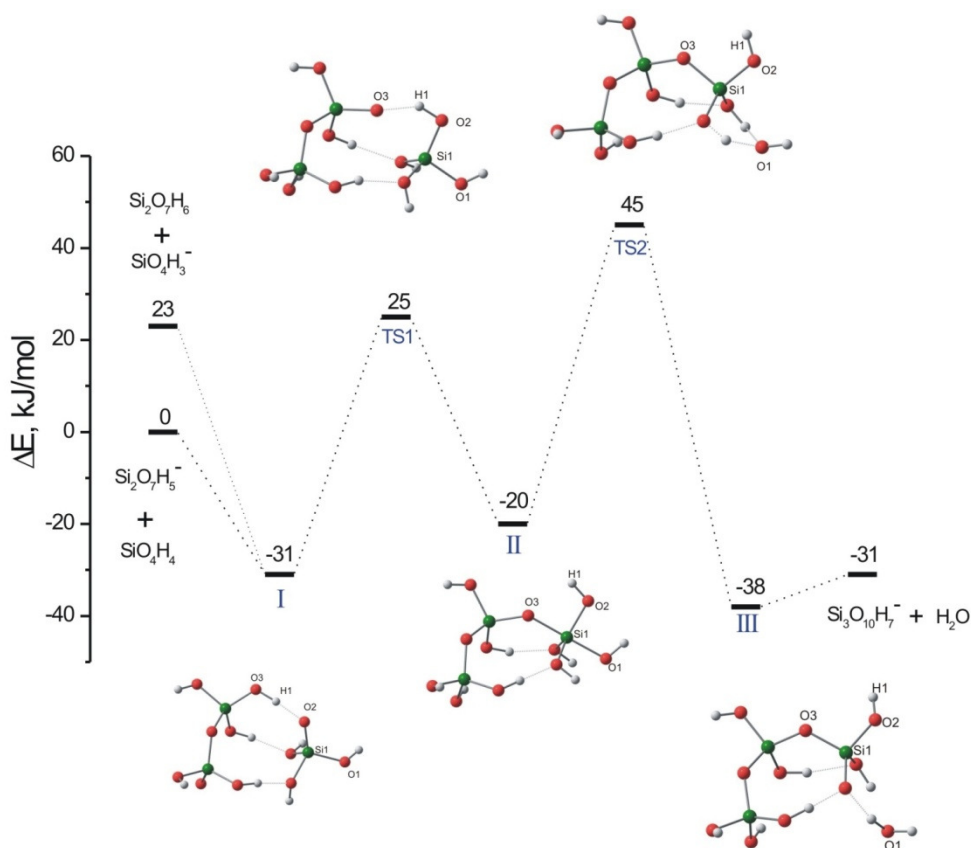
Fig 2.2. The neutral mechanism of dimerization reaction (B3LYP/6-31+G(d,p) – COSMO)

2.3.1.2. Formation of the linear trimer

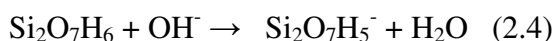
a. Anionic mechanism:

Table 2.2: Selected distances (Å) of intermediates and transition states along the anionic pathway of trimer formation reaction.

Distance	O3-H1	O2-H1	O3-Si1	O1-Si1
I	1.032	1.518	3.590	1.688
TS1	1.596	1.010	2.631	1.694
II	2.183	0.965	1.780	1.785
TS2	2.505	0.965	1.690	2.520
III	2.736	0.964	1.685	3.279

**Fig 2.3.** The anionic mechanism of the trimerization reaction (B3LYP/6-31+G(d,p) – COSMO)

In basic environment, the OH⁻ ion deprotonates the oligomers species to form the monocharged anions. The first deprotonation reaction of monomer and dimer are given by equation (2.3) and equation (2.4);



The calculated values of deprotonation free energy of monomer and dimer are -64 kJ/mol and -92 kJ/mol, respectively [16]. Thus, formation of the anionic dimer is more favourable than that of the anionic monomer in the high pH environment. The product of the dimerization reaction is a monocharged anion. For this reason, the reaction between anionic dimer and one monomer is more favourable than between neutral dimer and anionic monomer. The difference in energy between the two set of reactants is 23 kJ/mol. Hence, the reactants for trimerization reactions are mainly an anionic dimer and a monomer. Both a neutral monomer attack on an anionic dimer and an anionic monomer attack on neutral dimer will lead to the same intermediate structure (I). Therefore, these two mechanisms are essentially the same.

Whereas one would expect also in the complex of dimer and monomer, formed upon reaction, that the dimer would remain anionic this is not found. In the pre-transition state complex from which Si-O-Si bond occurs, proton transfer has taken place. It is due to the large hydrogen bonding of the hydroxyl groups of dimers with the hydroxyl groups of monomer. It causes an increase in the basicity of the monomer silicate anion.

The anionic pathway is very similar to the mechanism of dimerization and occurs in two steps. First, the formation of a Si-O-Si bond with a barrier of 56 kJ/mol. As in the case of dimerization, proton transfer occurs again in the transition state also. The intermediate is a five-coordinated complex with a geometry similar to the case of the dimer. The most favourable approach of the monomer is to form an almost cyclic-like structure. H-bonding controls the preferred conformation. It explains why the linear trimer has a cyclic-like conformation as has also been found by others.^[12,13] Second, the hydroxyl group leaves and H transfer occurs at the same time. The leaving group is a water molecule. This second step has a barrier equal to 64 kJ/mol. The overall barrier of trimerization reaction is 76 kJ/mol, which is similar as the value found for dimerization.

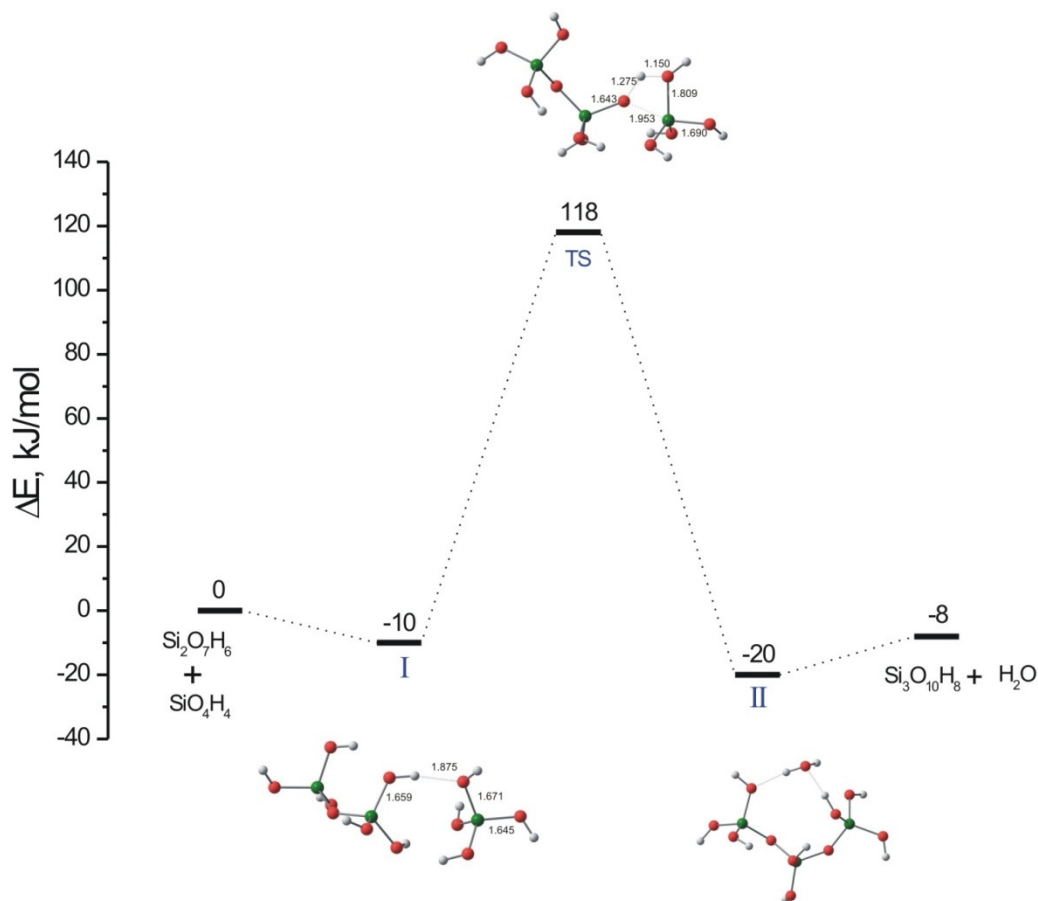
Neutral mechanism:

Fig 2.4. The neutral mechanism of the trimerization reaction (B3LYP/6-31+G(d,p) – COSMO)

The neutral mechanism of the reaction of dimer silica and one monosilicic acid is presented in Fig 2.4. The pathway is very similar to dimerization; the complex reactant turns into the product via a transition state with hydrogen transfer. The barrier of this process is 128 kJ/mol which again is higher than for the case of the anionic mechanism.

2.3.1.3. Formation of the 3-ring:

Formation of the 3-ring has been suggested before to occur via an intramolecular condensation reaction [12,16]. Calculations on the thermodynamics indicate that the 3-ring is a stable product

in solution [16]. Here we will study the mechanism of 3-membered ring formation via the internal condensation reaction according to the anionic and neutral route.

The anionic mechanism

Table 2.3: Selected distances (Å) of intermediates and transition state along the anion paths of 3-ring closure reaction.

Distance	O3-H1	O2-H1	O3-Si1	O1-Si1
II	1.706	1.007	2.980	1.647
TS1	1.952	0.973	2.250	1.671
III	3.285	0.966	1.733	1.799
TS2	2.953	1.016	1.689	2.496
IV	3.406	0.975	1.694	3.294

There are two important differences with the two previously discussed anionic reactions. First of all for ring closure, intramolecular hydrogen bridges between the hydroxyl groups of the molecules have to be broken in order to create a geometry so that internal ring closure can actually happen. This causes the unfavourable energies of intermediates (Fig 2.5.II) (a pre-transition state configuration) and intermediate (Fig 2.5.III) with five-coordinated Si. The activation energy for initial SiO-Si bond formation (Fig 2.5.TS1) is relatively low (36 kJ/mol) because now no proton is transferred. This is the other important difference with the previous anionic dimerization and oligomerization steps.

The water removal step has the same activation barrier as for linear species. The overall barrier of 3-ring formation is 99 kJ/mol, which is much higher than that of dimerization and linear trimerization. We will analyse the consequences of this finding in the discussion section.

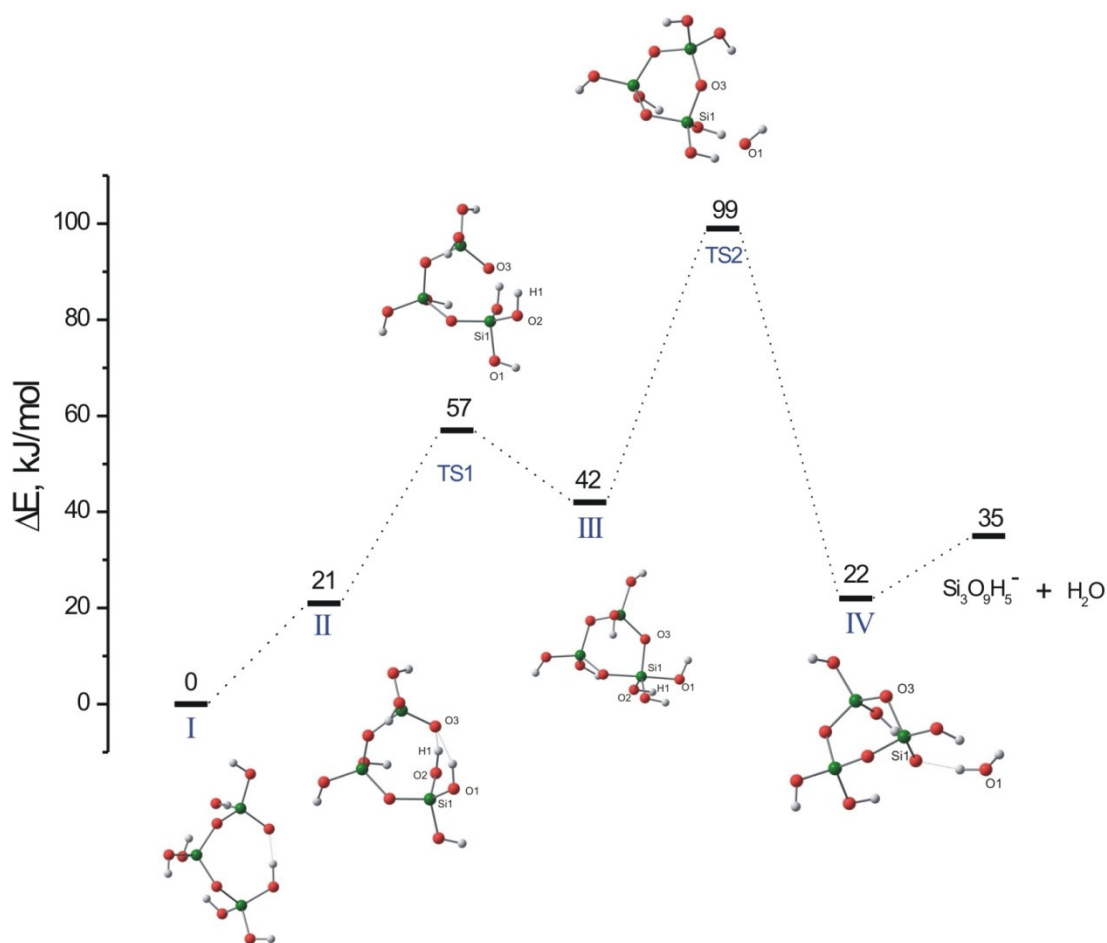


Fig 2.5. The anionic mechanism of 3-ring formation (B3LYP/6-31+G(d,p) – COSMO)

The neutral mechanism:

The ring closure reaction may also take place via the hydrogen transfer mechanism between neutral species as in Figure 2.6. The neutral linear trimer changes conformation. The two ends of the chain approach each other. For the transition state, which is very similar to the case of dimer, a hydrogen transfers to a hydroxyl group. After that, a water molecule will leave of the cluster and a 3-ring is formed. The activation energy is 135kJ/mol, which is higher than the overall barrier of anionic mechanism. Again, this neutral route is not favourable.

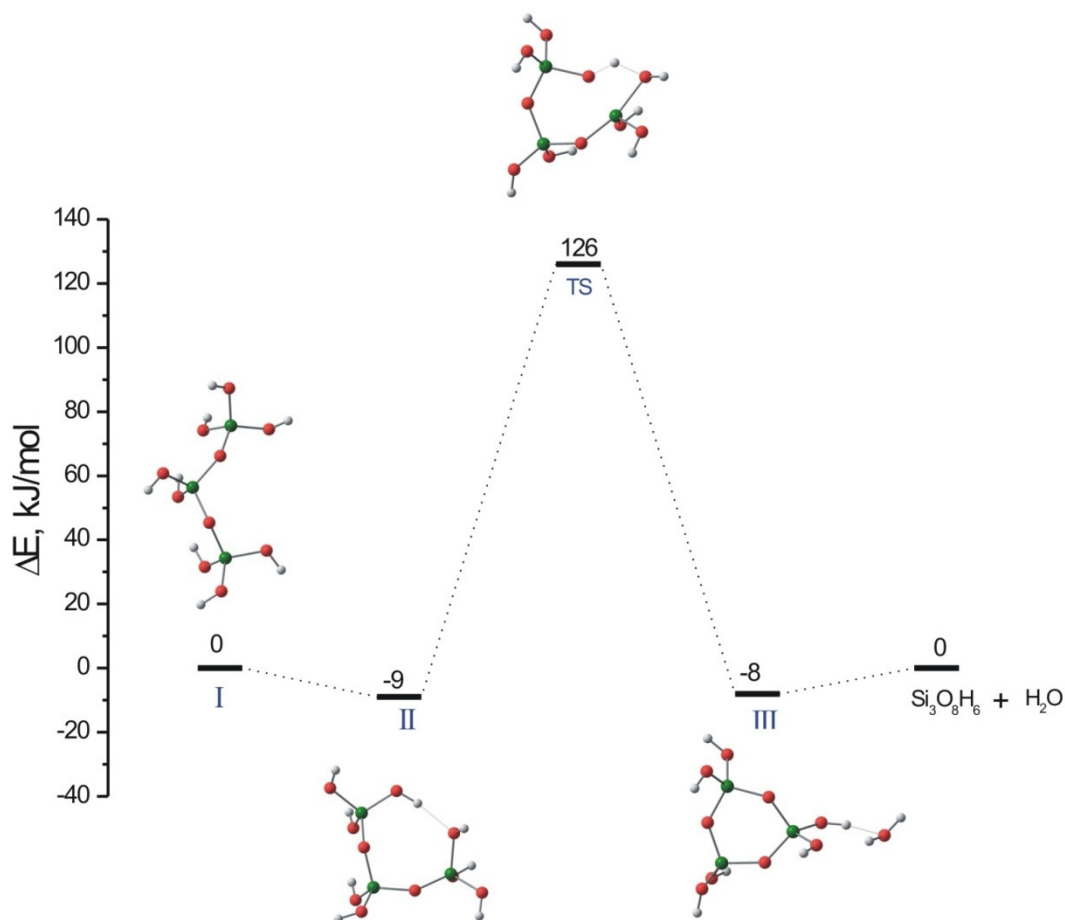


Fig 2.6. The neutral mechanism of 3-ring formation (B3LYP/6-31+G(d,p) – COSMO)

Table 2.4: Comparison of the anionic mechanism and neutral mechanism for the silica condensation reaction. The overall activation barriers are calculated using B3LYP/6-31+G(d,p) and COSMO solvent model.

	Anionic mechanism	Neutral mechanism
Reactants species	1 neutral + 1 anionic	2 neutral
Steps	- SiO-Si bond formation - Water removal	Hydrogen transfer with SiO-Si bond formation
Intermediate	Five-fold silicon	
Overall barrier (kJ/mol)		
Dimer	78	127
Trimer	76	128
3-membered ring	99	135

Data on the two mechanisms (anionic and neutral) are summarised in table 2.4. The anionic pathway, which has two steps, SiO-Si bond formation and subsequent water removal, is clearly the most favourable route for the silica condensation reaction. Our observations are in agreement with the general condition of silica condensation [1,2]. It is interesting to note that the second step in the anionic mechanism is more difficult than the former.

2.3.2. The tetramers

Here we report on the silica condensation reaction for larger clusters. From the previous section, we concluded that the anionic mechanism is the favourable path for silica condensation. Therefore, we only consider the anionic route for the formation of tetramer species.

Formation of linear tetramer and branched tetramer:

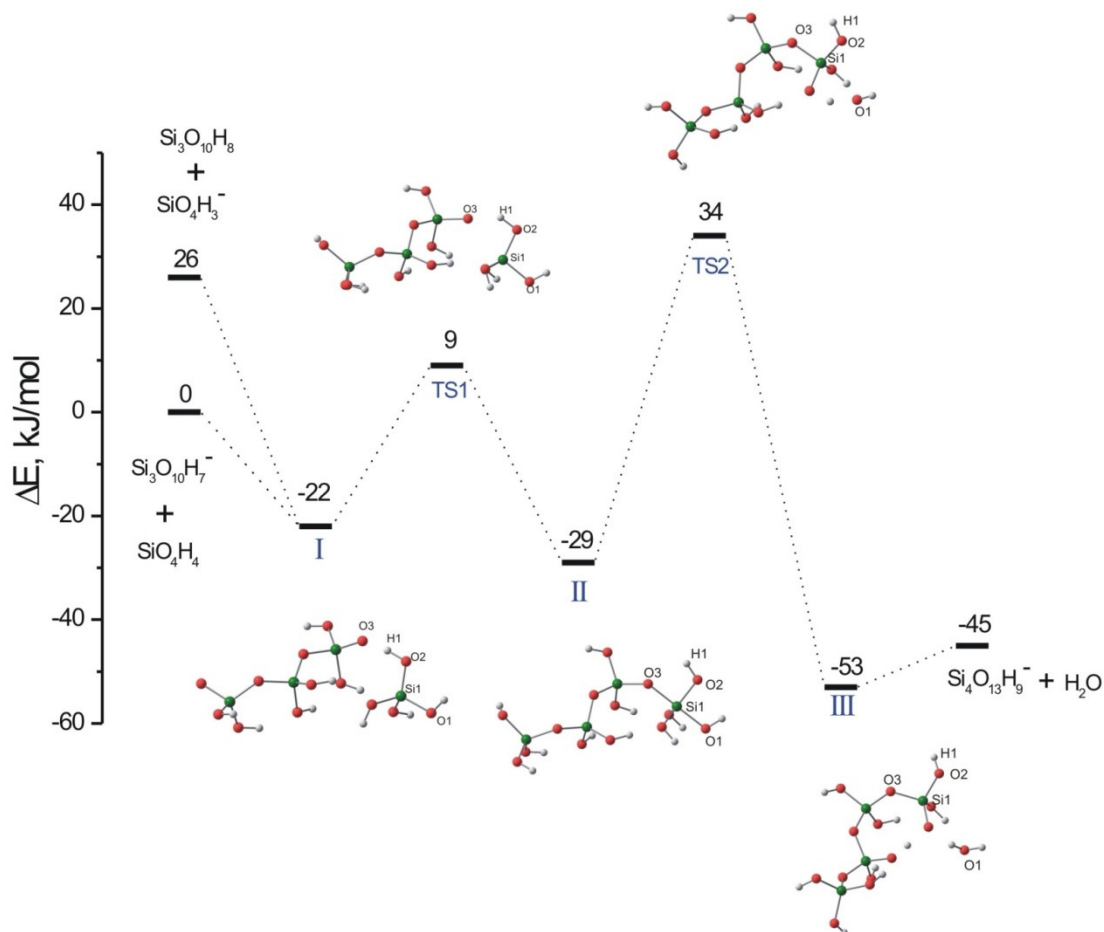


Fig 2.7. The anionic mechanism of linear tetramer formation from a linear trimer and a monomer (B3LYP/6-31+G(d,p) – COSMO)

A linear tetramer and branched tetramer can be formed from the same reactants: an anionic linear trimer and a monomer. Fig 2.7 and Fig 2.8 show the routes of formation for the two species.

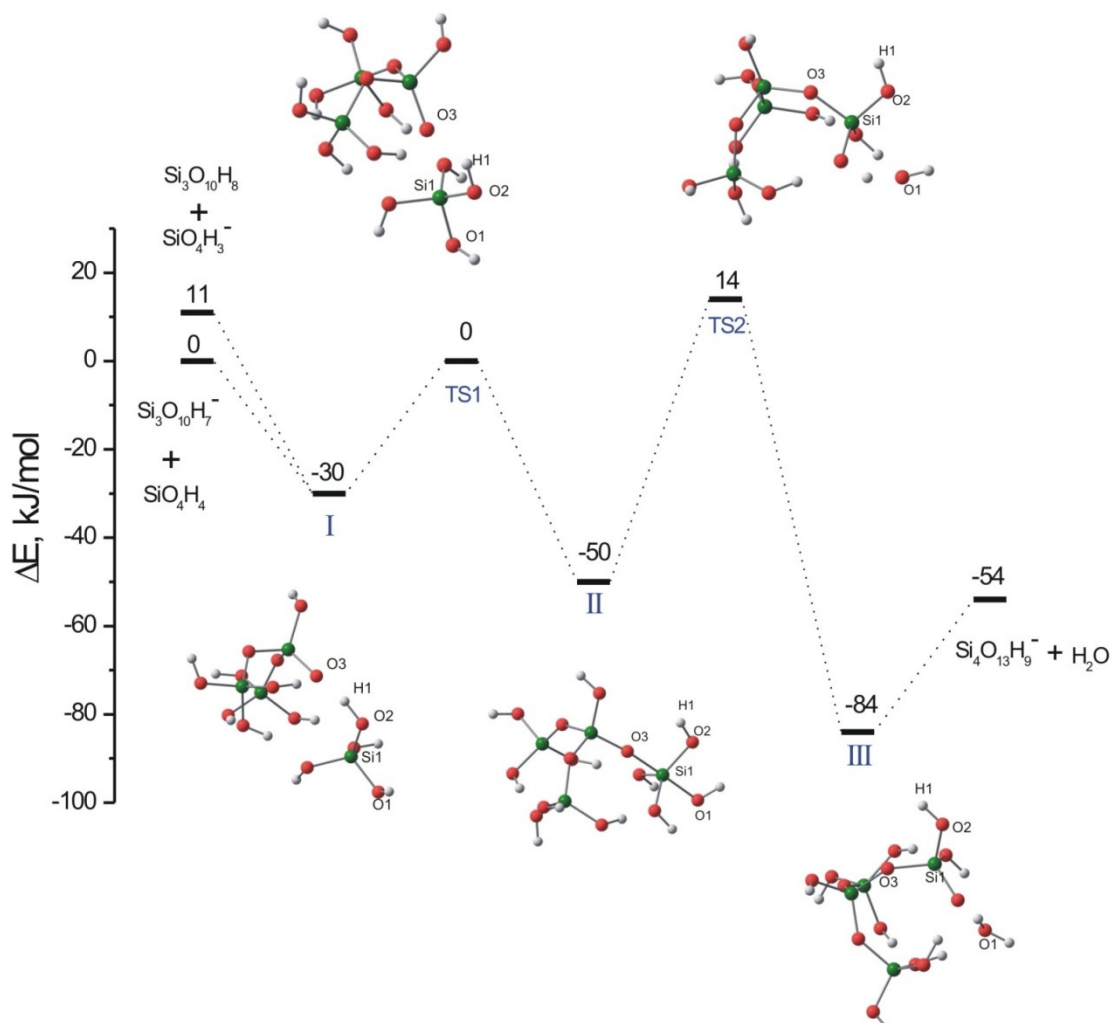


Fig 2.8. The anionic mechanism of branched tetramer formation from a linear trimer and a monomer (B3LYP/6-31+G(d,p) – COSMO)

Different from the cases of anionic dimerization and linear trimer formation, there is no proton transfer between monomer and oligomer in the pre-transition state (complex Fig 2.7.I) of SiO-Si bond formation. Now there is no stabilization of negative charge on the monomeric silicate anion in the complex with oligomer. The oligomeric hydrogen bonds remain saturated by

intramolecular hydrogen bonds. As a consequence the activation barrier for SiO-Si bond formation is the same as that found in the trimer cyclization reaction. Secondly intermediate (Fig 2.7.II), with five coordinated Si, is stabilized because of the many intramolecular hydrogen bonds possible in this complex. The first barrier of SiO-Si formation and the second barrier of water removal are 31 kJ/mol and 63 kJ/mol respectively. Hydrogen bonding effects explain the finding that the overall barrier of linear tetramer formation reaction is only 56 kJ/mol, while the overall barriers for dimerization and trimerization are 76 kJ/mol and 78 kJ/mol, respectively.

Table 2.5: Selected distances (Å) of the intermediates and transition state along the anion paths of formation of linear tetramer.

Distance	O3-H1	O2-H1	O3-Si1	O1-Si1
I	1.352	1.089	3.251	1.672
TS1	1.601	1.008	2.654	1.691
II	2.188	0.965	1.785	1.781
TS2	2.483	0.965	1.695	2.439
III	2.756	0.965	1.683	3.285

Table 2.6: Selected distances (Å) of intermediates and transition state along the anionic paths of formation of branched tetramer.

Distance	O3-H1	O2-H1	O3-Si1	O1-Si1
I	1.409	1.055	3.285	1.668
TS1	1.686	0.996	2.598	1.692
II	2.248	0.965	1.760	1.783
TS2	2.498	0.965	1.681	2.455
III	2.651	0.964	1.670	3.321

The anionic mechanism of branched tetramer formation from a linear trimer and a monomer is shown in Fig 2.8. The mechanism is very similar to the case of formation of the linear tetramer. The mechanism with two steps takes place with barriers of 30 kJ/mol and 64 kJ/mol,

respectively. For the same reasons as mentioned for linear tetramer formation, the phenomenon of hydrogen transfer at the first step does not occur. Consequently, this reaction has a low activation barrier of the SiO-Si formation (30 kJ/mol). The overall barrier (44 kJ/mol) is again low because of stabilisation of intermediate (Fig 2.8.II) by hydrogen bonding.

We predict that the formation of higher oligomers as pentamers and hexamers would have very similar barriers as found for the case of linear and branched tetramer formation. Essentially because of the role of hydrogen bond, the formation of these complexes may be expected to be quite similar.

4-ring formation:

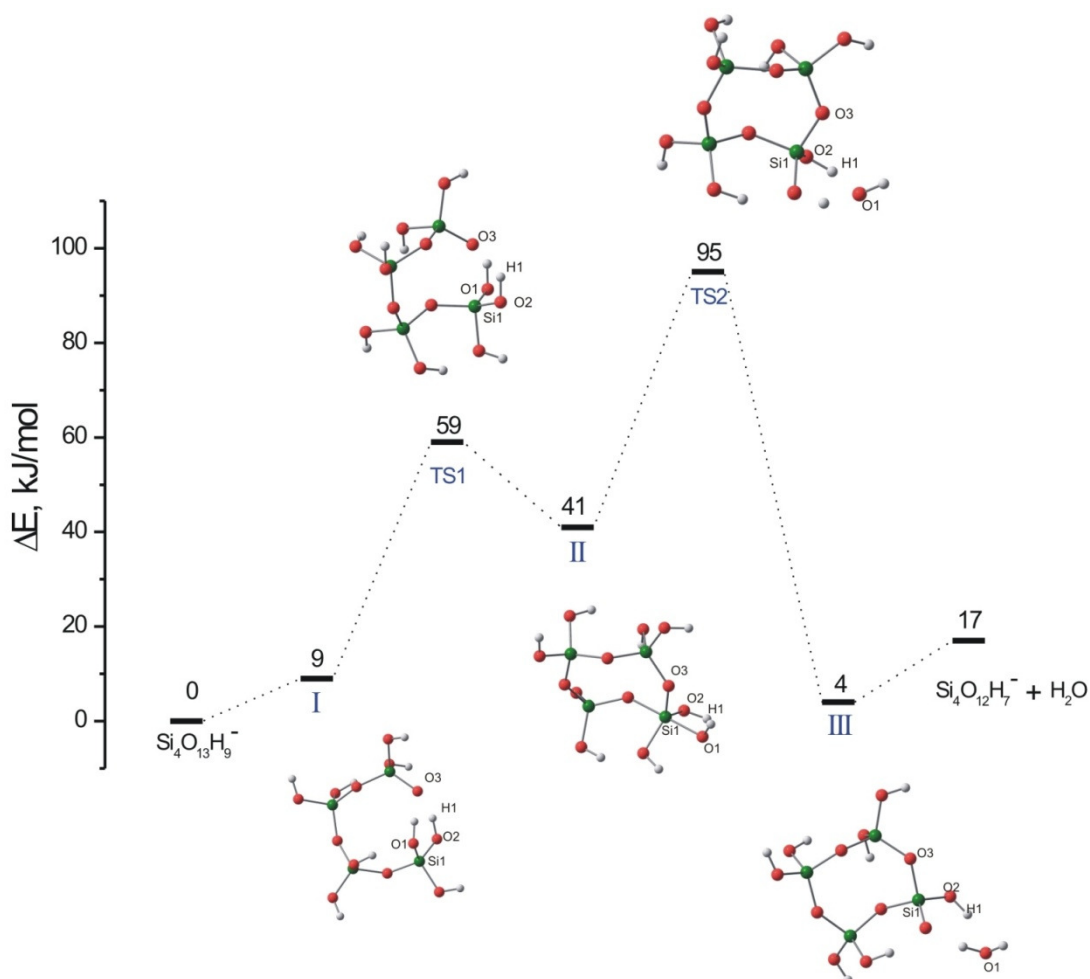


Fig 2.9. The anion mechanism of 4-ring formation from a linear tetramer (B3LYP/6-31+G(d,p) – COSMO)

The case of 4-ring formation is similar to the 3-ring mechanism. The linear tetramer has several internal hydrogen bonds. They have to be broken for formation of the reactive cyclic intermediate. The energies of the different elementary reactions steps is similar as that of the trimer ring closure reaction. Similar to the case of 3-ring closure, the overall barrier of 4-ring formation is 95 kJ/mol.

Table 2.7: Selected distances (Å) of the intermediates and transition state along the anion paths of 4-ring closure reaction

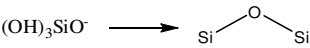
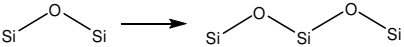
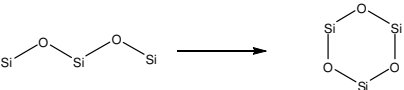
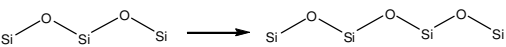
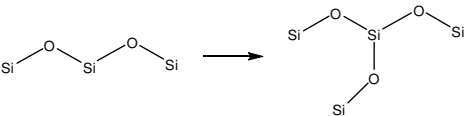
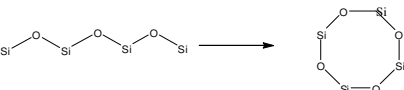
Distance	O3-H1	O2-H1	O3-Si1	O1-Si1
I	1.709	1.001	3.168	1.663
TS1	1.986	0.975	2.392	1.660
II	3.305	0.966	1.726	1.789
TS2	3.007	0.987	1.684	2.484
III	3.399	0.975	1.688	3.311

2.4. DISCUSSION

The overall energetics of the oligomerization reactions considered is summarised in Fig.10. One notes the relatively high barriers of the initial oligomerization steps and the low barriers for consecutive linear and branched oligomer formation. This result implies that higher oligomer formation should occur rapidly once the initial oligomers have been formed. This agree with experimental observation [1,2]. In contrast, the ring closure reactions are found to have high barriers. These rates should be relatively slow. This does not agree with experimental observation that always shows significant ring formation [10,11]. From the analyses of our results given earlier we deduced that the main reason for the barriers is the reduction of the internal hydrogen bonds when the ring closure occurs. In agreement with this we find (see table 2.8) the values of E_{act2} are the same for all reactions. We suggest that the main reason for the difference between experiment and theory is the absence of explicit water molecules in the

simulation. Embedding the reactions in a water environment will create many hydrogen bonds with water. This will tend to counteract the hydrogen bonds change energies we found to have responsible for many of the differences in our calculated results. This we intend to study in consecutive study.

Table 2.8: Calculated activation barriers (kJ/mol) for the condensation reactions forming silicate clusters from monomeric to tetrameric species via the anionic mechanism. For the linear and branched oligomers, the reactants are a silicate anion and a monomer $\text{Si}(\text{OH})_4$ to form the larger silicate anion and water as products. For the internal condensations, the reactants are the silicate anion that leads to the monocharged ring and a water as products. E_{act1} is the activation barrier of SiO-Si bond formation step, E_{act2} is the activation barrier of water removal step. The overall-barrier is the difference in energy between highest transition state and the initial complex formed that leads to the first transition state intermediate.

Condensation reaction	Gas phase					COSMO model				
	E_{act1}	E_{act2}	Overall-barrier	ΔE	ΔH^a	E_{act1}	E_{act2}	Overall-barrier	ΔE	ΔH^a
	52	61	52	-87	-92	57	66	78	-28	-42
	41	62	41	-60	-68	56	64	76	-30	-69
	28	51	68	60	69	57	57	99	35	49
	20	57	20	-87	-51	31	63	56	-45	-74
	22	62	31	-121	N/a	30	64	44	-54	N/a
	34	57	71	64	37	59	54	95	17	18

^a Ref 16: calculated ΔH values using BLYP/DNP at 450K, COSMO model for solvation energy.

We have considered two possible pathways for the silica condensation reaction. The anionic and neutral mechanism of the formation of dimer, trimer and 3-membered ring silicate species have been investigated. The calculated overall-barrier of anionic route is always lower than the neutral route. This finding agrees with experiment [1,2] that finds rapid oligomerization in basic solutions.

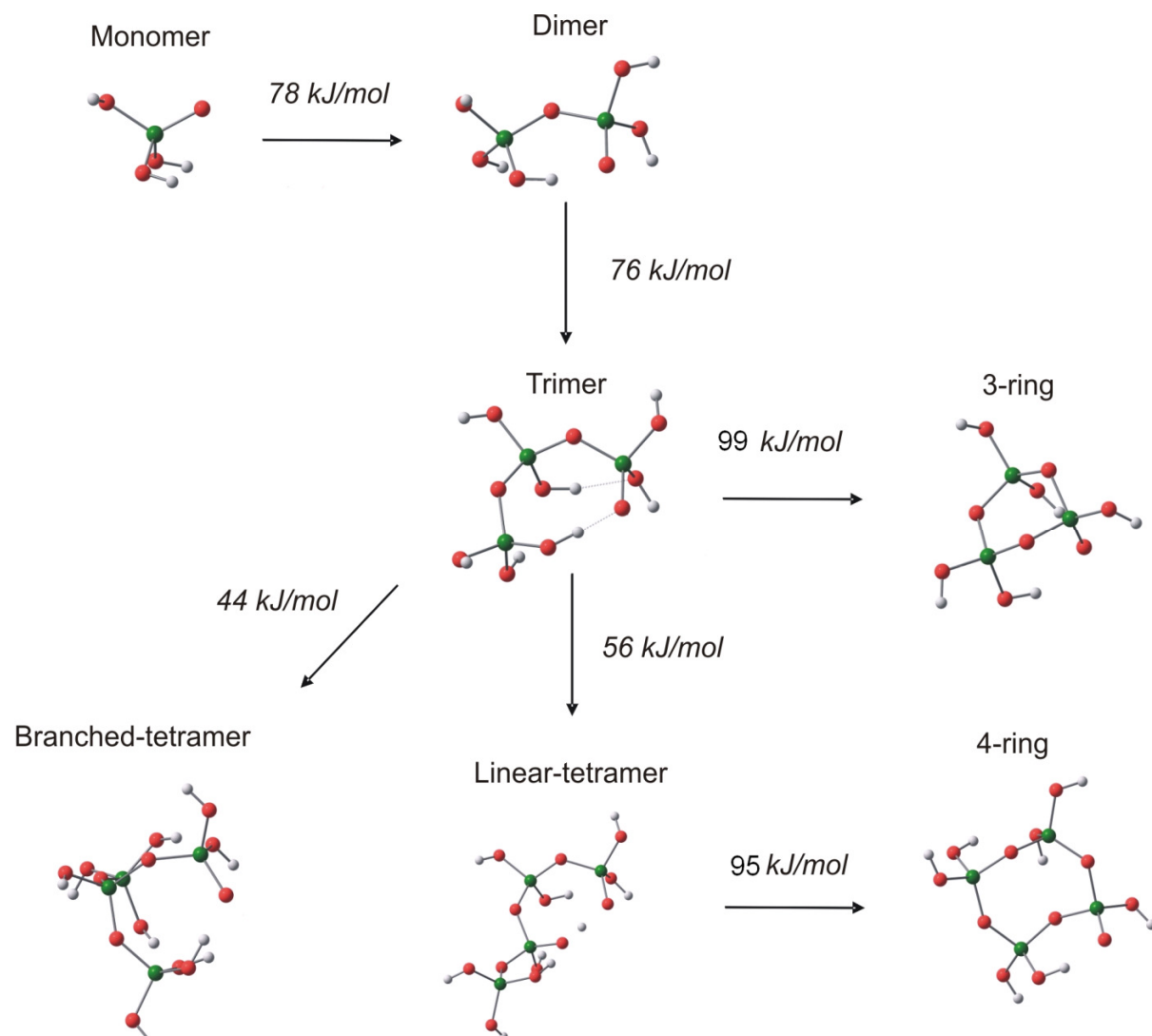


Fig 2.10. B3LYP/6-31+G(d,p)- COSMO results: condensation reaction map of the formation from dimer to tetramer and the ring structure with calculated overall activation barriers (kJ/mol).

The anionic mechanism has 2 steps. The first step is SiO-Si linkage formation which results in an intermediate with a five-coordinated silicon complex. The prediction of this five-coordinated silicon is supported by experimental work [23] which shows the presence of this kind of complex during the hydrothermal synthesis of zeolites. The hydrogen-bond is very important factor in the initial reactant complex. It is found that at the initial step of SiO-Si formation, the hydrogen can also transfer between the two reactants (in the case of dimer and trimer). This derives from the fact that the deprotonation energy of silicate species increased when the size of oligomer increases [16]. The second step is the removal of water of that intermediate to create the product in the oligomerization process. It is found that the second step has the higher barrier. Cluster size does not have an effect on the activation barrier of water removal in the noncyclic addition reaction. For linear oligomer formation from dimer to tetramer, this barrier is in range 63-66 kJ/mol. The activation barrier of water removal step for internal ring closure reaction is similar for 3-ring and 4-ring formation.

Other thermodynamic properties calculations of the oligomerization reaction were reported by Mora-Fonz et al. [16]. The authors used the BLYP method with the COSMO model to evaluate the free energy of silica condensation reaction. One of their conclusions was that the reaction concerning the mono charged silica species is favourable in high pH environment. The ring formation was also suggested to occur via an internal condensation reaction. Our thermodynamic results are comparable with that of the previous studies [12,13,16]. Additionally, this mechanism study adds to their observation that the kinetics also prefers the anionic route compared to the neutral pathway.

The size of the oligomer has an effect on the mechanism and activation barrier of the silica condensation mainly due to the differences in hydrogen bonding. In the first step of the SiO-Si bond formation reaction, there is a hydrogen transfer between the reactants in the formation of the dimer and trimer. This phenomenon has an important contribution to the activation energy of the SiO-Si linkage formation step. The activation barrier of this step is higher when there is hydrogen transfer, because the O-H bond has to be broken to create O-Si bond. For larger oligomers or ring formations, there is no such hydrogen transfer. Subsequently, the barrier energy for SiO-Si formation is lower than the case of smaller oligomer.

In the experimental studies of zeolite synthesis, the dominant species depends sensitively on reaction conditions, solvent used and presence or absence of structure directing agent (SDA) [10, 11]. The mechanism that we proposed can be influenced by the present of SDA. But we expect that there would be a little variation in the bond distance and geometry of the intermediates and transition states. However, we also note that there can be large deviations in the relation energies of the oligomers because the presence of such organic templating agents is likely to increase the stability of particular anionic silica species [30]. In this study, we limited ourselves to the case of pure silica condensation reaction without the presence of SDA compound. A detailed study of the interaction with SDA molecules requires careful considerations of salvation effects with water [30].

2.5./ CONCLUSIONS

In the present study, the reaction mechanism of silica condensation was investigated using DFT calculations for various structures of silicate oligomers. There are two different reaction paths for the condensation reaction: one reaction path proceeds via neutral species and the other occurs via the anionic species. We have investigated an anionic mechanism that occurs in two steps. The first step is the formation of the SiO-Si linkage bond between two reactants. The second one is the removal of the water group from the intermediate to form a product. We infer that the water removal is the most difficult step in reaction pathway. Based on the calculated activation barriers of silicate formation, the anionic pathway is kinetically preferred over the neutral one. Thus, the polymerization of silicate species mainly concerns the anionic species. This remark is good agreement with experimental and consistent with other theoretical studies.

This study continues previous theoretical work [12,13,16] that studied the formation of the silica oligomers. The ring closure reactions occur with high barriers because of loss of intramolecular hydrogen bonds.

The decrease of the overall activation barrier for the formation of higher linear and branched molecules is ascribed to more favourable hydrogen bonding effects for these cases.

The finding of the importance of inter- and intramolecular hydrogen bonding to the relative activation barriers of SiO-Si bond formation in different complexes has several important consequences. First of all presence of water solvent may change the differences in overall barriers found significantly because hydrogen bonding with water molecules will alter hydrogen

bond effects. Secondly SiO-Si bond formation on surfaces may proceed with high barriers, because also here opportunities for hydrogen bonding are reduced.

REFERENCES

- [1] Brinker, C.J.; Scherer, G.W. *Sol-Gel Science*, Academic Press, Boston, **1990**.
- [2] Iler, R. K. *The Chemistry of Silica*, John Wiley & Sons : New York, **1979**.
- [3] Cundy, C. S.; Cox, P. A. *Chem. Rev.* **2003**, *103*, 663-701
- [4] Knight, C. T. G.; Kinrade, S. D. *J. Phys. Chem. B* **2002**, *106*, 3329.
- [5] Kirschhock, C. E. A.; Ravishankar, R.; Verspeurt, F.; Grobet, P. J.; Jacobs, P. A.; Martens, J. A. *J. Phys. Chem. B* **2002**, *106*, 3333.
- [6] Felmy, A. R.; Cho, H.; Rustad, J. R.; Mason, M. J. *J. Solution Chem.* **2001**, *30*, 509.
- [7] de Moor, P.-P. E. A.; Beelen, T. P. M.; van Santen, R. A.; Beck, L.W.; Davis, M. E. *J. Phys. Chem. B* **2000**, *104*, 7600.
- [8] de Moor, P.-P. E. A.; Beelen, T. P. M.; van Santen, R. A.; Tsuji, K.; Davis, M. E. *Chem. Mater.* **1999**, *11*, 36.
- [9] Kirschhock, C. E. A.; Ravishankar, R.; Verspeurt, F.; Grobet, P. J.; Jacobs, P. A.; Martens, J. A. *J. Phys. Chem. B* **1999**, *103*, 4965.
- [10] Bussian, P.; Sobott, F.; Brutschy, B.; Schrader, W.; Schüth, F. *Angew Chem, Int. Ed.* **2000**, *39*, 3901.
- [11] Pelster, S.A.; Schrader, W.; Schüth, F. *J. Am. Chem. Soc.* **2006**, *128*, 4310.
- [12] Pereira, J. C. G.; Catlow, C. R. A.; Price, G. D. *J. Phys. Chem. A* **1999**, *103*, 3252.
- [13] Pereira, J. C. G.; Catlow, C. R. A.; Price, G. D. *J. Phys. Chem. A* **1999**, *103*, 3268.
- [14] Pereira, J. C. G.; Catlow, C. R. A.; Price, G. D. *Chem. Commun.*, **1998**, 1387.
- [15] Tossell, J.A. *Geochimica et Cosmochimica Acta* **2005**, *69*, 283.
- [16] Mora-Fonz, M.J.; Catlow, C.R. A.; Lewis, D. W. *Angew Chem. Int. Ed.* **2005**, *44*, 3082.
- [17] Xiao, Y. T.; Lasaga, A.C. *Geochim. Et Cosmo Acta* **1996**, *60*, 2283.
- [18] Criscenti, L. J.; Kubicki, J. D.; Brantley, S. L. *J. Phys. Chem. A* **2006**, *110*, 198.
- [19] Pelmenschikov, A.; Leszczynski, J.; Pettersson, L. G. M. *J. Phys. Chem. A* **2001**, *105*, 9528.
- [20] Pereira, J. C. G.; Catlow, C. R. A.; Price, G. D.; Almeida, R.M. *J. Sol-gel Science and Technology* **1997**, *8*, 55.
- [21] Rao N. Z.; Gelb, L. D. *J. Phys. Chem. B* **2004**, *108*, 12418.
- [22] Catlow, C. R. A.; Coombes, D. S.; Lewis, D. W.; Pereira, J. C. G. *Chem. Mater* **1998**, *10*, 3249.
- [23] Becke, A.D. *Phys. Rev. A* **1988**, *38*, 3098.; Becke, A.D. *J. Chem. Phys.* **1993**, *98*, 1372.; Becke, A.D. *J. Chem. Phys.* **1993**, *98*, 5648.
- [24] Backer, J.; Muir, M.; Andzelm J.; Scheiner, A. In: Laird, B.B.; Ross, R.B.; Ziegler, T. Editors, *Chemical Applications of Density-Functional Theory, ACS Symposium Series* **1996**, vol.629, American Chemical Society, Washington, DC.
- [25] Frisch, M. J.; Trucks, G. W.; Schlegel, H. B.; Scuseria, G. E.; Robb, M. A.; Cheeseman, J. R.; Zakrzewski, V. G.; Montgomery, J. A.; Stratmann, R. E.; Burant, J. C.; Dapprich, S.; Millam, J. M.; Daniels, A. D.; Kudin, K. N.; Strain, M. C.; Farkas, O.; Tomasi, J.; Barone, V.; Cossi, M.; Cammi, R.; Mennucci, B.; Pomelli, C.; Adamo, C.; Clifford, S.; Ochterski, J.; Petersson, G. A.; Ayala, P. Y.; Cui, Q.; Morokuma, K.; Malick, D. K.; Rabuck, A. D.; Raghavachari, K.; Foresman, J. B.; Cioslowski, J.; Ortiz, J. V.; Stefanov, B.; Liu, G.; Liashenko, A.; Piskorz, P.; Komaromi, I.; Gomperts, R.; Martin, R. L.; Fox, D. J.; Keith, T.; Al-Laham, M. A.; Peng, C. Y.; Nanayakkara, A.; Gonzalez, C.; Challacombe, M.; Gill, P. M. W.; Johnson, B. G.; Chen, W.; Wong, M. W.; Andres, J. L.; Head-Gordon, M.; Replogle, E. S.; Pople, J. A. *Gaussian 03 (Revision B.05)*, Gaussian, Inc., Pittsburgh PA, 2003.

- [26] Takano, Y.; Houk, K. N. *J. Chem. Theory Comput.* **2005**, *1*, 70.
- [27] Herreros, B.; Klinowski, J. *J. Phys. Chem.*, **1995**, *99*, 1025.
- [28] Burggraf, L. W.; Davies, L.P.; Gordon, M.S. in *Ultrastructure Processing of Advanced Materials*, ed. D. R. Uhlmann and D.R. Ulrich, Wiley, **1992**, p.47
- [29] Rabinovich, E. M.; Jackson, K. A.; Kopylow, N. A. *Mater. Res. Soc. Symp. Proc* **1990**, *172*, 29.
- [30] Lewis, D. W.; Catlow, C. R. A.; Thomas, J. M. *Faraday Discuss* **1997**, *106*, 451.

CHAPTER 3

The Role Of Water In Silicate Oligomerization Reaction

Here we apply Car-Parrinello Molecular Dynamics simulations with explicit inclusion of water molecules to investigate the reaction pathway for the anionic bond formation of siliceous oligomers. The rates of SiO-Si bond formation of linear or ring containing silicate oligomers become substantially enhanced, compared to gas phase results. The formation of 3-ring oligomer is more favorable than the formation of higher branched and ring silica oligomers.

3.1 INTRODUCTION

The silica condensation reaction is the key elementary reaction step of silica sol-gel chemistry [1,2] as well as alumino-silicate synthesis [3]. Understanding how alumino-silicates as zeolites nucleate and grow is of fundamental scientific and technological importance. Numerous experimental [4-11] and theoretical studies [12-21] have been devoted to investigate molecular aspects of the kinetics and thermodynamics of silicate oligomers at prenucleation conditions.

Most of previous theoretical studies have focused on the thermodynamic properties of silica condensation reaction using cluster models in gas phase and continuum solvent models. For example, an early study on the energies of the dimerization reaction of monosilic acid was reported by Tossel [15]. Using the COSMO solvent model, Tossel studied the free energy of reaction changes by varying temperature and dielectric constants of the solvent. The author found that the condensation reaction is more favorable at high temperature than at room temperature. Free energies of the silica condensation reaction in neutral and alkaline environment have been recently presented by Mora-Fonz et al.[16,17]. It was found that the formation of the small ring fragment is favourable in high pH media.

There is still limited information on the activation barriers that control the rate of the SiO-Si formation step in real solutions. From previous computational studies of the reaction models in the gas phase, it became apparent that formation of inter-molecular or intra-molecular hydrogen bonds is an important aspect. Computational studies including water molecules explicitly are essential to establish further the role of such hydrogen bonding effects [22]. Previously in chapter 2, we found that especially the relative rates of formation of silicate ring containing oligomers compared to that of linear silicate oligomers were affected by intra-molecular hydrogen bonding differences. The gas phase calculations [21] indicated significantly higher barriers for ring formation than for linear and branched oligomer formation. This disagrees with experimental observations in the water phase.

Here we report on an ab initio density-functional theory based molecular dynamics simulation study of the silica condensation reaction in aqueous solution.

3.2 COMPUTATIONAL DETAILS

Earlier we concluded, in agreement with experiment, that silica oligomerization proceeds through an anionic intermediate species [21]. Therefore, we have used this preferred anionic pathway (scheme 3.1)

to investigate the formation of dimer to branched tetramer, 3-ring and 4-ring oligomers species. Simulations [23,24,25] were performed employing the Car-Parrinello method as implemented in the CPMD package. We considered a system consisting of one silicic acid $\text{Si}(\text{OH})_4$ and its deprotonated form $\text{Si}(\text{OH})_3\text{O}^-$ with 64 water molecules. The simulation cell is a periodically replicated cubic box with a size corresponding to a density of solution around $1\text{g}/\text{cm}^3$ at ambient conditions. The temperature is set at $T=350\text{K}$ and imposed with a Nose-Hoover thermostat. The electronic structure was calculated using the Kohn-Sham formulation of density functional theory (DFT) and employing the BLYP functional [26,27]. BLYP has proven to give an accurate description of the structure and dynamics of water [28-30] and silica-water interaction [31]. Typically, simulations runs consisted of a short equilibration run (1ps) with the temperature of 350K imposed by velocity scaling, followed by a 10 ps production run. This allowed for sufficient relaxation and sampling of the orientational and translational motion. The Car-Parrinello equations of motion have been integrated using a time step of 6 a.u. Deuterium has been utilized instead of hydrogen to allow a larger time step. Therefore, in the discussion below (Molecular Dynamics Simulations), it should be kept in mind that all species that include hydrogen atoms are in fact deuterium containing species.

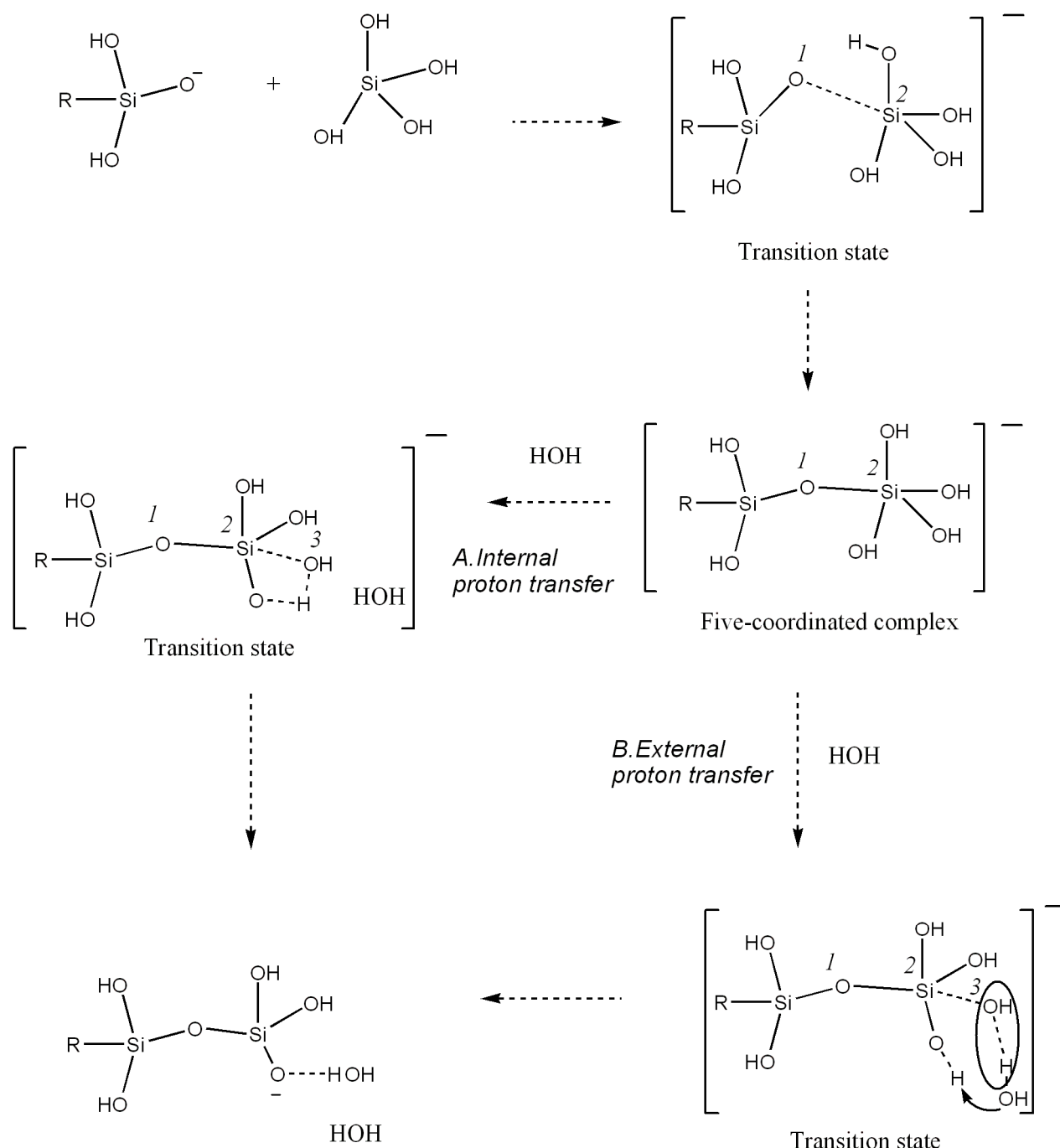
To evaluate the free energy change ΔA , the phase space along the reaction path has been explored by the constrained dynamic method [32], keeping the $r(\text{Si-O})$ length constrained. The reaction free-energy profile was determined by imposing a reaction pathway using the constrained molecular dynamics. Starting from the an equilibrated system the distance $r(\text{Si-O})$ is changed stepwise with intervals of 0.1-0.2 Å from the reactant value to the product value. At each value of the imposed $r(\text{Si-O})$ distance, the system is equilibrated for 1 ps, followed by a 10 ps trajectory for the which the average constraint force required to maintain the imposed $r(\text{Si-O})$ distance was measured. The applied method of constraint ensures that configurations typical for a reaction pathway are properly sampled. The free energy is obtained by thermodynamic integration of the average constraint force along the imposed reaction path. It was determined numerically by a polynomial fit through the measured constrained force:

$$\Delta A = - \int_{\zeta_1}^{\zeta_2} f(\zeta) d\zeta \quad (3.1)$$

where ζ is the value of the constrained reaction coordinate, f is the mean force to hold the system at reaction coordinate ζ and λ is the Lagrange multiplier on the constraint which is proportional to the force due to constraint. Note that all ΔA values are free energies calculated at constant volume;

therefore they are Helmholtz's free energies. However, for most reactions the volume change during the reaction is fairly small (including the interactions, considered in this paper); therefore, ΔA is approximately equal to ΔG under ambient pressure.

Scheme 3.1: Intermediates according to the anionic mechanism of the silica condensation reaction (schematics). Two proton transfer mechanisms are compared.



To calculate the internal energy U of the reactant state and product state, we estimate the average internal energy of 3000 configurations of the system at equilibrium state. The standard error of the energies was calculated according to the block average method presented by Allen and Tildesley [33].

As the rate of condensation reaction is outside the timescale accessible to ab-initio molecular dynamics (~ 10 ps), the reactive events are enforced by using the method of constraints [32]. Starting from the equilibrium configuration, the first step of OSi-O bond formation was controlled by varying the distance between the O1 and Si2 atoms respectively at fixed positions (See scheme 3.1). Subsequently, the reactive event of water removal was controlled by varying at fixed values the distance between Si2 and O3 atoms. The final state of the first step is 5-fold silica intermediate; this structure is also the beginning state of the second step.

3.3 RESULTS AND DISCUSSION

3.3.1./ Radial distribution functions (RDF)

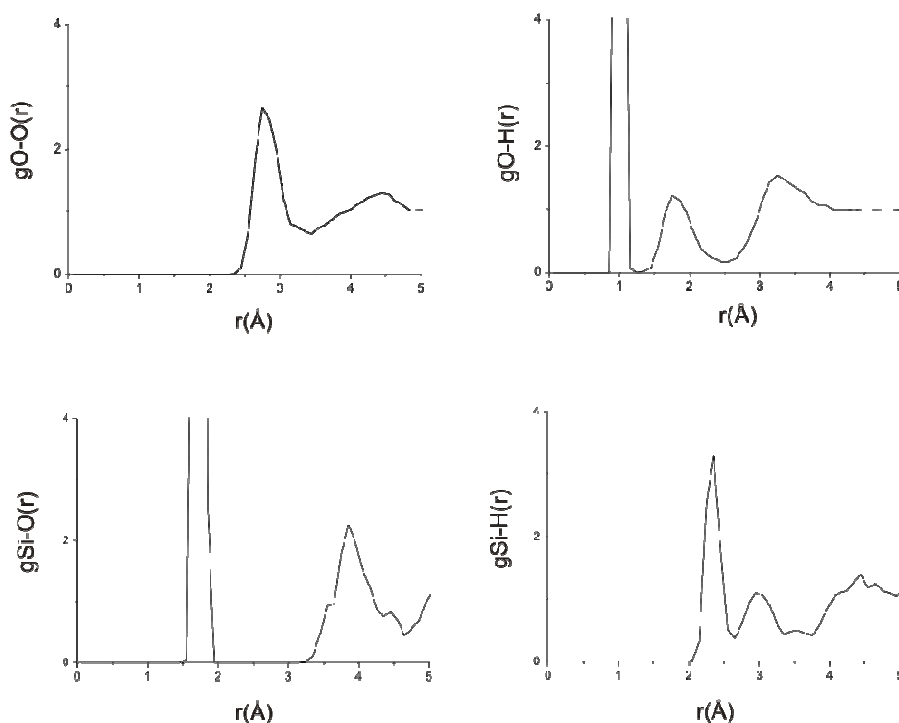


Figure 3.1: a) oxygen-oxygen, (b) oxygen-hydrogen, silicon-oxygen (c) and (d) silicon-hydrogen radial distribution functions (RDFs) obtained from the last 10 ps of the simulation of the reactant state in the dimerization reaction.

An important quantity for characterizing chemical structures in liquid water is radial distribution functions (RDF). In Figure 3.1, we depict the silicon-oxygen $g_{\text{Si-O}}(r)$, silicon-hydrogen $g_{\text{Si-H}}(r)$, oxygen-oxygen $g_{\text{O-O}}(r)$ and oxygen-hydrogen $g_{\text{O-H}}(r)$ obtained from 10ps run after the equilibration step. The main contribution of the oxygen-oxygen and the oxygen-hydrogen RDF is from water structure. The maximum value of the oxygen-oxygen RDF obtained from our simulation is in good agreement with other theoretical studies of pure water [33,34]. This indicates that the silicate species is very well solvated. The typical shape of oxygen-hydrogen RDF of oxygen-hydrogen with the average distance for hydrogen bond of 1.97\AA is observed. We define the hydrogen bond as the distance between oxygen atom and hydrogen atom r_{OH} in the range between 1.5\AA and 2.5\AA . A hydrogen bond is called internal when both the hydrogen atom and the oxygen atom belong to the silicate species, and called external when one atom belongs to the silica oligomer and the other belongs to water molecules. We will use these definitions to discuss the stabilities of various silica structures in later section.

3.3.2./ Dimerization and Trimerization

In our simulations, the initial state is defined as the configuration where one anionic oligomer has a hydrogen bond with one silicic acid monomer. In the case of dimerization, the reactant state contains one silicic acid and its deprotonated form. To prepare the simulation in an aqueous box, the initial geometries of the silica species are taken from our previous gas phase simulations [21] and then solvated with 64 water molecules.

A general accepted mechanism of silica condensation reaction in high pH contains two steps. The first step is $-\text{OSi-O}-$ bond formation. During this step one oxygen atom of monomeric silicic acid connects with one silicon atom of another silicate to form a stable 5-silicon coordinated intermediate. The second step is water removal: one hydroxyl group will depart from the 5-silicon coordinated structure with a hydrogen transfer process occurring at the same time. The products are higher oligomeric silicates and one water molecule (Scheme 3.1).

The free-energy profile of each step is obtained by integrating the calculated constraint force with the method described in the computation and details section. The first point and the last point of each step which have no constrained force applied are obtained after 10ps of production run. The first point of each step is taken as the reference to get the free energy integration of the reaction. Two steps are

connected by the intermediate structure, where the final state of first step is the first state of the second step.

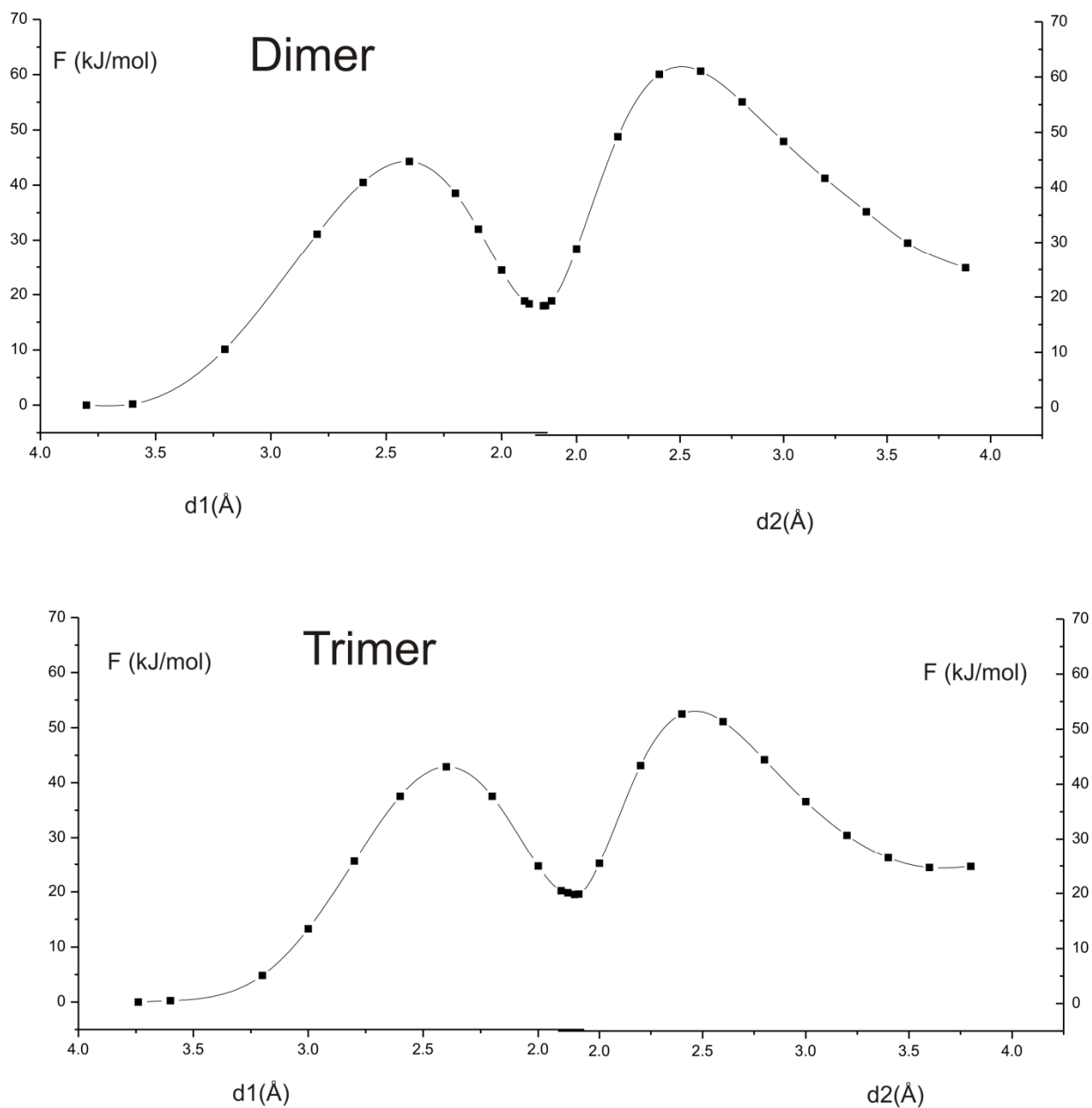


Figure 3.3: Calculated free-energy profile along the reaction path of silica dimerization and trimerization. The free-energy profile is obtained by integrating the connecting line through the calculated constraint force points. Dimerization reaction has an internal proton transfer mechanism. Trimerization reaction has an external proton transfer mechanism.

The first step of the dimerization reaction mechanism is depicted in Figure 3.1. During the process, one oxygen atom of the monomer approaches the Si atom of another monomer. When the distance between two atoms is 1.8 Å, then the bond OSi-O is formed between the two monomers. The product of this step is a 5-fold silicon which is generally observed in theoretical and experimental works. We observe that at 350K, the first activation barrier of dimerization is around 45 kJ/mol.

The second step of the dimerization reaction is a water cleavage process (Figure 3.2). This step is modelled by sampling the distance between the moving oxygen and the silicon atom (Scheme 3.1). During the process, one hydrogen atom will transfer to a hydroxyl group with the result a water cleavage of the 5-silicon coordinated structure to form the final product dimer. This dimer species will be used as a reactant for further reaction (trimerization). Hence, the oligomerization of silica in solution is the process of adding step by step one monomeric silicic acid to a silica chain.

Figure 3.3 shows the calculated free-energy profile of the dimerization reaction with two activation barriers. Our previous calculations of this reaction with a continuous solvent model COSMO found a higher barrier for the second step compared to the first one. The reduction in relative barriers in the aqueous solution calculations compared to the gas phase values (see Table 3.1) is due to the stabilization of the leaving hydroxyl by hydrogen bonds with solvent water molecules. In the continuum model solvent, individual interaction between water molecule and silica structure could not be observed.

The first step of trimerization and dimerization are very similar in reaction mechanism. The activation barriers of the two steps are also comparable (Table 3.1). The second step of trimerization reaction is depicted in Figure 3.2. During the water removal process, one water molecule from the environment will assist the hydroxyl group's cleavage. As the result, to remove OH group from the 5-silicon coordinated intermediate will cost less energy. This mechanism could not be observed in the previous simulation in the gas phase or the continuum solvent model.

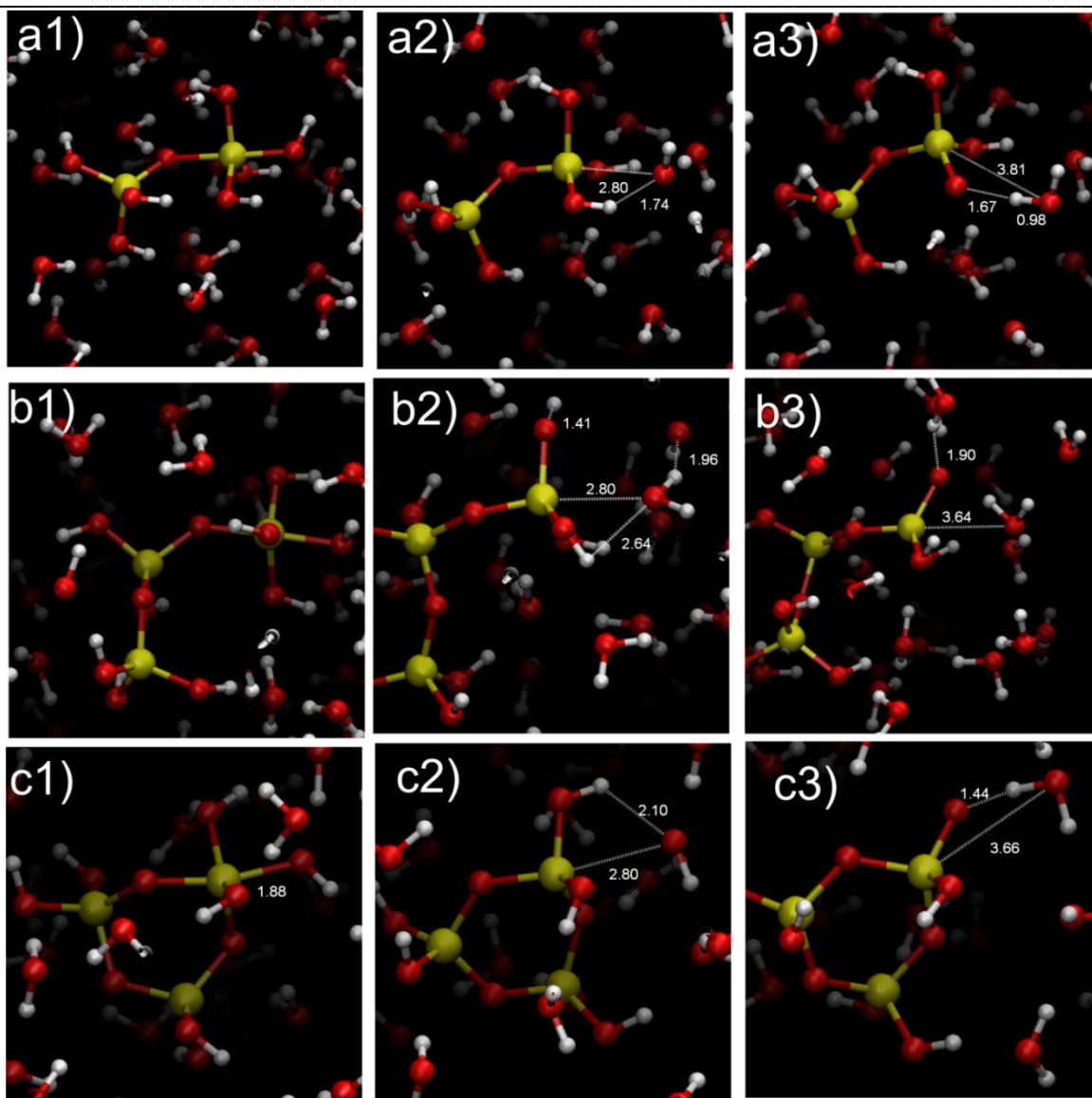


Figure 3.2: Snapshots of representative configurations of ab initio molecular dynamics simulations of the second step (water removal) anionic mechanism to form a dimer (a), trimer (b) and 3-ring species. More detailed snapshots are presented in Supporting Information. White, red, and yellow indicate hydrogen, oxygen, and silicon atoms, respectively. Numbers indicate bond lengths [\AA].

a1, b1, c1: The intermediate five-fold silicon complex. This species is stable in aqueous media.

a2, b2, c2: During the process: differences in the hydrogen bonds network and interactions between silicate and water molecules.

a3, b3, c3: Water cleavage has been completed. The geometry is fully relaxed after 30ps.

The second step of dimerization and trimerization has a different mechanism and barrier height. Water molecules create a hydrogen network environment that assists the water removal process that concludes the SiO-Si formation process. For the dimer, the hydroxyl leaving group forms a water molecule by reacting with an internal hydrogen atom of the dimer (Figure 3.2). The results of simulations of the

consecutive oligomerization step from dimer to linear trimer are shown in Figure 3.3. The second step in which a hydroxyl group leaves the barrier is lower for trimerization (~ 33 kJ/mol) than for dimerization (~ 42 kJ/mol). This is due to an essential difference in the reaction path, with in this case the leaving hydroxyl taking up an external proton from water. The random reorganization of water shell around the silicate during reaction process is likely related to this difference. The hydrogen bond network around the leaving hydroxyl group and nearby trimer's oxygens is unfavourable for internal proton transfer.

3.3.3/ Closure reaction of 3-ring and 4-ring

Experimental study of the first nucleation stage of zeolite synthesis shows a relative high concentration of the 3-ring oligomer [4-10]. During the last decade, many theoretical studies have focused on the formation of these small ring oligomers in first hours of zeolite synthesis. In high pH environment, the ring closure reaction mechanism has two steps. As for the linear species, the first step is the internal interaction to form an intermediate ring with a 5-silicon coordinated structure. The second step is to remove the hydroxyl group and form the final ring product.

Figure 3.4 provides the calculated free energy profile of the internal condensation reaction from linear trimer to form the three-ring silica. The barrier energy of this step in gas phase employing the continuum COSMO model was very high due to the loss of internal hydrogen bonds.^[21] However, in the simulation with explicit water solvent, a lower barrier (~ 35kJ/mol) is found for the initial SiO-Si bond formation step. This barrier height is reduced since the interaction between the silica and water molecules compensates for the necessary loss of intra molecular hydrogen bonds.

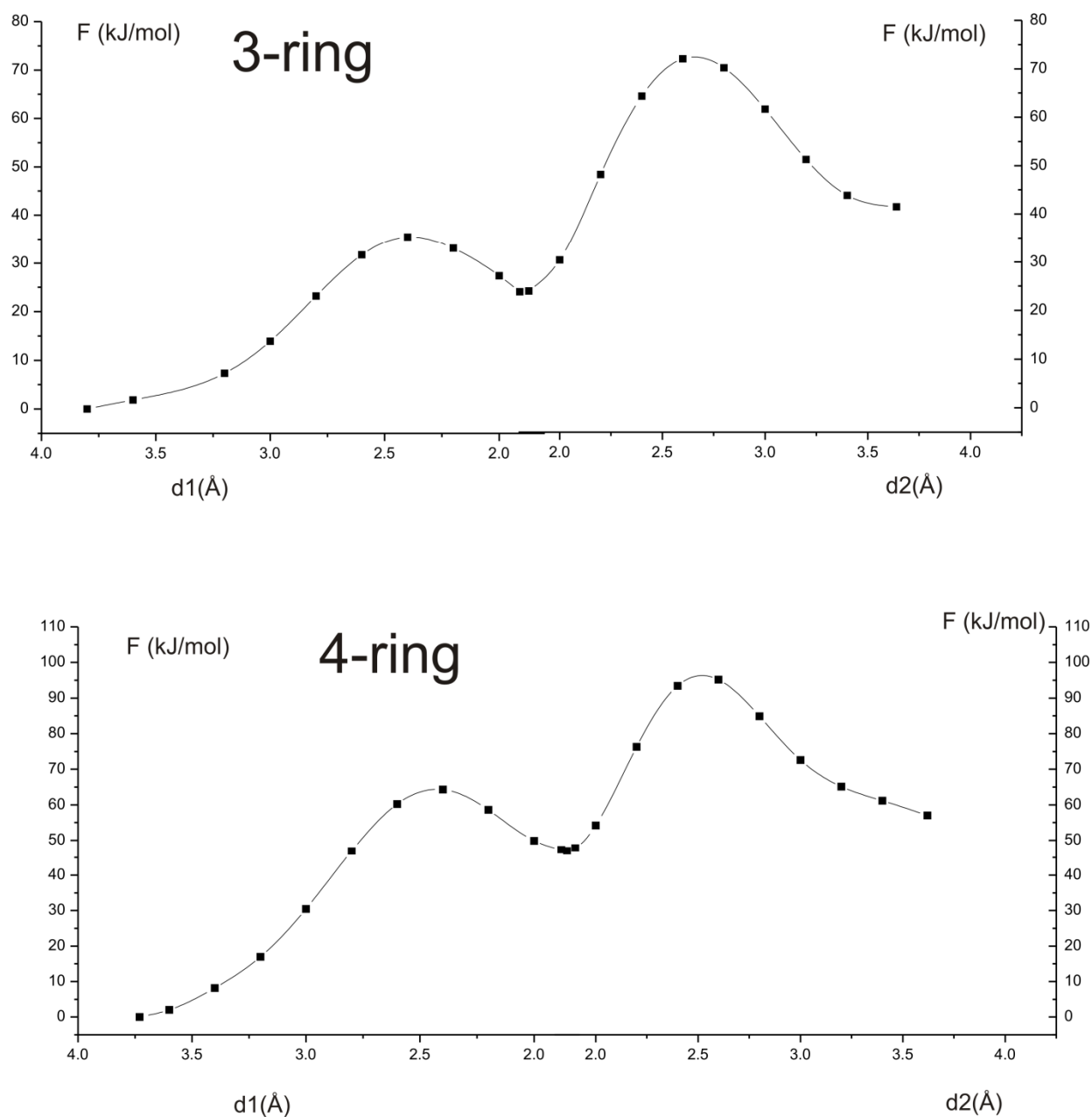


Figure 3.4: Calculated free-energy profile along the reaction path of 3-ring and 4-ring formation. The free-energy profile is obtained by integrating the connecting line through the calculated constraint force points. Both reactions have an internal proton transfer mechanism.

For the cyclic trimer formation the leaving hydroxyl reacts again with the internal proton transfer (Figure 3.2). The barrier difference for the rates of this step of cyclic and linear trimer formation has not changed compared to the gas phase.

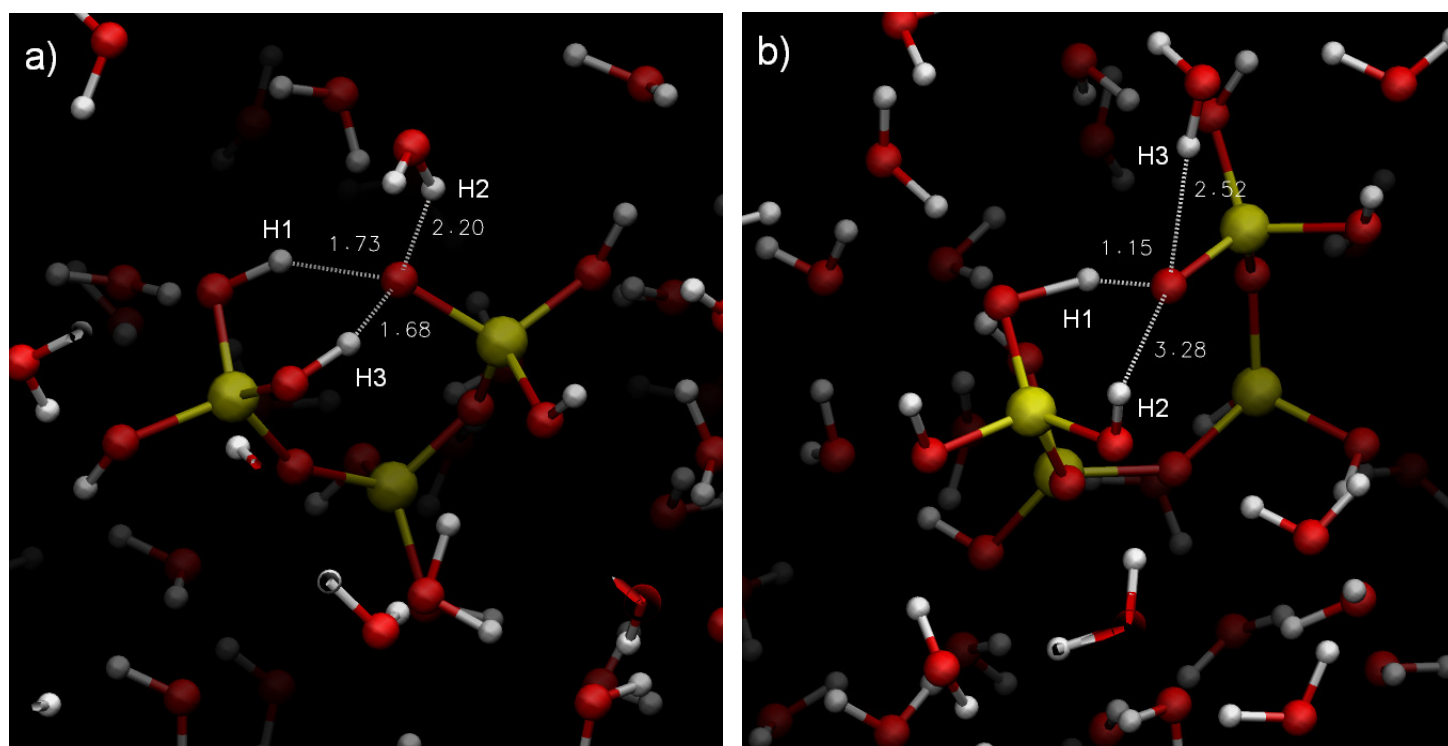


Figure 3.5: Snapshots of representative configurations of the transition state of the SiO-Si bond formation step to form 3-ring (a) and 4-ring (b) silica. White, red, and yellow indicate hydrogen, oxygen, and silicon atoms, respectively. Numbers indicate bond lengths [\AA].

a.) 3-ring transition state: There are 2 internal hydrogen bonds, 1 external hydrogen bond with water

b.) 4-ring transition state: There are 1 internal hydrogen bond, 1 external hydrogen bond with water

Similar to 3-ring formation, the energy profile of the process from linear tetramer leading to 4-ring product is depicted in Figure 3.4. Interestingly, the activation barrier of the first step OSi-O bond formation of the 4-ring is higher than that of the 3-ring. We analyze the hydrogen bonds of the oxygen atom which makes a bond with Si during the trajectory of the transition state. In the case of the 3-ring formation, that oxygen atom has more internal hydrogen bonds than in the case of the 4-ring formation (Figure 3.5). During the simulation, there are two internal hydrogen bonds and one external hydrogen bond for 3-ring. There are only one internal hydrogen bond and two external hydrogen bonds active oxygen of 4-ring (Figure 3.6). The disparity of the first activation barrier between 3-ring and 4-ring formation may also be due to the electrostatic nature of the oxygen atom. In the 3-ring, it is more

negatively charged than in the 4-ring. Hence the interaction $[O^{\delta-} \dots Si^{\delta+}]$ of 3-ring is stronger and more favorable for the SiO-Si bond formation step.

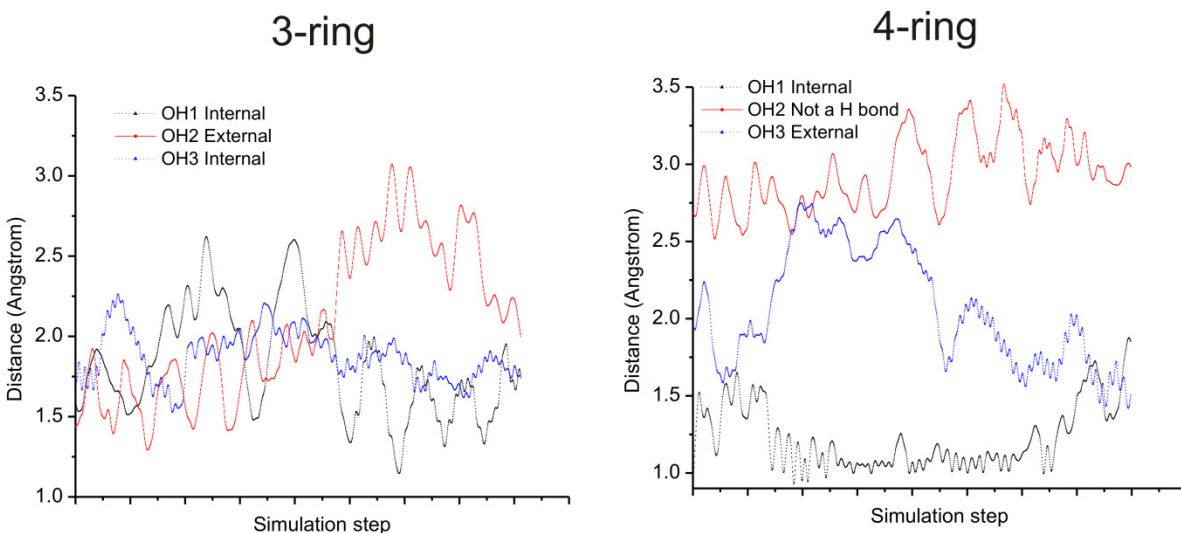


Figure 3.6: Distance between an active oxygen atom and internal/external hydrogen atom in the transition state of SiO-Si bond formation step to form the 3-ring (a) and 4-ring (b) silica oligomer.

The second step of water removal of the 3-ring and of the 4-ring formation has a comparable barrier (50 kJ/mol) and a similar mechanism. Due to the differences of the first activation barrier, the overall barrier of 4-ring (95 kJ/mol) is higher and that that of 3-ring formation (70 kJ/mol). This means that 3-ring formation is more favorable than 4-ring formation. This observation indicates that during the first stage of pure silica oligomerization process, the 3-ring species will have a significant concentration.

3.3.4./ Branched tetramer formation

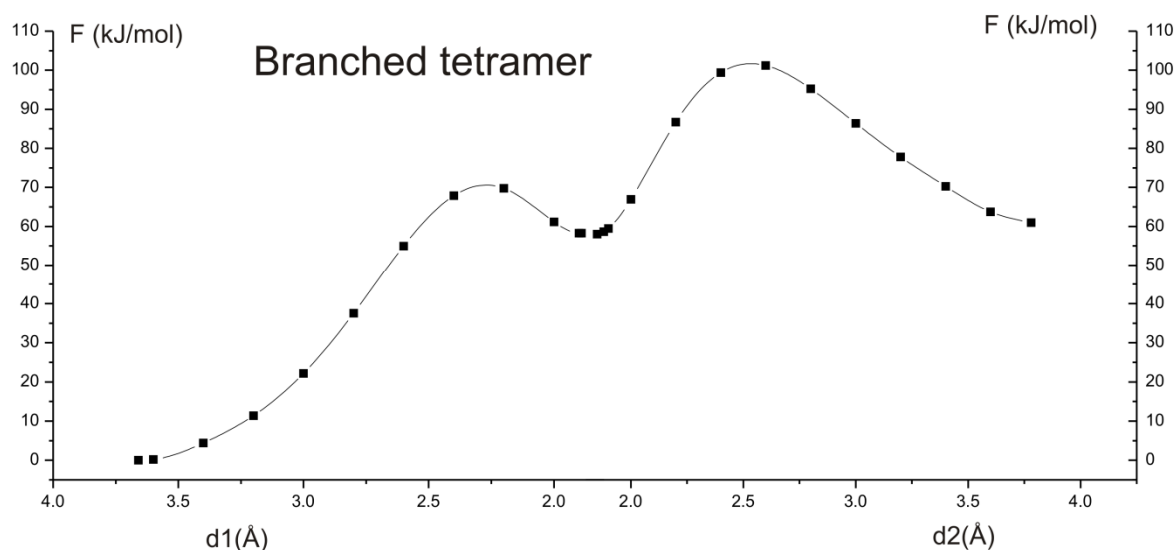


Figure 3.7: Calculated free-energy profile along the reaction path of branched tetramer formation. The free-energy profile is obtained by integrating the connecting line through the calculated constraint force points. The reaction has an internal proton transfer mechanism.

The branched tetramer is formed from a linear trimer and one monomer and has a very comparable mechanism with dimerization and trimerization. Figure 3.7 gives a picture of the free energy profile of the branched tetramer formation. Compared to silica structures containing 3-silicon (linear trimer and 3-ring), the branched tetramer has a higher activation barrier for the first step, SiO-Si bond formation. This distinction may come from the different charged state of the oxygen of the interaction [$O^{\delta-} \dots Si^{\delta+}$]. The oxygen of oligomers containing 4 Si atoms is less negatively charged than oligomers containing 3 Si atoms. As the consequence, the first step to form the 4-ring and the branched tetramer has a higher barrier (65 kJ/mol) than that of the 3-ring and the linear trimer (45 kJ/mol). Our prediction is that the formation of higher oligomer such as pentamer or hexamer would have an even higher activation barrier for the first step SiO-Si bond formation.

The water removal step of the branched tetramer formation is comparable that step of the 3-ring and the 4-ring formation; an internal proton transfer process. The overall barrier of the branched tetramer formation is higher than that of lower oligomers. This trend is different from the previous simulation in continuum model where the branched oligomer formation has a significant low barrier. This implies that

explicit water simulation is very important to study the reaction related to hydrogen bonds in water solution. In a continuum solvent model without explicit water, there is no external hydrogen bond, hence the stabilities of the system is dominated by the internal hydrogen bonds.^[21] With the presence of water, the external hydrogen bonds between silica and water shell environment also contribute to the relative stabilities of the silica structure.

3.4. The role of water molecules in the silica condensation reaction.

One of the most important contributions of this work is that a model is used with explicit water molecules, which can describe the solvation shell of water and the chemical properties of silica in solution much better than earlier cluster approach. The movement of atoms and molecules during the reaction, especially those involved in the hydrogen bonds are captured accurately. Furthermore, this approach can provide new insight in the participation of water molecules in the reaction process.

To estimate to contribution of entropy to the total free energy, the internal energy U is calculated as in the computational details section above. Then the $T\Delta S$ is determined by the fundamental equation $T\Delta S = \Delta U - \Delta A$. The entropy change ΔS of the system comes from the entropy change of silica oligomer and from water environment $\Delta S = \Delta S_{silica} + \Delta S_{water}$

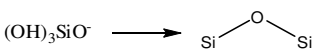

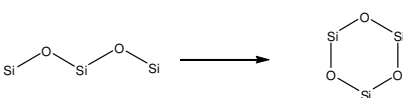
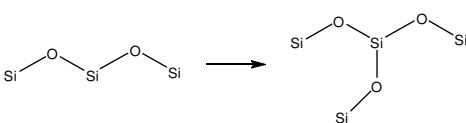
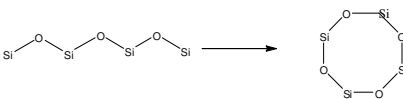
Table 3.1 summarizes the thermodynamic property of all oligomerization reaction. The table clearly demonstrates that incorporating explicit water molecule in the model significantly alters the picture. Compared to the continuum water model, the total reaction free energy becomes more unfavorable due to significant entropy decrease and yields an exothermic reaction enthalpy. This should be related to an overall change of the solvation shell, that has a structure that is dominated by hydrogen bonds. Note that the entropy change upon creating a hydrogen bond is of the order of -30kJ/mol [35]. According to experimental studies and MP2 calculations [35] $T\Delta S$ of one hydrogen bond of a water dimer at 373K is around -30 kJ/mol. Note also that one water molecule is produced in silica condensation reactions. This indicates that the water molecule arrangement is important.

In brief, the total free energy of reaction is unfavorable due to reorganization of waters which results in a significant negative contribution to the entropy of the system. The results show that the enthalpy of silica oligomerization reaction is exothermic. This observation is in good agreement with experimental studies of sol-gel formation and zeolite synthesis [1,2].

Table 3.1: Calculated free energy (kJ/mol) for the condensation reactions forming dimer, linear trimer, 3-ring, 4-ring and branched tetramer via the anionic mechanism. E_{act1} is the activation barrier of the SiO-Si bond formation step, E_{act2} is the activation barrier of the water removal step. The overall-barrier is the difference in energy between highest point and the lowest point along the reaction coordinates, ΔA is the reaction free energy (the difference in energy between the final state and the initial state), ΔU and $T\Delta S$ is the internal energy of reaction and entropy contribution to the reaction, respectively. The unit of all calculated values is kJ/mol. The trimerization reaction has an external proton transfer mechanism. All other reactions have an internal proton transfer mechanism.

^a Ref 21: calculated single point energies values using B3LYP/6-31+G(d,p), COSMO model for solvation energy. The difference in relative reaction energy calculated (single point energy calculation with the same silica geometry in gas phase) between CPMD/BLYP and B3LYP was estimated around 5 kJ/mol.

[*]: The thermodynamic properties of the reaction are not evaluated from the initial reactant and the final product but from the stable intermediate state in the reaction process.

Condensation reaction	CPMD model (explicit water included)						COSMO model [Ref 21] ^a (no explicit water included)			
	E_{act1}	E_{act2}	Overall-barrier	$\Delta A^{[*]}$	ΔU	$T\Delta S$ 350K	E_{act1}	E_{act2}	Overall-barrier	$\Delta E^{[*]}$
	44	42	61	25	-66	-91	57	66	78	-9
	43	33	53	25	-96	-121	56	64	76	-7
	35	48	72	41	-116	-157	57	57	99	22
	69	43	101	60	-95	-155	30	64	44	-54
	64	48	95	57	-71	-128	59	54	95	4

3.5. SUMMARY AND CONCLUSIONS

Our results show that it is essential to include explicitly water molecules in silica condensation and sol-gel chemistry computational studies. The rate limiting step is not the water removal step as in the gas phase simulation [21]. The overall barrier is mostly depends on the first barrier of the SiO-Si bond formation. The activation barrier of the water removal step depends on the mechanism of water assisted internal or external proton transfer, independent from the size of oligomer.

The kinetic and thermodynamic trends of formation of higher oligomers from dimer silica are found to be quite different between explicit solvent simulations (this chapter) and gas phase simulation [21]. The gas phase model proposes that the linear and branched higher silica structure are more favorable than the 3-ring and 4-ring. In contrast, this study in solution observed that 3-ring formation is more favorable than the formation of higher branched and ring silica oligomers. As a consequence, the 3-ring silica structure will be a dominant species during the first stage of pre-nucleation process in pure silica condensation. This is in good agreement with experimental studies of the early stage of zeolite synthesis.

In conclusion, our results show that it is essential to include explicitly water molecules in silica condensation and sol-gel chemistry computational studies. The rates of SiO-Si bond formation of linear or ring containing silicate oligomers become substantially enhanced, compared to gas phase results. The formation of 3-ring oligomer is less unfavorable than the formation of higher branched and ring silica oligomers. The unfavourable thermodynamics is mainly due to changes in water entropy that results from water molecules arrangement. Water molecules are also essential to assist proton transfer and form stabilization hydrogen bond.

References

1. C. J. Brinker and G. W. Scherer, Academic Press, Boston, 1990.
2. R. K. Iler, *The Chemistry of Silica*, John Wiley & Sons New York, 1979.
3. C. S. Cundy and P. A. Cox, *Chem. Rev.*, 2003, **103**, 663-702.
4. C. T. G. Knight and S. D. Kinrade, *J. Phys. Chem. B*, 2002, **106**, 3329-3332.
5. C. E. A. Kirschhock, R. Ravishankar, F. Verspeurt, P. J. Grobet, P. A. Jacobs and J. A. Martens, *J. Phys. Chem. B* 2002, **106**, 3333.
6. A. R. Felmy, H. Cho, J. R. Rustad and M. J. Mason, *Journal of Solution Chemistry*, 2001, **30**, 509-525.
7. P. P. E. A. de Moor, T. P. M. Beelen, R. A. van Santen, L. W. Beck and M. E. Davis, *J. Phys. Chem. B*, 2000, **104**, 7600-7611.

8. P. P. E. A. de Moor, T. P. M. Beelen, R. A. van Santen, K. Tsuji and M. E. Davis, *Chem. Mater.*, 1999, **11**, 36-43.
9. C. E. A. Kirschhock, R. Ravishankar, F. Verspeurt, P. J. Grobet, P. A. Jacobs and J. A. Martens, *J. Phys. Chem. B*, 1999, **103**, 4965-4971.
10. P. Bussian., F. Sobott., B. Brutschy, W. Schrader and F. Schüter, *Angewandte Chemie*, 2000, **39**, 3901-3905.
11. S. A. Pelster, W. Schrader and F. Schuth, *J. Am. Chem. Soc.*, 2006, **128**, 4310.
12. J. C. G. Pereira, C. R. A. Catlow and G. D. Price, *J. Phys. Chem. A*, 1999, **103**, 3252-3267.
13. J. C. G. Pereira, C. R. A. Catlow and G. D. Price, *J. Phys. Chem. A*, 1999, **103**, 3268-3284.
14. J. C. G. Pereira, C. R. A. Catlow and G. D. Price, *Chem. Commun.*, 1998, 1387.
15. J. A. Tossell, *Geochimica et Cosmochimica Acta*, 2005, **69**, 283-291.
16. M. J. Mora-Fonz, C. R. A. Catlow and D. Lewis, *Angew Chem. Int. Ed.*, 2005, **44**, 3082.
17. M. J. Mora-Fonz, C. R. A. Catlow and D. W. Lewis, *J. Phys. Chem. C*, 2007, **111**, 18155-18158.
18. J. C. G. Pereira, C. R. A. Catlow, G. D. Price and R. M. Almeida, *J. Sol-gel Science and Technology*, 1997, **8**, 55.
19. N. Z. Rao and L. D. Gelb, *J. Phys. Chem. B*, 2004, **108**, 12418-12428.
20. C. R. A. Catlow, D. S. Coombes, D. W. Lewis and J. C. G. Pereira, *Chem. Mater.*, 1998, **10**, 3249-3265.
21. T. T. Trinh, A. P. J. Jansen and R. A. vanSanten, *J. Phys. Chem. B*, 2006, **110**, 23099-23106.
22. T. S. vanErp and E. J. Meijer, *Angew. Chem. Int. Ed.*, 2004, **43**, 1660.
23. R. Car and M. Parrinello, *Phys. Rev. Lett.*, 1985, **55**, 2471.
24. CPMD, <http://www.cpmc.org/>, Copyright IBM Corp 1990-2008, Copyright MPI für Festkörperforschung Stuttgart 1997-2001.
25. Calculations were performed with the CPMD package, version 3.11.(<http://www.cpmc.org/>). Electronic states are expanded in plane waves with a wavenumber of up to 70 Ry. The mass associated with the fictitious electronic degree-of-freedom is 700 a.u. The time-step in the numerically integrated equations-of-motion is 0.145 fs. In these simulations, the hydrogen atom mass was set to 2.014102 amu.
26. N. Trouiller and J. L. Martins, *Phys. Rev. B.*, 1991, **43**, 1993.
27. C. Lee, W. Yang and R. G. Parr, *Phys. Rev. B.*, 1988, **37**, 785.
28. K. Laasonen, M. Sprik, M. Parrinello and R. Car, *J. Chem. Phys.*, 1993, **99**, 9080.
29. M. Sprik, J. Hutter and M. Parrinello, *J. Chem. Phys.*, 1996, **105**, 1142.
30. P. L. Silvestrelli and M. Parrinello, *J. Chem. Phys.*, 1999, **111**, 3572.
31. C. Mischler, J. R. Horbach, W. Kob and K. Binder, *J. Phys. Condens. Matter.*, 2005, **17**, 4005.
32. E. A. Carter, G. J. Ciccotti, T. Hynes and R. Kapral, *Chem. Phys. Lett.*, 1989, **156**, 472.
33. M. P. Allen and D. J. Tildesley, *Computer Simulation of Liquids*, Oxford University Press, Oxford U.K., 1987.
34. H. S. Lee and M. E. Tuckerman, *J. Chem. Phys.*, 2006, **125**, 154507.
35. O. Leonid, I. Gorb and J. Leszczynskij, *J. Comput. Chem.*, 2007, **28**, 1598.

CHAPTER 4

Effect Of Counter Ion On The Silica Oligomerization Reaction

Silica condensation reaction were studied in solution in the presence of two counter ions (Li^+ and NH_4^+). Ab-initio molecular dynamics simulations as implemented in CP2K/Quickstep have been used to construct reaction energy diagrams including transition state free energies. Contact with Li^+ as well as NH_4^+ increases the activation energies of the dimerization step compared to the situation of no contact. NH_4^+ has no effect on consecutive oligomerization step. Hence NH_4^+ will increase the relative formation rate of larger oligomer.

4.1 INTRODUCTION

Theoretical modeling of zeolite synthesis has been attractive for many scientists. Many different approaches have been used to date, using both quantum chemical and classical molecular mechanics techniques. Many electronic structure calculations [16-28] have been performed to reveal information about the mechanism of the elementary reaction in pre-nucleation stage.

Free energies of the silica condensation reaction have been recently presented by Mora-Fonz et al. [20, 28]. The authors found that the formation of the small ring fragment is thermodynamically favorable in high pH media. Especially, it is important to include explicitly water molecule and counter ion to the silica model [28]. At different solution pH, the silica condensation reaction has a different mechanism and activation barrier [27, 30]. It is generally accepted that the reaction occurs in high pH solution when an anionic mechanism is operational. This is more favorable and has a lower activation barrier than the neutral mechanism [27,28] Catlow et al.[29] have carried out MD simulations of silica precursors and a structure directing agent. They found that long range electrostatic interactions are of crucial importance. Without these interactions, the investigated complexes tended to dissociate rather than agglomerate.

In chapter 3, it was found that the water molecule in environment has an important role on the silica condensation reaction. Water stabilizes the silicate oligomer with external hydrogen bonding. Water also assists the hydrogen transfer process in the water removal step. The effect of counter ion was not investigated before. Understanding the electrostatic effect is also important to explore the chemistry of silica oligomerization process.

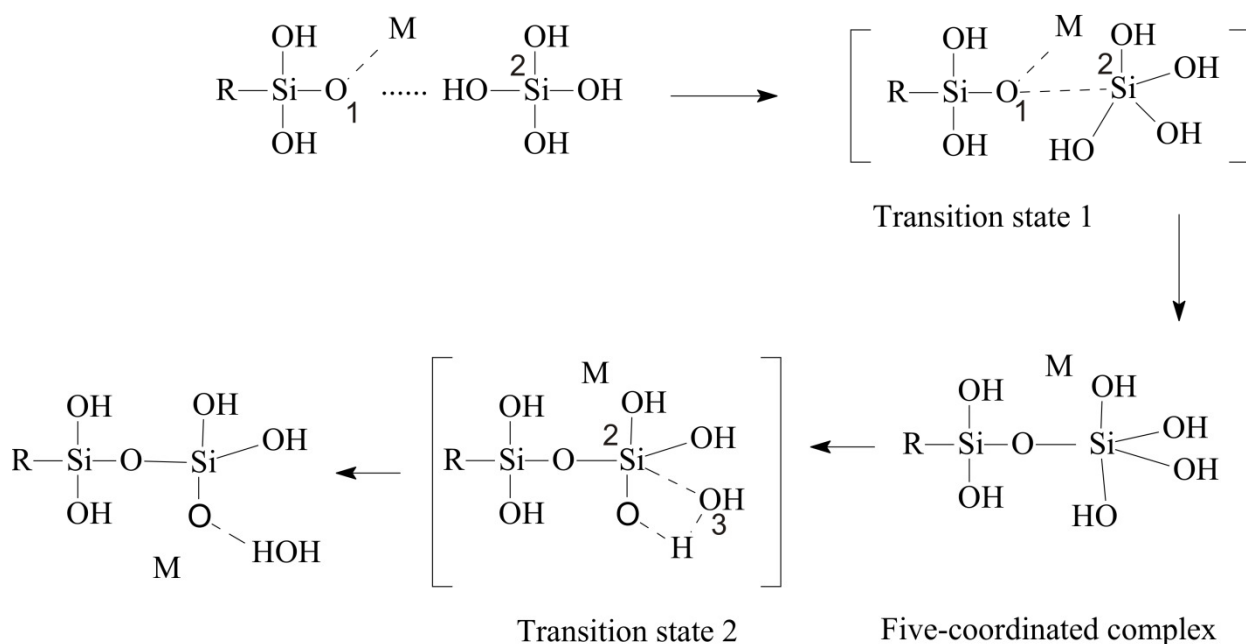
Here we report on an ab initio density-functional theory based molecular dynamics simulation study of the silica condensation reaction in aqueous solution with two cation Li^+ and NH_4^+ .

4.2 COMPUTATIONAL DETAILS

Earlier we concluded, in agreement with experiment, that silica oligomerization proceeds through an anionic intermediate species [27]. Therefore, we have used this preferred anionic pathway (scheme 4.1) to investigate the formation of dimer to branched tetramer and 3-ring species.

We performed DFT-based molecular dynamics simulations using Quickstep[30] which is part of the CP2K program package [31]. It uses a Born-Oppenheimer molecular dynamics (BOMD) algorithm, meaning that it calculates the optimal electron density every time step and from that the forces on the ions. It employs the Gaussian and plane waves (GPW) method [32], which makes efficient and accurate density-functional calculations of large systems possible [33]. We used Goedecker-Teter-Hutter (GTH) pseudopotentials [34,35], the BLYP functional [36,37] and DZVP-MOLOPT basis set [38]. The density cutoff was 200 Ry and the time step 1 fs. A Nosé-Hoover thermostat [39] with a chain length of 3 and a time constant of 1000 fs fixed the temperature at 350K. Every SCF step, the electronic gradient was converged to 10^{-5} Hartree with the orbital transformation method. We considered a system consisting of one silicic acid $\text{Si}(\text{OH})_4$ and its deprotonated form $\text{Si}(\text{OH})_3\text{O}^-$ with 64 water molecules. The counter ion is Li^+ and NH_4^+ . The simulation cell is a periodically replicated cubic box with a size corresponding to a density of solution around $1\text{g}/\text{cm}^3$ at ambient conditions.

Scheme 4.1: Anionic mechanism of the silica condensation reaction with counter ion contain two steps (schematics). M is Li or NH_4 . The first step is SiO-Si bond formation can be effected by cation M. The second step is water removal independent of cation position (water assisted).



To evaluate the free energy ΔF , the phase space along the reaction path has been explored by the constrained dynamic method [40], keeping the $r(\text{Si-O})$ length constrained. After short equilibration (1ps) at 350K by velocity scaling, the equations of motion have been integrated with a time step of 6 a.u. for a time about 10 ps in the NVT ensemble, and the change in the free energy value between states 1 and 2 has been calculated using the thermodynamic integration method with polynomial fit function:

$$\Delta F = - \int_{\zeta_1}^{\zeta_2} f_{\zeta} d\zeta; \quad (4.1)$$

where ζ is the value of the constrained reaction coordinate, f is the mean force to hold the system at reaction coordinate ζ . Note that all ΔF values are free energies calculated at constant volume; therefore they are Helmholtz's free energies. However, for most reactions the volume change of the reaction is fairly small (including the interactions, considered in this paper); therefore, ΔF is approximately equal to ΔG under ambient pressure.

As the rate of condensation reaction is outside the timescale accessible to ab-initio molecular dynamics (~ 10 ps), the reactive events are enforced by using the method of constraints. Starting from the equilibrium configuration, the first step of OSi-O bond formation was controlled by varying the distance between the O1 and Si2 atoms respectively at fixed positions (See scheme 1). Subsequently, the reactive event of water removal was controlled by varying at fixed values the distance between Si2 and O3 atoms. The final state of the first step is 5-fold silica intermediate; this structure is also the beginning state of the second step. Molecular graphics in this chapter is done with VMD [41].

4.3. RESULTS AND DISCUSSION

4.3.1. Radial Distribution Functions (RDF)

An important quantity for characterizing chemical structures in liquid water is the radial distribution functions (RDF). In Figure 4.1, we depict the silicon-oxygen $g_{\text{Si-O}}(r)$, silicon-hydrogen $g_{\text{Si-H}}(r)$, oxygen-oxygen $g_{\text{O-O}}(r)$ and oxygen-hydrogen $g_{\text{O-H}}(r)$ obtained from 10ps run after the equilibration step. The main contribution to the RDF of the oxygen-oxygen and the

oxygen-hydrogen is from water structure. The maximum value of the oxygen-oxygen RDF obtained from our simulation is in good agreement with other theoretical studies of pure water.^[42] The typical shape of oxygen-hydrogen RDF of oxygen-hydrogen with the average distance for hydrogen bond of 1.97\AA is observed. RDF of cation Li^+ in our system is also presented in Figure 4.1.

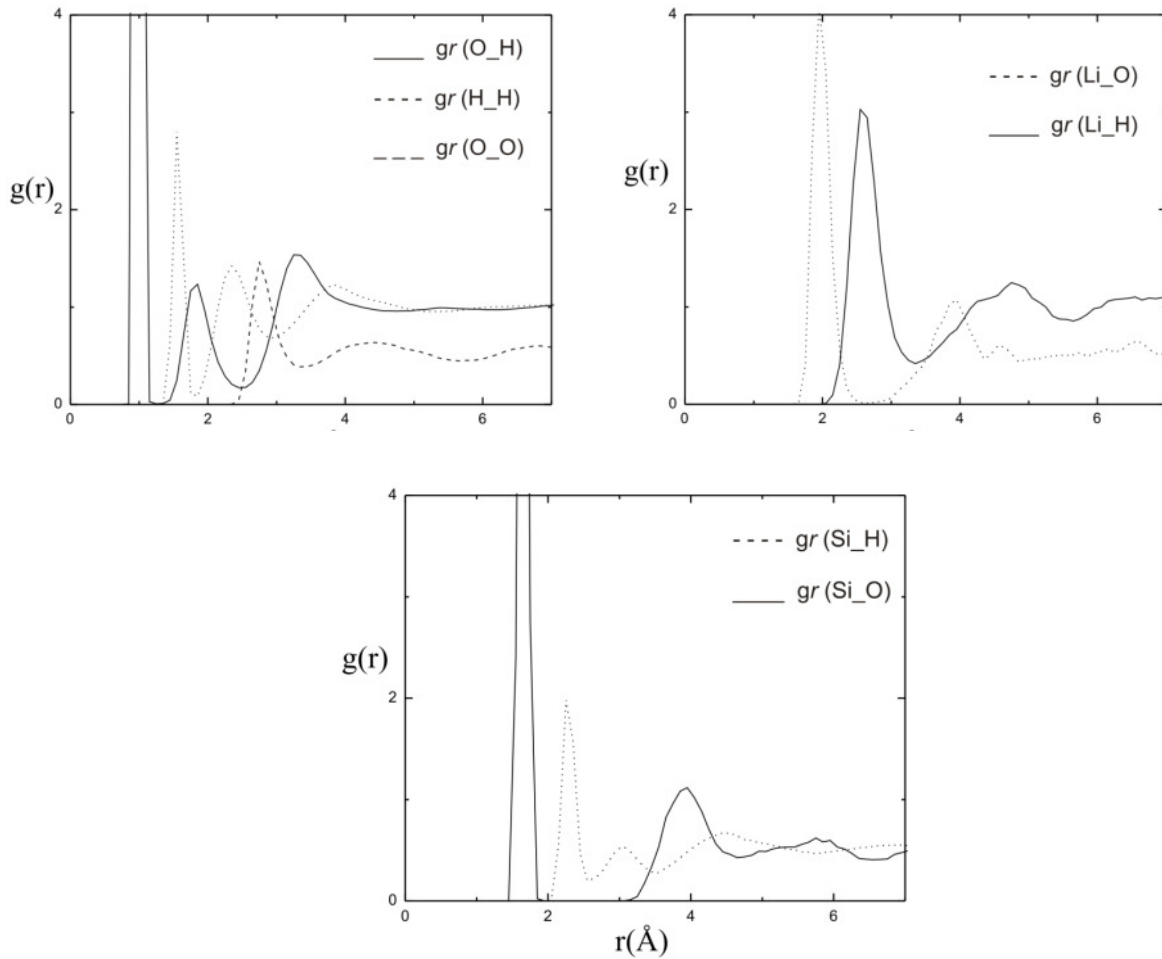


Figure 4.1: Radical distribution function of oxygen and hydrogen atom is mainly from water contributions (a). Radical distribution function with Li (b). Radical distribution function with Si (c)

We obtain a shape of RDF $g_{\text{Li-O}}(r)$ and $g_{\text{Li-H}}(r)$ depicted in Fig 4.1C are comparable to other report. The value of first peak of Li-O is around 2.0\AA , in agreement with previous simulations [43]. The coordination number of the cation Li^+ with water is 4. This observation is consistent with recent experimental data and other simulation.[43,44] In our system, the coordination of Li^+ consist of 4 water molecules [$\text{Li}^+(\text{OH}_2)_4$] or of three water molecules and with one oxygen of silica [$\text{Li}^+(\text{OH}_2)_3 \text{OSi}(\text{OH})_2\text{-R}$].

In contrast, NH_4^+ has 4 strong hydrogen bonds with water oxygen or with oxygen of silica. During the 10ps simulation at 350K, we observed that there is a rapid rotation of ammonium in water. Figure 4.2 shows the rapid exchange position of two hydrogen atoms of ammonium cation.

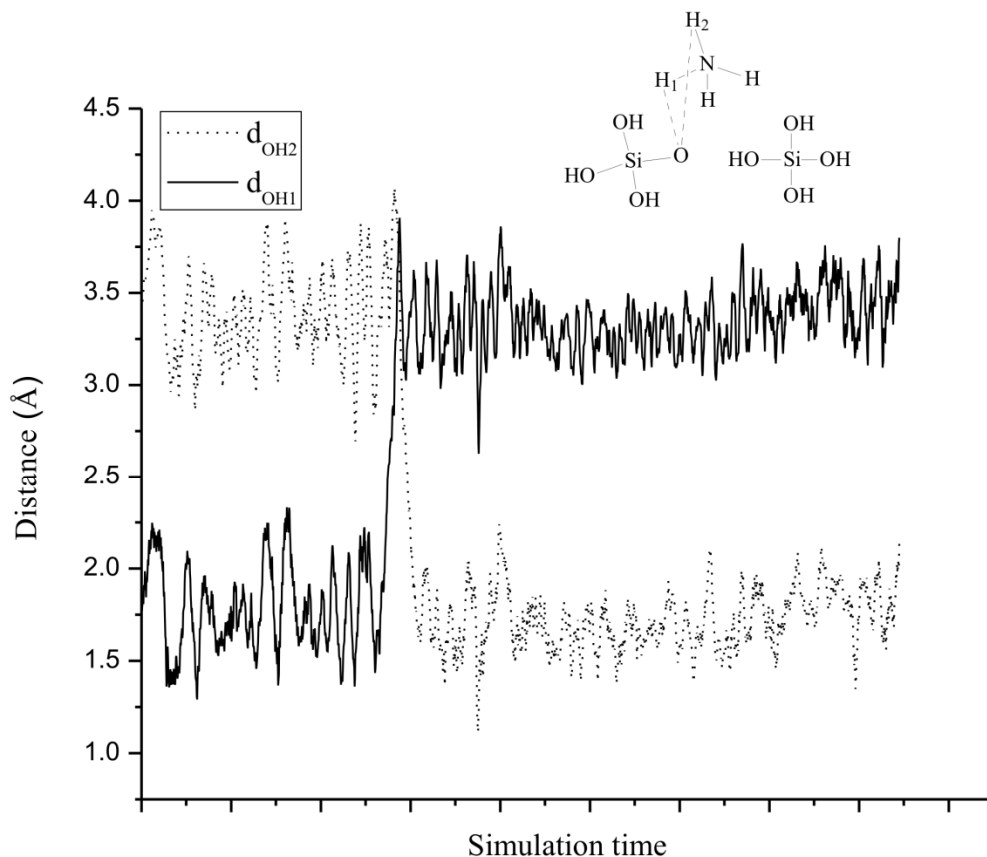


Figure 4.2: Rapid rotation of ammonium cation. The two hydrogen atom H1 and H2 exchange its position during the simulation.

4.3.2 Silica Oligomerization Reaction

A general accepted mechanism of silica condensation reaction in high pH consists of two steps. The first step is SiO-Si bond formation. During this step one oxygen atom of monomeric silicic acid connects with one silicon atom of another silicate to form a stable 5-silicon coordinated intermediate. The second step is water removal: one hydroxyl group will depart from the 5-silicon coordinated structure with a hydrogen transfer process occurring at the same time. The products are higher oligomeric silicates and one water molecule (Scheme 4.1).

Table 4.1: Calculated free energy (kJ/mol) for the condensation reactions forming dimer, linear trimer, 3-ring and branched tetramer via the anionic mechanism with presence of counter ion Li^+ and NH_4^+ at 350K. E_{act1} is the activation barrier of the SiO-Si bond formation step, E_{act2} is the activation barrier of the water removal step. The overall-barrier is the difference in energy between highest point and the lowest point along the reaction coordinates, ΔF is the reaction free energy (the difference in energy between the final state and the initial state). The unit of all calculated values is kJ/mol.

Cation/product of condensation reaction	E_{act1}	E_{act2}	E_{overall}	ΔF
Li^+				
Dimer	70	39	98	37
Trimer	78	46	108	56
3ring	83	44	111	80
Iso-tetramer	60	35	80	42
NH_4^+				
Dimer	106	35	120	75
Trimer	63	22	73	24
3ring	54	34	82	47
Iso-tetramer	62	42	88	50
Without cation ^{[45]*}				
Dimer	44	42	61	25
Trimer	43	33	53	25
3ring	35	48	72	41
Iso-tetramer	69	43	101	60

^[*] Simulation with the same size of system, Car-Parinello Molecular dynamics at 350K.

In our simulations, the initial state is defined as the configuration where one anionic oligomer has a hydrogen bond with one silicic acid monomer. In the case of dimerization, the reactant state contains one silicic acid and its deprotonated form. To prepare the simulation in an aqueous box,

the initial geometries of the silica species are taken from our previous gas phase simulations [27] and then solvated with 64 water molecules. After equilibration (1 ps) at 350 K by velocity scaling, the production run with 10 ps in the NVT ensemble with Nose-Hoover thermostats.

The free-energy profile of each step is obtained by integrating the calculated constraint force with the method described in the computation and details section. The first point and the last point of each step which have no constrained force applied are obtained after 10ps of production run. The first point of each step is taken as the reference to get the free energy integration of the reaction. Two steps are connected by the intermediate structure, where the final state of first step is the first state of the second step.

Silica oligomerization with Li^+ counter ion

This section will describe the mechanism and free energy profile of the silica condensation reaction to form dimer, trimer, 3-ring and iso-tetramer oligomer with Li^+ in solution as the counter ion.

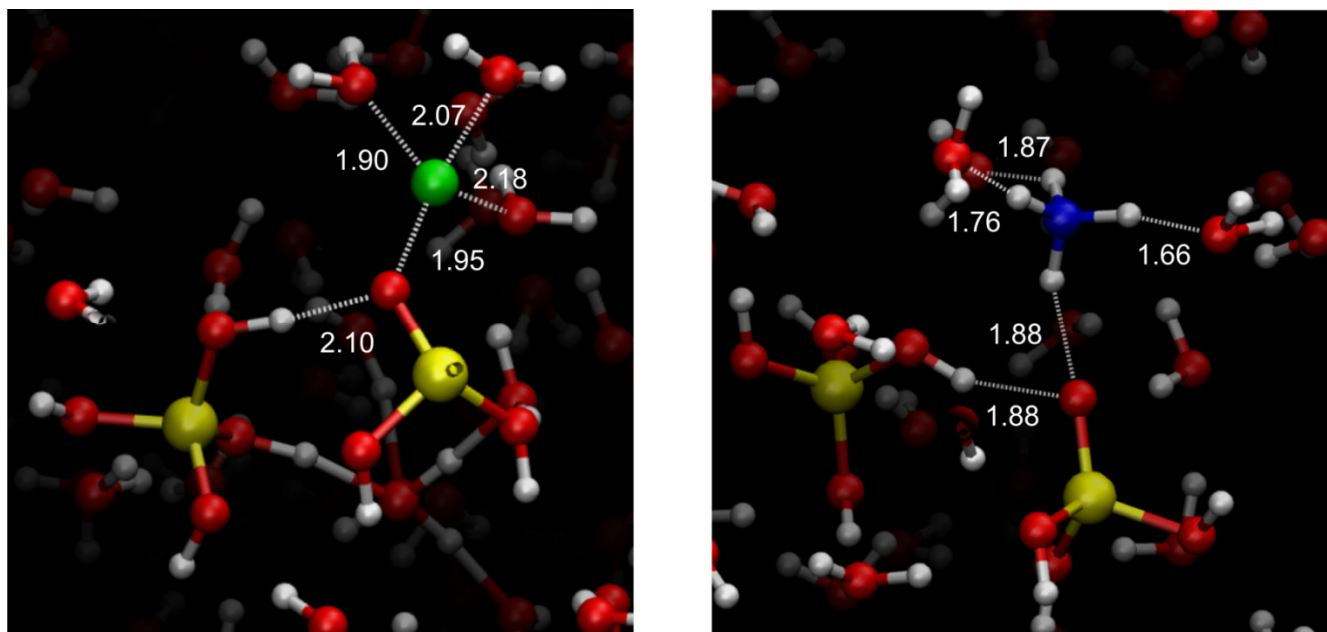


Figure 4.3: Snapshot of the system in reactant state in the case of dimer formation after 10ps of equilibrium. The number of coordination of Li^+ is 4 (a). NH_4^+ has 4 dynamic hydrogen-bond with water and silica species (b).

The initial silica geometry was taken from our previous gas phase simulation. After the silica structure is solvated with 64 water molecules, we generated a random position of cation Li^+ in the box and performed a equilibrium 15ps run. The trajectory and energy profile was checked to warranty that the system is in equilibrium state. A snapshot of the reactant state which is depicted

in Figure 4.3 shows that cation Li^+ has a coordination number of 4 (3 with water and 1 with silica). The distances between Li^+ and water oxygen and between Li^+ and oxygen of silica are comparable (around 2\AA).

The first step of the dimerization reaction mechanism is controlled by a constrained values of a SiO-Si distance as described in section 2. During the process, one oxygen atom of the monomer approaches the Si atom of another monomer. When the distance between two atoms is around 1.8\AA , then the bond OSi-O is formed between the two monomers. The product of this step is a 5-fold silicon which is generally observed in theoretical and experimental works. We observe that at 350K, the first activation barrier of dimerization is around 70 kJ/mol. In the case without cation, this first barrier of dimerization reaction is only 44 kJ/mol [45]. The higher energy may due to the electrostatic interaction of cation Li^+ . The positive charge of this cation may reduce the interaction of activate oxygen and silicon atom. Thus the attraction of $[\text{SiO}^\delta \dots \text{Si}^{\delta+}]$ will be less favourable for SiO-Si bonding. The second step of the dimerization reaction is a water cleavage process. This step is modelled by sampling the distance between the corresponding oxygen atom and silicon atom (Scheme 4.1). During the process, one hydrogen atom of silica will transfer to a hydroxyl group with the result a water cleavage of the 5-silicon coordinated structure to form the final product dimer. This dimer species will be a reactant for further oligomerization reaction. Figure 4.4 shows the calculated free-energy profile of the dimerization reaction with two activation barriers. Our previous calculations of this reaction with a continuous solvent model COSMO found a higher barrier for the second step compared to the first one. The reduction in relative barriers in the aqueous solution calculations compared to the gas phase values is due to the stabilization of the leaving hydroxyl by hydrogen bonds with solvent water molecules. In the continuum model solvent, individual interaction between water molecule and silica structure could not be observed. With the explicit model, the barrier of water removal step does not depends on the presence of cation Li^+ , the barrier is found comparable to that of the case without cation [45] (around 40 kJ/mol).

The trimerization reaction of one dimer silica and one monomeric silica has a similar mechanism. After the equilibrium, the position of cation Li^+ in reactant state is located quite far away from the negative centre of the silica (around 4\AA). The cation is preferred in the water solvent with 4 coordinators. During the SiO-Si formation step, the Li^+ does not approach the silica structure. The water removal step of trimerization reaction takes place with the same mechanism with that of dimerization reaction. The activation barriers of the first step and second step are 78 kJ/mol and 46 kJ/mol respectively (Table 4.1).

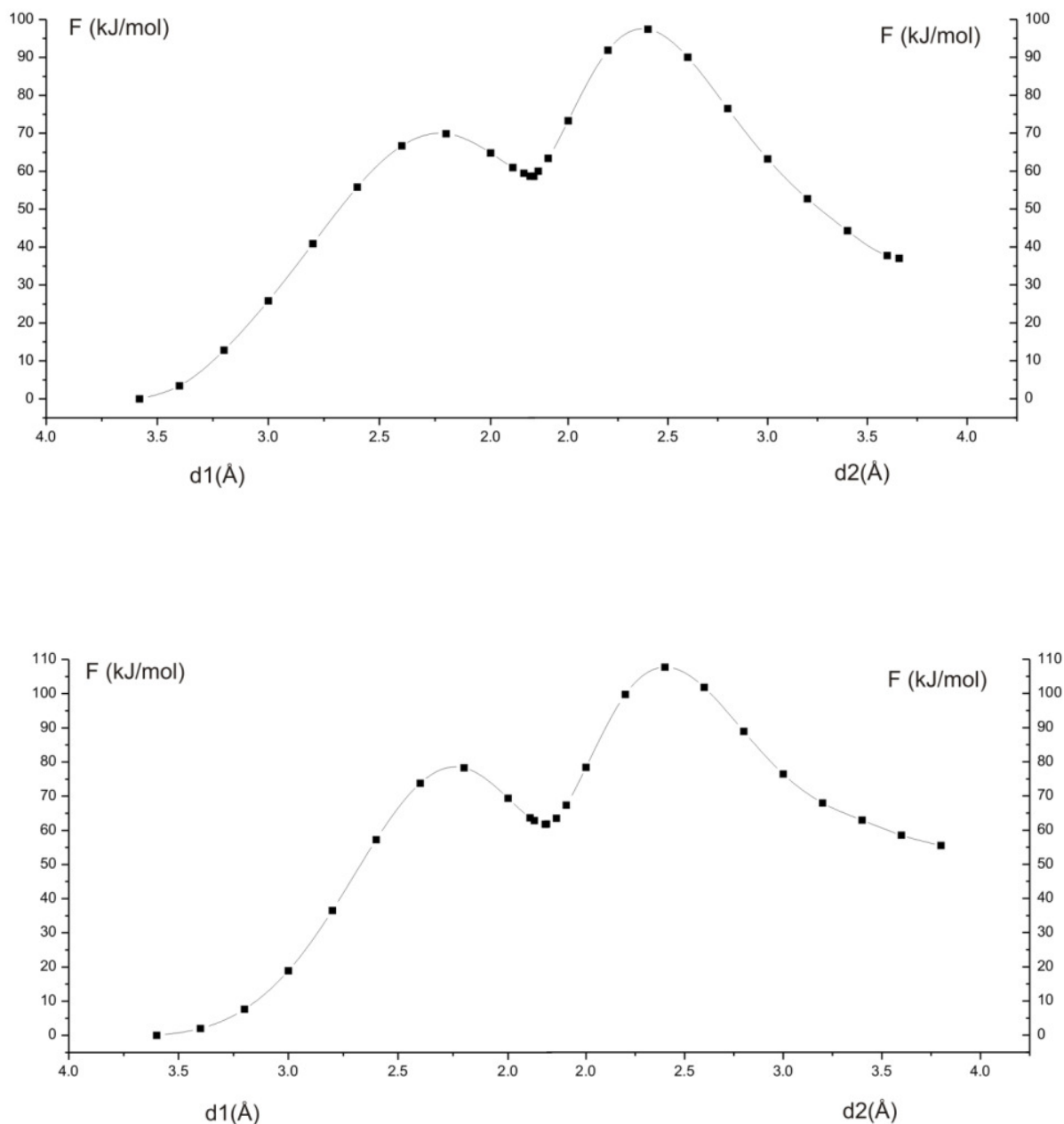


Figure 4.4 : Calculated free-energy profile along the reaction path of silica dimerization and trimerization in the case of cation Li^+ . The free-energy profile is obtained by integrating the connecting line through the calculated constraint force points.

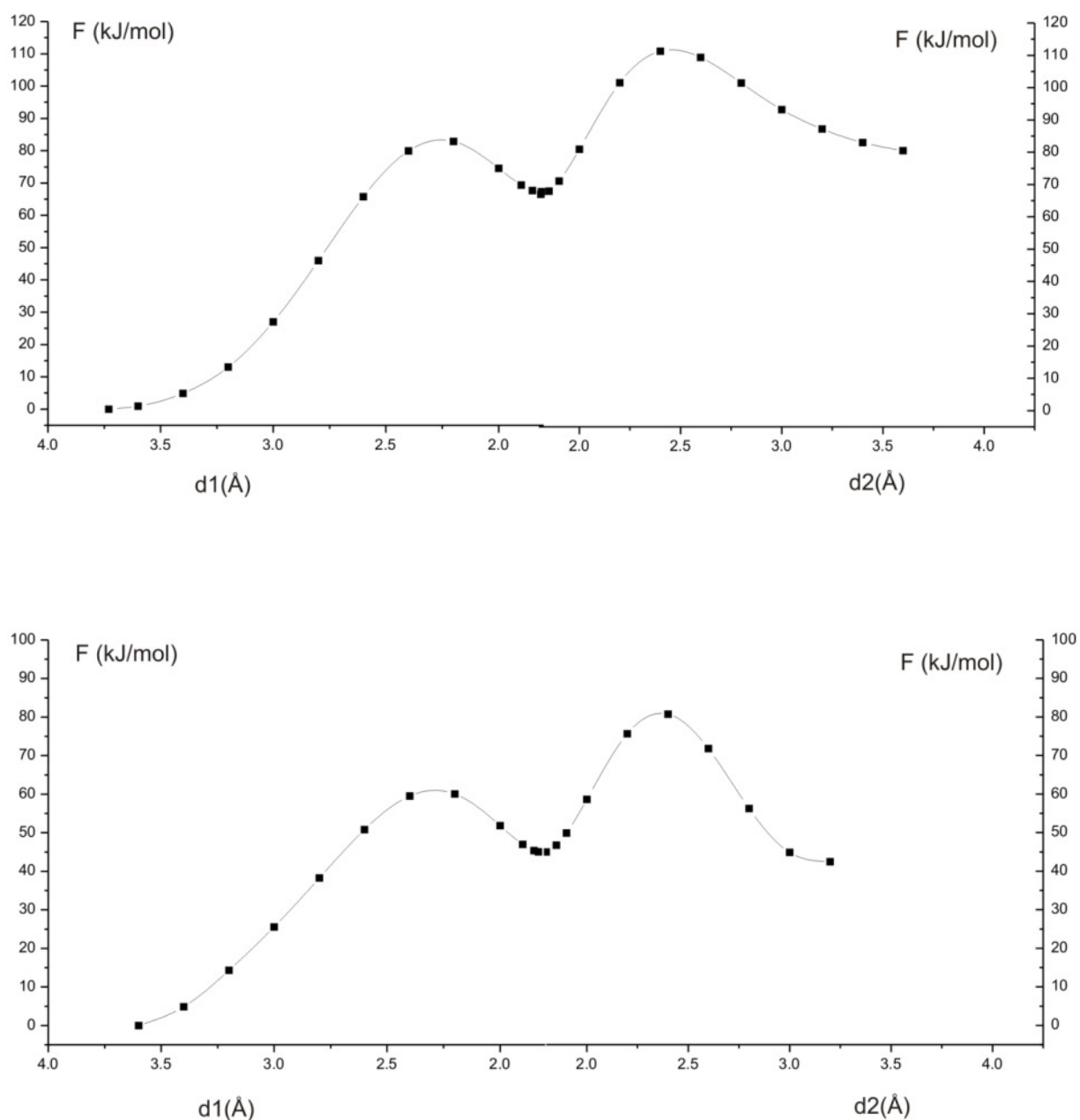


Figure 4.5 Calculated free-energy profile along the reaction path of 3-ring and branched tetramer formation in the case of cation Li^+ . The free-energy profile is obtained by integrating the connecting line through the calculated constraint force points.

Figure 4.5 provides the calculated free energy profile of the internal condensation reaction from linear trimer to form the three-ring silica. In this reaction, the SiO-Si bonding step provokes the conformations change of linear trimer. The simulation in gas phase reported a high activation barrier due to the loss of internal hydrogen bonding [27]. In solution without cation, a lower

barrier is found for the initial SiO-Si bond formation step [45] because of the external hydrogen bond of water compensate for the loss of internal hydrogen bond. A higher activation energy is found with the case of cation Li^+ . This may come from the different reorganization of hydrogen bonding around silica when Li^+ is present. The barrier of the first step of 3-ring closure is even higher than that of the dimerization and trimerization reaction. For the cyclic trimer formation the water removal step is similar to the case of dimerization with a low barrier (44 kJ/mol).

From the linear trimer the further oligomerization reaction can proceed to form a branched tetramer with a very comparable mechanism with dimerization and trimerization reaction. Figure 4.5 gives a picture of the free energy profile of the branched tetramer formation. Compared to silica structures containing 3-silicon (linear trimer and 3-ring), the branched tetramer has a slightly lower activation barrier for the first step, SiO-Si bond formation. The water removal step of the branched tetramer formation is comparable that step of the 3-ring. In the case of Li^+ , linear trimer is preferred to react further to higher oligomer than to create a ring structure.

Silica oligomerization with NH_4^+ counter ion

The oligomerization mechanism of silica in solution with NH_4^+ follows the mechanism in scheme 4.1. NH_4^+ and Li^+ both have a single charge. There are different effects of these two cations on the activation barrier of silica condensation. This may come from the dissimilar role of the cations in the hydrogen bond network of water around silica structure. NH_4^+ can provide 4 strong hydrogen-bonding meanwhile Li^+ is not involved in reconstructing the water hydrogen bond network .

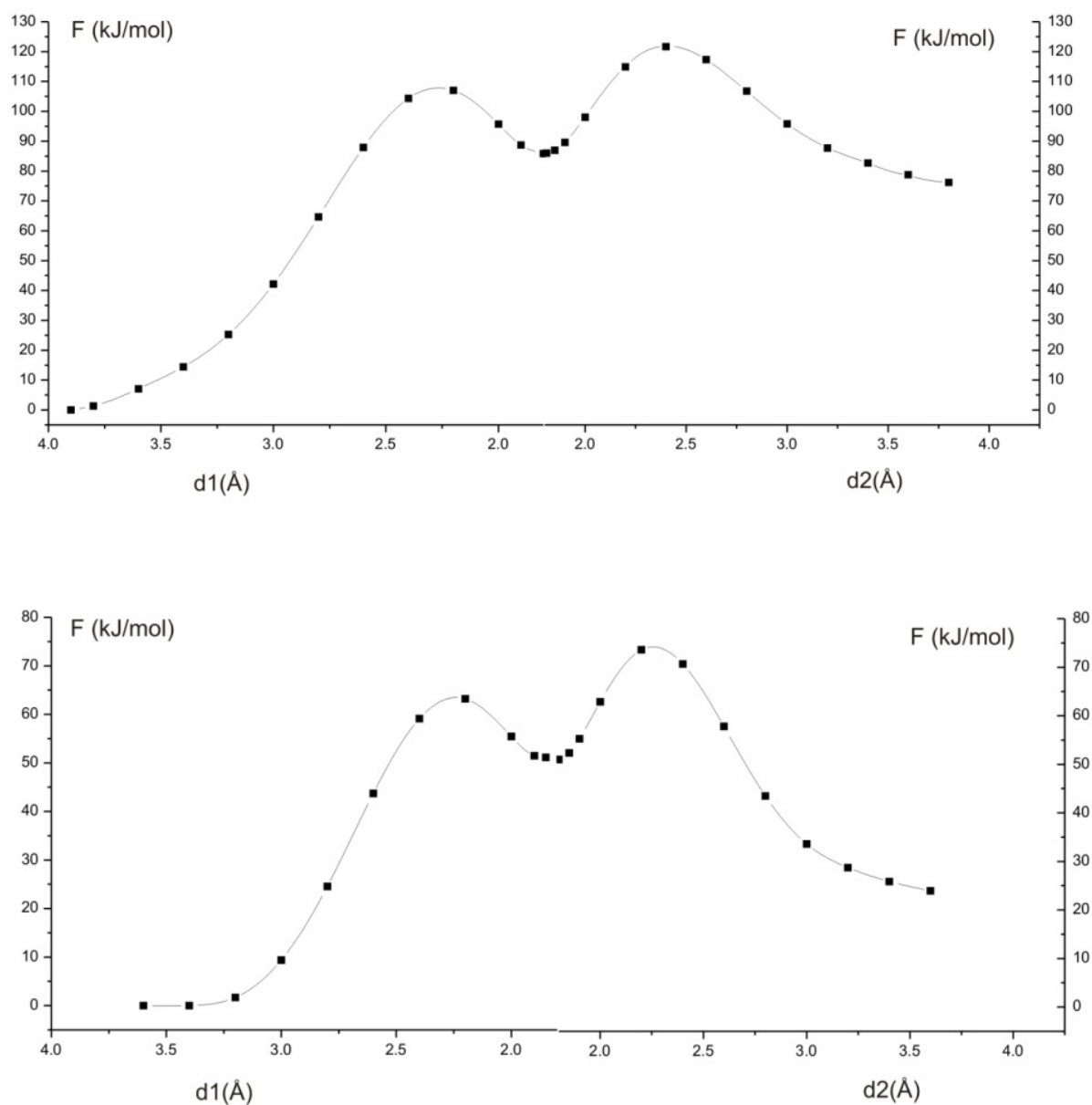


Figure 4.6: Calculated free-energy profile along the reaction path of silica dimerization and trimerization in the case of cation NH_4^+ . The free-energy profile is obtained by integrating the connecting line through the calculated constraint force points.

The initial position of cation NH_4^+ is also randomly generated around the negative centre of silica. A snapshot of the reactant state of dimerization reaction with NH_4^+ counter ion is depicted in Figure 4.3. The cation has a hydrogen-bonding with an oxygen atom of silica. The other 3 hydrogen-bonds are with water molecules. These interactions are strong with a short distance

around 1.8-1.9Å. When the dimerization reaction take place, one monomer will approach the other monomer and a new SiO-Si bond will be made. We observed that the position of NH_4^+ changes according the reaction coordinate. The movement of NH_4^+ is not only a translation but also a rapid rotation. During the first step of dimerization, the deprotonation of NH_4^+ is not observed. A snapshot of the transition state is presented in Figure 4.7. We noticed that the ammonium cation has an interaction with the reactive centre by a hydrogen-bonding. In this situation, NH_4^+ will weaken the internal hydrogen bond between the two monomers in the transition state. The activation barrier of SiO-Si bond formation in the case of NH_4^+ (106 kJ/mol) is higher than the case of Li^+ (70 kJ/mol). The water removal step is assisted by water molecule similarly as in the Li^+ case.

Compared to the dimerization reaction, further oligomerization to the linear trimer from the dimer silica has a lower first step activation barrier (only 63 kJ/mol). The initial position of the ammonium cation is now quite far away from the negative centre. It prefers to stay in the water phase with 4 hydrogen bonds with water molecules. This may due to the fact that the negative charge is more delocalized in the dimer than in the monomer. Thus, the electrostatic attraction of the dimer with NH_4^+ is less important. During the first step, the position of NH_4^+ remains far away from the silica. Figure 4.7 shows that in the case of trimerization, the transition state of SiO-Si bond formation step is not effected by the cation NH_4^+ . The distance between cation and silica oxygen is too large. After the water removal step with a barrier of 22 kJ/mol, the linear trimer is formed.

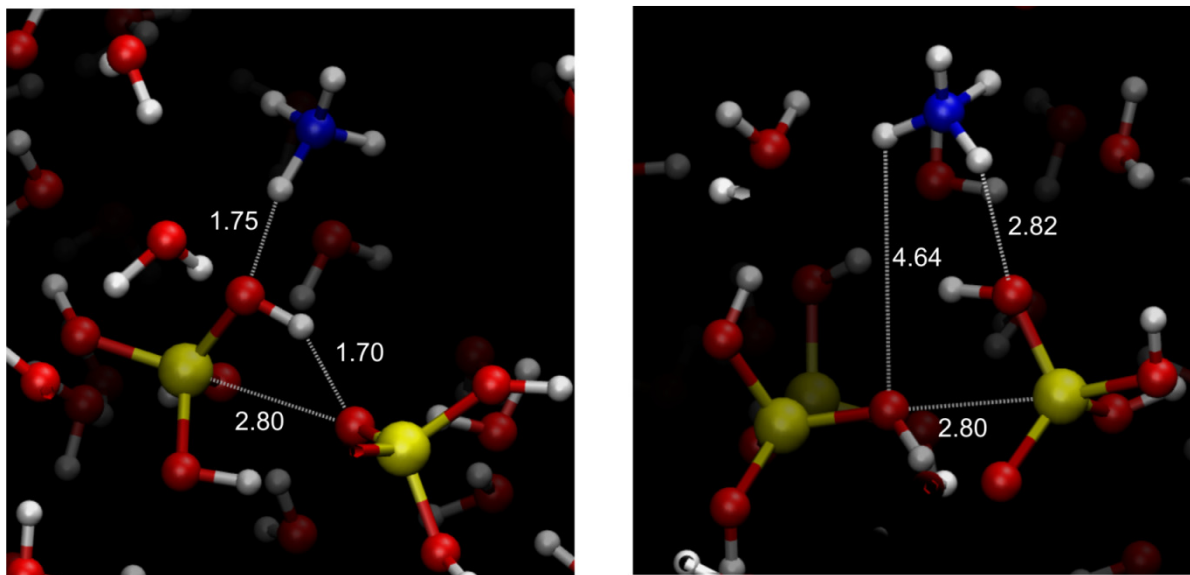


Figure 4.7: Snapshot of the system near the transition state in the case of NH_4^+ after 10ps of production run. In dimerization reaction, ion NH_4^+ stays close to the reactive center and have a

hydrogen-bonding with oxygen of silica structure (a). In trimerization reaction, the position of NH_4^+ is far away from the reactive center and does not have a hydrogen-bonding with silica structure (b). In both pictures, hydrogen bonding with water is not shown for a better visibility.

The 3-ring closure reaction from the linear trimer was also investigated. Figure 4.8 depicts the energy profile of this process. The results show that it is more favourable to form a SiO-Si bond than in the case of dimerization and trimerization. In this step, the conformation of linear trimer has to be changed to a more cyclic shape in order to complete ring closure. Simulation in gas phase gave a high activation energy due to loss of internal hydrogen [27]. In solution, water molecules can enhance the conformation change by providing more hydrogen bonds with silica trimer. In the case of Li^+ , there is no hydrogen bond effect to the water structure and this barrier is still a high value (83 kJ/mol). With NH_4^+ , the transition state structure is even more stabilized, activation barrier is only 54 kJ/mol.

The further oligomerization reaction can proceed to form a branched tetramer following the anionic mechanism in scheme 4.1. Figure 4.8 gives a picture of the free energy profile of the process. The branched tetramer formation has a comparable activation barrier as the trimer formation but slightly higher than 3-ring closure. Thus, in the case of NH_4^+ the linear trimer is preferred to closure of the ring than to react further to branched tetramer.

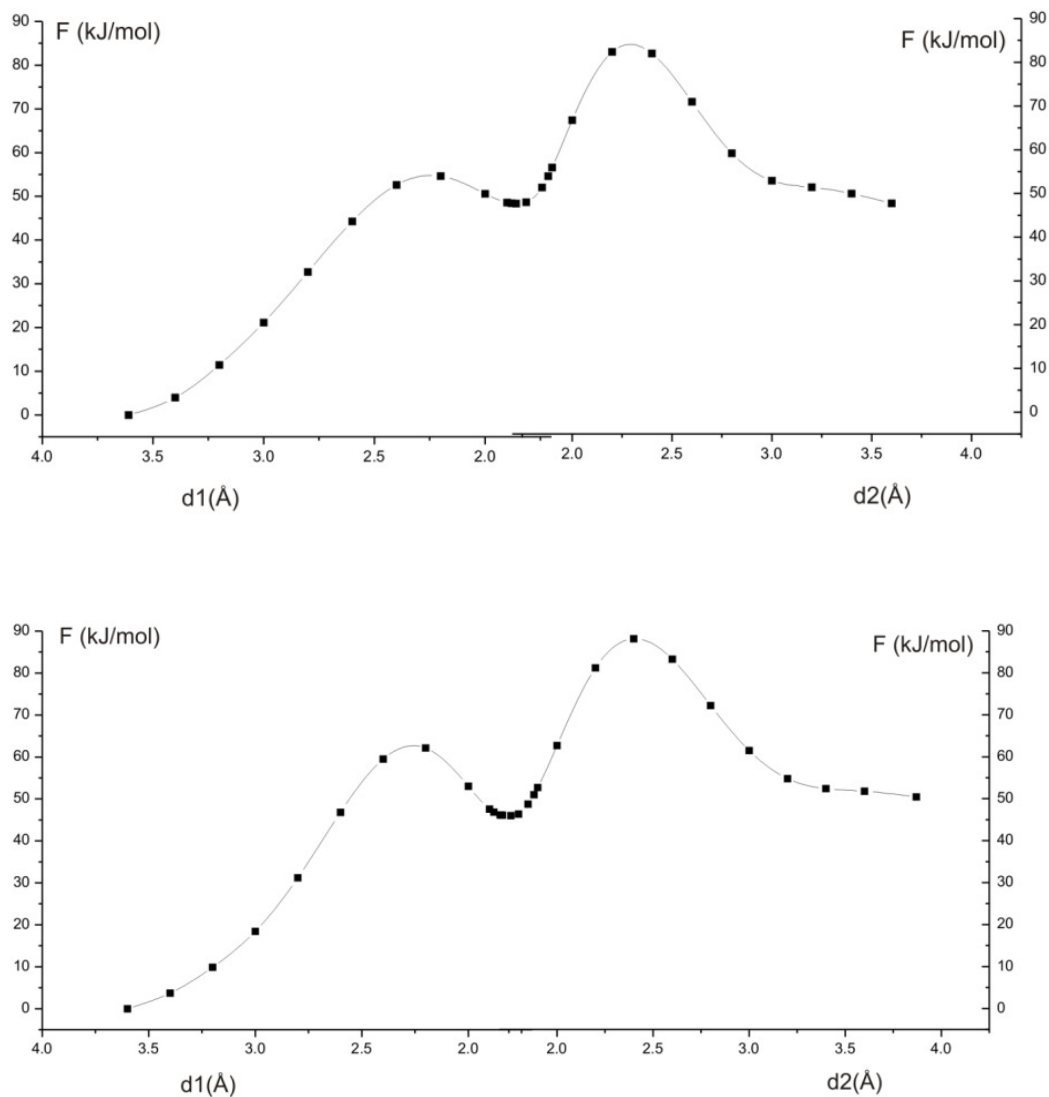


Figure 4.8 Calculated free-energy profile along the reaction path of 3-ring and branched tetramer formation in the case of cation NH_4^+ . The free-energy profile is obtained by integrating the connecting line through the calculated constraint force points.

4.4. DISCUSSION

Using ab-initio molecular dynamics, we investigated the anionic mechanism of the silica condensation reaction in the presence of counter ions Li^+ and NH_4^+ respectively. The results illustrate the importance of electrostatic versus hydrogen bonding effects for a reaction in the water phase.

Without cation, the activation barrier of SiO-Si bond formation has been found to have a low value (~ 40 kJ/mol) [45]. In this study, the positive charge Li^+ and NH_4^+ reduces the interaction $[\text{SiO}^\delta-\text{Si}^{\delta+}]$. This is the reason for the increase of the activation barrier of the first reaction step of the dimerization process.

Reorganization of the water structure is mainly controlled by hydrogen bonding. It has an considerable effect on the relative stabilities of silica species in solution especially the transition state structures. The first activation barrier strongly depends on the hydrogen bonding effects. In the transition state of dimerization, the position of Li^+ is very close to the silica centre ($\sim 2\text{\AA}$) but there is no hydrogen bonding to the reactive oxygen. Its presence only slightly increases the activation barrier of SiO-Si bond formation of the silicate anion. In contrast, NH_4^+ has a strong hydrogen bond with this reactive oxygen (Figure 4.3). It increase significantly the activation barrier. For the first step of the dimerization reaction, the hydrogen bonding effects are more important than the electrostatic interaction.

Table 4.2: Average distance (\AA) between cation M^+ (M is Li or NH_4) and active oxygen in the reactant state and near transition state during the first step of oligomerization reaction.

Reaction	Li^+		NH_4^+	
	Reactant	Transition state	Reactant	Transition state
Dimerization	2.01	1.92	3.07	1.75
Trimerization	3.80	4.15	6.15	5.20
3-ring formation	4.15	4.07	3.93	5.11
Branched tetramer formation	5.59	5.83	5.46	5.27

As mentioned the electrostatic interaction dominates for Li^+ , for NH_4^+ hydrogen bonding type interactions dominate. The influence of the cation is only significant when the position of cation is near the reactive centre. In consecutive oligomerization reaction steps, the ammonium cation only weakly interacts with silica oxygen atom involved in the formation of new bond. As a consequence, in the presence of ammonium the activation barriers of higher oligomerization reaction are much lower than the dimerization reaction. Our results imply that the relative rate of higher oligomer formation is larger in the case of NH_4^+ compared to Li^+ .

When we compare formation of ring structure oligomers we found that the activation barrier for three ring formation in the presence of NH_4^+ is lower than formed in the presence of Li^+ . Oligomer ring structures are experimentally observed in the silica oligomerization reaction in the presence of organic base [4-14].

Table 4.1 summarizes the thermodynamic property of all oligomerization reaction. According to experimental studies and MP2 calculations [46] TΔS of one hydrogen bond of a water dimer at 373K is around -30 kJ/mol. In this study one water molecule is produced in silica condensation reaction. This indicates that the water molecule arrangement is important. The total free energy of reaction is unfavorable due to reorganization of waters which has an important contribution to the entropy of the system. This remark is consistent with the previous simulation in water phase[45] (chapter3).

4.5. CONCLUSIONS

In this paper, we use ab-initio molecular dynamic simulation with a model including explicitly water molecules and counter ion (Li^+ and NH_4^+) to investigate the silica condensation reaction. The rate limiting step is not the water removal step as in the gas phase simulation [27]. The activation barrier of the water removal step depends only on the water assisted, which is independent of the size of oligomer. The overall barrier mostly depends on the initial barrier of the SiO-Si bond formation. The position of cation has a strong effect on the barrier height of this step. When close to the reactive center of the dimerization reaction, Li^+ does not change strongly the activation barrier, meanwhile NH_4^+ increase significantly the activation barrier.

The relative rates of formation of the higher oligomers from dimer silica are found to be quite different between Li^+ and NH_4^+ case. The presence of Li^+ favor the linear and branched higher silica structure over the 3-ring. In contrast, with NH_4^+ in solution we observed that 3-ring formation is more favorable than the formation of higher branched silica oligomers.

In conclusion, our results show that it is essential to include explicitly the counter ion in silica condensation computational studies. The positive charge of counter ion increases the rates of SiO-Si bond formation. For the first step of the dimerization reaction, the hydrogen bonding effects are more important than the electrostatic interaction. In consecutive oligomerization reaction steps, the cation has a weak effect on activation barrier. The unfavourable thermodynamics is mainly due to changes in water entropy that results from water molecules arrangement.

REFERENCES

1. C. J. Brinker and G. W. Scherer, Academic Press, Boston, 1990.
2. R. K. Iler, *The Chemistry of Silica*, John Wiley & Sons New York, 1979.
3. C. S. Cundy and P. A. Cox, *Chem. Rev.*, 2003, **103**, 663-702.
4. C. T. G. Knight and S. D. Kinrade, *J. Phys. Chem. B*, 2002, **106**, 3329-3332.
5. C. E. A. Kirschhock, R. Ravishankar, F. Verspeurt, P. J. Grobet, P. A. Jacobs and J. A. Martens, *J. Phys. Chem. B* 2002, **106**, 3333.
6. A. R. Felmy, H. Cho, J. R. Rustad and M. J. Mason, *Journal of Solution Chemistry*, 2001, **30**, 509-525.
7. P. P. E. A. de Moor, T. P. M. Beelen, R. A. van Santen, L. W. Beck and M. E. Davis, *J. Phys. Chem. B*, 2000, **104**, 7600-7611.
8. P. P. E. A. de Moor, T. P. M. Beelen, R. A. van Santen, K. Tsuji and M. E. Davis, *Chem. Mater.*, 1999, **11**, 36-43.
9. C. E. A. Kirschhock, R. Ravishankar, F. Verspeurt, P. J. Grobet, P. A. Jacobs and J. A. Martens, *J. Phys. Chem. B*, 1999, **103**, 4965-4971.
10. P. Bussian., F. Sobott., B. Brutschy, W. Schrader and F. Schüter, *Angewandte Chemie*, 2000, **39**, 3901-3905.
11. S. A. Pelster, W. Schrader and F. Schuth, *J. Am. Chem. Soc.*, 2006, **128**, 4310.
12. S. L. Burkett and M. E. Davis, *Chem. Mater.* , 1995, **7**, 920.
13. S. L. Burkett and M. E. Davis, *Chem. Mater.* , 1995, **7**, 1453.
14. S. L. Burkett and M. E. Davis, *Chem. Mater.* , 1994, **98**, 4647.
15. J. D. Rimer, O. Trofymlyuk, R. F. Lobo, A. Navrotsky and D. G. Vlachos, *J. Phys. Chem. C*, 2008, **112**, 14754-14761.
16. J. C. G. Pereira, C. R. A. Catlow and G. D. Price, *J. Phys. Chem. A*, 1999, **103**, 3252-3267.
17. J. C. G. Pereira, C. R. A. Catlow and G. D. Price, *J. Phys. Chem. A*, 1999, **103**, 3268-3284.
18. J. C. G. Pereira, C. R. A. Catlow and G. D. Price, *Chem. Commun*, 1998, 1387.
19. J. A. Tossell, *Geochimica et Cosmochimica Acta*, 2005, **69**, 283-291.
20. M. J. Mora-Fonz, C. R. A. Catlow and D. Lewis, *Angew Chem. Int. Ed.*, 2005, **44**, 3082.
21. Y. T. Xiao and A. C. Lasaga, *Geochim. Et Cosmo Acta* 1996, **60**, 2283.
22. L. J. Criscenti, J. D. Kubicki and S. L. Brantley, *J. Phys. Chem. A*, 2006, **110**, 198-206.
23. A. Pelmenschikov, J. Leszczynski and L. G. M. Pettersson, *J. Phys. Chem. A*, 2001, **105**, 9528-9532.
24. J. C. G. Pereira, C. R. A. Catlow, G. D. Price and R. M. Almeida, *J. Sol-gel Science and Technology*, 1997, **8**, 55.
25. N. Z. Rao and L. D. Gelb, *J. Phys. Chem. B*, 2004, **108**, 12418-12428.
26. J. R. B. Gomes, M. N. D. S. Cordeiro and M. Jorge, *Geochimica et Cosmochimica Acta*, 2008, **72**, 4421-4439.
27. T. T. Trinh, A. P. J. Jansen and R. A. vanSanten, *J. Phys. Chem. B*, 2006, **110**, 23099-23106.
28. M. J. Mora-Fonz, C. R. A. Catlow and D. W. Lewis, *J. Phys. Chem. C*, 2007, **111**, 18155-18158.
29. C. R. A. Catlow, D. S. Coombes, D. W. Lewis and J. C. G. Pereira, *Chem. Mater.*, 1998, **10**, 3249-3265.
30. VandeVondele, J.; Krack, M.; Mohamed, F.; Parrinello, M.; Chassaing, T.; Hutter, J. *Comp. Phys. Comm.* 2005, **167**, 103.
31. <http://cp2k.berlios.de>. CP2K developers home page, October 23, 2007.
32. Lippert, G.; Hutter, J.; Parrinello, M. *Mol. Phys.* 1997, **92**, 477.
33. Sulpizi, M.; Rauegi, S.; VandeVondele, J.; Carloni, P.; Sprik, M. *J. Phys. Chem. B* 2007, **111**, 3969.
34. Goedecker, S.; Teter, M.; Hutter, J. *Phys. Rev. B* 1996, **54**, 1703.

35. Hartwigsen, C.; Goedecker, S.; Hutter, J. *Phys. Re .B* 1998, 58,3641.
36. Becke, A. D. *Phys. Re .A* 1988, 38, 3098.
37. Lee, C.; Yang, W.; Parr, R. G. *Phys. Re .B* 1988, 37, 785.
38. VandeVondele, J; Hutter, J *Chem Phys*, **2007**, 127 , 114105
39. Hoover, W. G. *Phys. Re .A* 1985, 31, 1695.
40. Carter, E. A.; Ciccotti, G. J.; Hynes, T.; Kapral, R. *Chem. Phys. Lett.* **1989**, 156, 472.
41. Humphrey, W., Dalke, A. and Schulten, K., "VMD - Visual Molecular Dynamics", *J. Molec. Graphics*, 1996, vol. 14, pp. 33-38. <http://www.ks.uiuc.edu/Research/vmd/>
42. Mischler, C.; Horbach, J. R.; Kob, W.; Binder, K. *J. Phys. Condens. Matter.* **2005**, 17, 4005
43. H. H. Loeffler and B. M. Rode, *J. Chem. Phys* 2002, **117**, 110.
44. S. Varma and S. B. Rempe, *Biophysical Chemistry*, 2006, **124**, 192.
45. T. T. Trinh, A. P. J. Jansen, R. A. van Santen and E.J. Meijer. *Phys Chem Chem Phys* 2009 (accepted)

46. Leonid, O.; Gorb, I.; Leszczynskij, J. *J. Comput. Chem.* **2007** 28, 1598

CHAPTER 5

Catalytic role of Tetrapropylammonium in silica oligomerization reaction

The mechanism of the oligomerization reaction of silica, the initial steps of silica formation with presence of organic compound tetrapropylammonium cation (TPA^+), has been studied by quantum chemical techniques. The solvent effect is included using the COSMO model. The formation of various oligomers (from dimer to 3-ring) with interaction of TPA^+ was investigated. The calculations show that TPA^+ has a catalytic role to enhance the first step of the anionic oligomerization mechanism which is the formation of the SiO-Si linkage between the reactants to form a five-coordinated silicon complex. TPA^+ also stabilize the oligomer structure, hence the condensation reaction is more favorable with the presence of organic compound.

5.1 INTRODUCTION

The silica condensation reaction is an essential elementary reaction step of sol-gel chemistry [1,2] and zeolite synthesis [3]. Understanding how zeolites nucleate and grow is of fundamental scientific and technological importance. Numerous experimental [4-15] and theoretical [16-31] studies have been devoted to investigate the silicate oligomers that occur in the pre-nucleation process of siliceous zeolite.

Various experimental techniques can be used to reveal the structural information about species in solution and nucleation processes. During the first hours of sol-gel reactions, various silicate oligomers are formed in solution. They can be dimers, trimers, tetramers, 3-rings, 4-rings, double 3-rings, double 4-rings or other larger oligomer. The dominant species depends sensitively on reaction conditions, solvent used and presence or absence of structure directing agent (SDA).[9,10] Pelster et al.[11] were able to track the evolution of different silica species undergoing condensation reactions in aqueous solutions. Using electrospray mass spectrometry (ESI MS) in conjunction with three different reactor systems, they were able to follow the growth of silica oligomers in solution. Burkett et al.[12–14] showed that using different ammonium salts as templating agents lead to different products. They identified the cubic octamer, prismatic hexamer, and cyclic-trimer as the predominate products when using TMA^+ , TEA^+ , and TPA^+ respectively. Recently, Rimer et al.[15] studied silica nanoparticle formation using microcalorimetry to measure the heats of reaction evolved from the addition of tetraethylorthosilicate (TEOS) to basic aqueous solutions of monovalent cations. They claimed that Na^+ , TMA^+ and TBA^+ behave similarly, while changes in the magnitude of enthalpy for TPA^+ solutions are 4 times larger. TPA^+ affects the enthalpy of nanoparticle formation. It is known that solutions of Na^+ , TMA^+ , and TBA^+ hydroxides do not lead to silicalite-1 formation, while those of TPA^+ do selectively generate the MFI framework type of silicalite-1.

Theoretical modeling of zeolite synthesis has proven to be a challenging task. Many different approaches have been used to date, using both quantum chemical and classical molecular mechanics techniques. Many electronic calculations [16-28] have been performed to reveal information about the mechanism of the elementary reaction in pre-nucleation stage. A study on the energies of the dimerization reaction of mono-silicic acid was reported by Tossel [19]. Using the COSMO solvent model, the author studied the free energy of reaction changes by varying temperature and dielectric constants of the solvent. The author found that the condensation reaction is more favorable at high temperature than at room temperature. Free energies of the

silica condensation reaction have been recently presented by Mora-Fonz et al. [20, 28] The authors found that the formation of the small ring fragment is thermodynamically favorable in high pH media. In different pH of solution, the silica condensation reaction has a different mechanism and activation barrier [27, 30]. It is generally accepted that the reaction occurs in high pH solution with an anionic mechanism is more favorable with a lower activation barrier [27, 28] Catlow et al. [29] have carried out MD simulations of silica precursors and a structure directing agent. They found that long range electrostatic interactions are of crucial importance. Without these interactions, the investigated complexes tended to dissociate rather than agglomerate.

However, there is still a glaring lack of insight into the exact role of the template molecules during the pre-nucleation stages of zeolite synthesis. Organic compound provide an electrostatic stabilization to silicate structures [29,31] but the contribution of weak Van-der-Waals interaction can also be important. Here we address the anionic reaction pathway with interaction of TPA⁺ presence. The MP2 approximation is applied in order to evaluate a VdW force between TPA⁺ and anionic silica fragment in the system.

5.2 COMPUTATIONAL DETAILS

In this chapter, Density Functional Theory (DFT) with the B3LYP [32] hybrid exchange-correlation functional and MP2 quantum method were used. The B3LYP method has been reported to provide excellent descriptions of various reaction profiles and particularly of geometries and vibrational properties of various molecules [33]. An accurate energy for the reaction in solution is formed from the equation (5.1):

$$\Delta E_{sol} = \Delta E_{gas} + \Delta ZPE + \Delta G_{solvation} \quad (5.1),$$

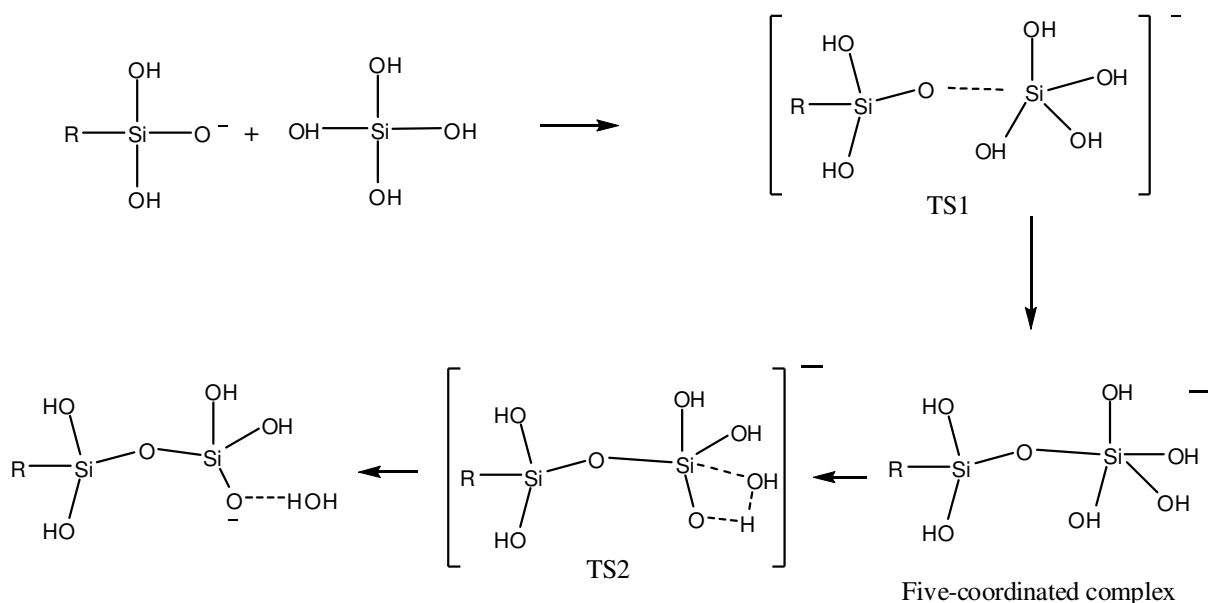
Where: ΔE_{sol} is the total energy in solution, ΔE_{gas} is the energy in gas phase calculation, ΔZPE is the zero point energy and $\Delta G_{solvation}$ is the solvation energy.

Geometry optimization and saddle point searches were all performed using the Gaussian 03 program[34]. The basis set used to expand the molecular orbital were all electron type 6-31+G(d,p). For all the systems considered we have determined equilibrium geometries in gas-phase and have evaluated vibrational frequencies. The transition states were obtained by requiring that one and only one of the eigenvalues of the Hessian matrix is negative. The solvation effect was included using the continuum solvation COSMO method implemented in GAUSSIAN03 package. The COSMO method has been reported to be an appropriate approach for studying the

silica reaction in solution[20-28]. The solvation energy and zero point energy were evaluated with B3LYP/6-31+G(d,p). The gas phase energy was obtained by a single point calculation of the MP2 level with triple zeta basis set 6-311G(d,p) using GAMESS –UK [35] program version 7.0 (except stated otherwise). This is an improvement of the method. The larger basis set is crucial for systems containing organic and inorganic species to compute the VdW contribution to the energy. To perform a MP2 calculation for such a system with more than 50 atoms almost reaches the limit of quantum computational chemistry at the present time. For investigating further oligomerization reaction of silica in contact with TPA^+ , this conventional MP2 method can not be applied.

For some species we calculated equilibrium geometries within the polarized continuum solvent model –COSMO. However, the change in bond distances in the COSMO optimization was always less than 0.01 Å. Therefore, we decided to use only the gas-phase equilibrium geometries in COSMO energy calculations, without reoptimizing the geometries

The calculations were performed on silica clusters with according to the anionic mechanism as sketched in scheme 5.1. This scheme illustrates the anionic mechanism; the polymerization reaction is initiated by a silicate anion. The monomer $\text{Si}(\text{OH})_4$ is added step by step into the chain by condensation reactions.



Scheme 5.1: Anionic mechanism of the silica condensation reaction. R = H, $(\text{OH})_3\text{Si}-[\text{Si}(\text{OH})_2]_n-$ (n=0-2).

We defined the overall-barrier as the difference in energy between the highest transition state and the initial complex formed that leads to the first transition state intermediate.

5.3 RESULTS

5.3.1 Interaction of TPA and silica

In a high pH environment, neutral monosilic acid is not thermodynamically favorable compared to its deprotonated form $\text{Si}(\text{OH})_3\text{O}^-$. In our calculations, tetrapropylammonium cation TPA^+ is positively charged. In the gas phase, obviously the main interaction of TPA^+ and anionic silica is electrostatic. In solution, the solvation energy can have an important effect to the relative stabilities of chemical compounds.

The anionic monomer has two possible ways of adsorption on the surface of TPA^+ . The geometries of these two structures are depicted in Figure 5.1. One structure has a short distance between the free oxygen atom and nitrogen atom of TPA^+ (Fig 5.1.A), in the other structure this distance is long (Fig 5.1.B).

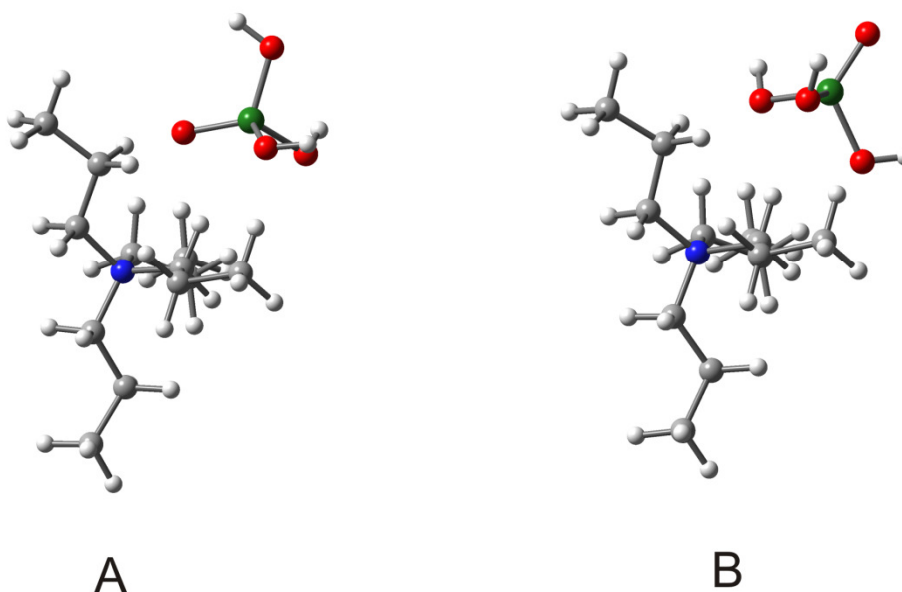


Fig 5.1. The two interaction structures between TPA^+ and anionic monomer of silica.

In the gas phase, the interaction between TPA^+ and anionic silica (Fig 5.1) has a very strong contribution of the electrostatic attraction. The closer the distance between the nitrogen atom and the oxygen atom is, the larger the electrostatic attraction. The interaction energy of structure *Fig.1 A* is 60 kJ/mol favorable compared with that in *Fig.1 B*. When the silicic acid is neutral, there is a major reduction of electrostatic energy. The coupling energy between TPA^+ and neutral monomer is only -33 kJ/mol, while that value between TPA^+ and anionic monomer is -322 kJ/mol. However, in solution each individual fragment has a favorable solvation energy because of its charged nature. This is the reason that the coupling process is not thermodynamic favorable in solution.

Table 5.1. Interaction Energy (kJ/mol) between TPA^+ and monomer silica calculated with various computational method and basis set. Energies have been corrected for the Basis Set Error Superposition (BSSE) with the counterpoise method [36]. The value in parentheses is for gas phase energy.

Method & basis set	B3LYP/6-31+g(d,p) COSMO (Gas)	B3LYP/6-311+g(2d,2p) COSMO (Gas)	MP2/6-311G(d,p) COSMO (Gas)	MP2/6-311+G(2d,2p) COSMO (Gas)	MP2/cc-pvtz COSMO (Gas)
$\text{M}^- + \text{TPA}^+ \rightarrow \text{TPA}^+ \dots \text{M}^-$ (A)	28 (-361)	33 (-354)	14 (-373)	11 (-376)	4 (-383)
$\text{M}^- + \text{TPA}^+ \rightarrow \text{TPA}^+ \dots \text{M}^-$ (B)	30 (-322)	38 (-314)	13 (-339)	13 (-339)	8 (-344)
$\text{M} + \text{TPA}^+ \rightarrow \text{TPA}^+ \dots \text{M}$	22 (-33)	28 (-26)	13 (-41)	12 (-42)	11 (-44)

The interaction energy obtained with various basis set for B3LYP and MP2 method is presented in Table 5.1. The size of the basis set is not a critical issue to calculate the energy implicating that all basis sets are large enough. The gas phase energy evaluated with the B3LYP method is always less favorable by 20 kJ/mol compared to the MP2 method. This results implies that B3LYP is not a good enough method to investigate the structure containing Van-der-Waals interactions, which is generally observed by other theoretical studies. In order to evaluate the energy of reaction, the MP2 level is an essential computational requirement to study the initial stage of the silica oligomerization with presence of organic compound.

5.3.2 Dimerization reaction

In high pH environment, the dominant silicate species will be anionic. Thermodynamic calculations show that in solution the OH⁻ ion will deprotonate the monomeric species to form mono-charged anion Si(OH)₃O⁻ [20]. These two monomeric silicas will interact with cation TPA⁺ to form the initial reactant structure in our simulation. The condensation reaction occurs through two reactions steps. The first step is the formation of the SiO-Si bond between two monomeric fragments, the second step is to remove water to form the dimer species. In the first step, one monomer Si(OH)₄ will approach the anionic monomeric species (coupled to TPA⁺) to a minimum distance to form a structure stabilised by strong hydrogen bonds (Fig 5.2. D_preocr).

The transition state corresponding to formation of the SiO-Si bond with one and only one negative frequency is showed in Fig 5.2. D_ts1. In this step, a reaction intermediate is formed with a five-coordinated silicon (Fig 5.1.D_cr). The presence of this five-fold complex has also been observed by Pereira et al.[18] when the dimerization reaction occurs in methanol environment and is acid catalysed. We also notice the elongated Si-O bond around the fivefold coordinated Si as in previous simulation without the presence of TPA⁺ [27]. The bond length of Si-O around fivefold coordinated Si is between 1.70 Å and 1.80 Å, whereas, the other Si-O bonds have a length of around 1.65 Å.

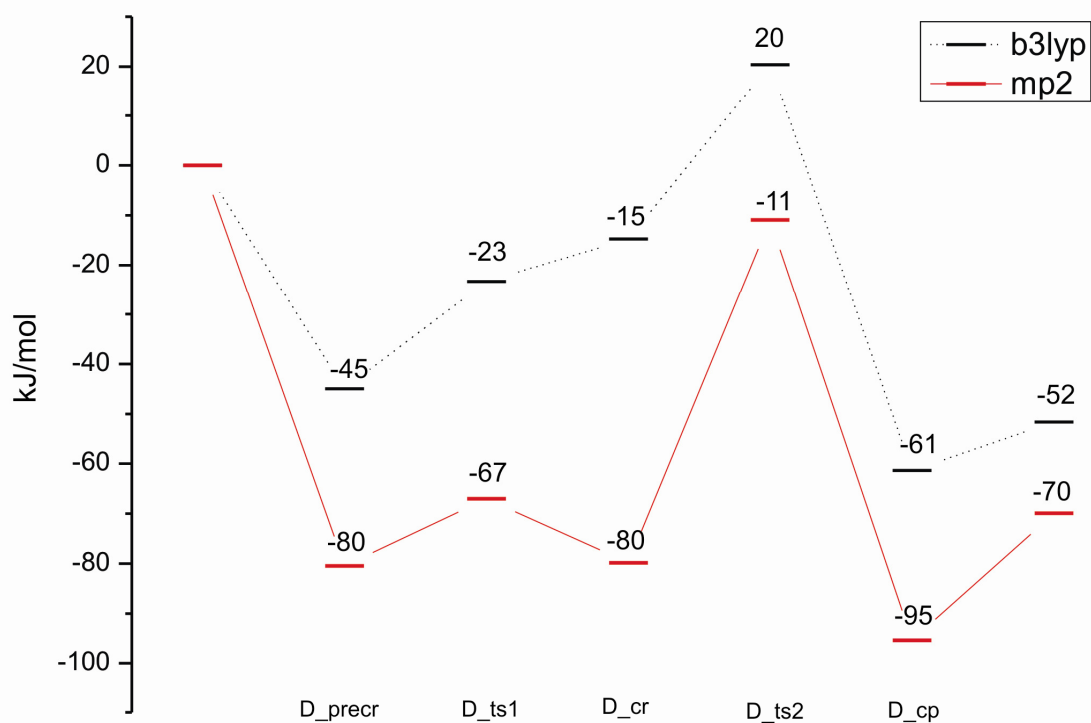


Fig 5.2. Energy profile (kJ/mol) of the dimerization reaction of silica. The reactants consist of an anionic monomer with interaction with TPA^+ and one monomer. The final products are an anionic dimer with interaction with TPA^+ (D_cp_pro) and water.

More interestingly, with the presence of TPA^+ , the barrier of OSi-O bond formation is reduced substantially. Without TPA^+ , this barrier has been reported 57 kJ/mol [27] and 69 kJ/mol [21]. In this chapter with TPA^+ present, the barrier is reduced to 22 kJ/mol with B3LYP and only 13 kJ/mol with MP2 approximation. This implies that TPA^+ stabilizes the transition state by electrostatic and Van-der-Walls interactions.

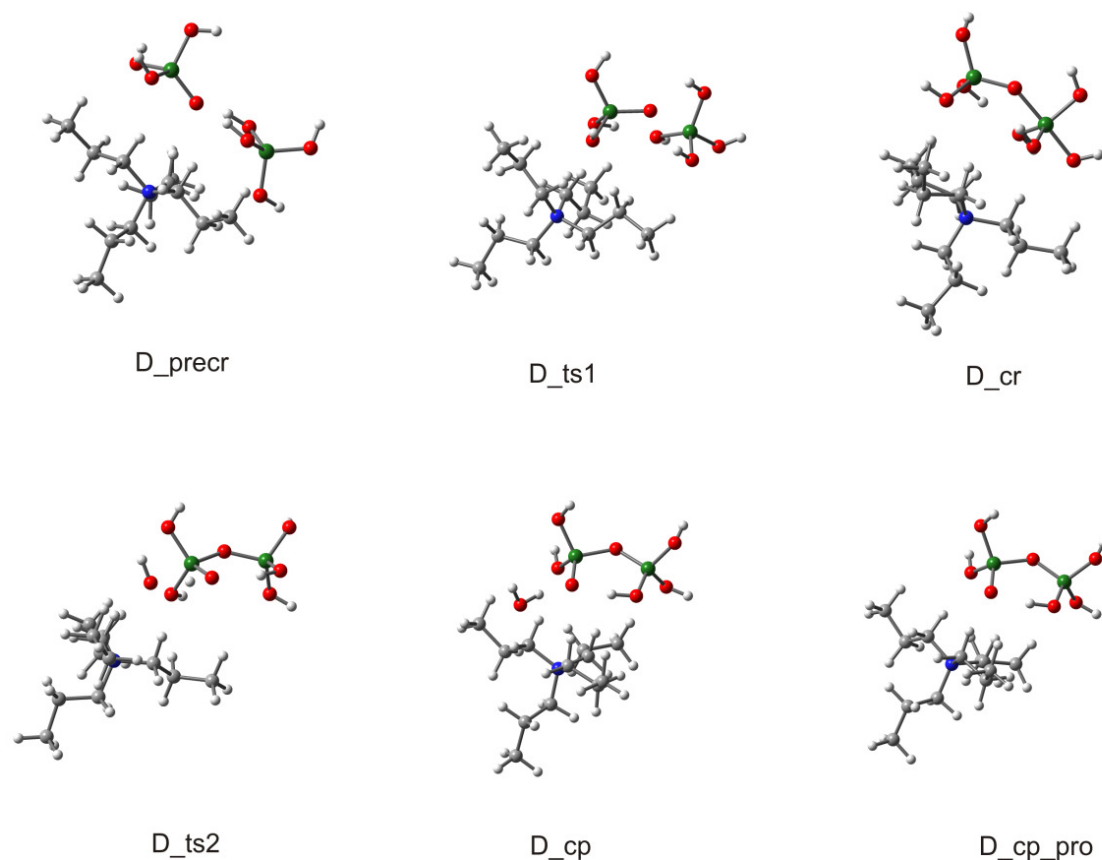


Fig 5.3. Structure of silica species for the dimerization of silica. White, red, green, blue, brown are Hydrogen, Oxygen, Silicon, Nitrogen and Carbon respectively.

In the gas phase, we calculated that pre-transition state (Fig 5.2. D_preocr) is more stable than the five-coordinated structure (Fig 5.2. D_cr) by 15 kJ/mol. However in COSMO solution, they have comparable stabilities, because of the different interaction energies with the solvent. The five-coordinated silicon has an advantage in the water phase. Therefore, including solvation is a crucial computational condition to explore the chemistry in solution. It can change completely the trend observed by gas phase calculations.

The most difficult reaction step is removal of the water molecule to form the dimer silica. The activation energy of this step is 69 kJ/mol. This value is comparable with that obtained from previous simulations without TPA⁺. Because of the continuum solvent model used, this barrier might be over estimated. In solution, the water removal step will be more favourable since it will be assisted by other water molecules. The hydrogen network helps to detach the hydroxyl group more easily from the five-fold complex. Hydrogen is transferred at the same time that a hydroxyl group starts to leave. As a result, the water molecule will be the leaving group and the product is

again an anionic dimer attached to TPA^+ which can initiate another condensation reaction to form a trimer.

The overall barrier of this two step dimerization reaction with TPA^+ is 69 kJ/mol. Whereas the first step of OSi-O bond formation is very encouraging with low barrier 13 kJ/mol, the rate limiting step is water removal. As mentioned above, the overall barrier could be lower because of the water supporting to remove hydroxyl group.

With the presence of TPA^+ , the dimerization reaction is thermodynamically favourable. Without TPA^+ in the model, the energy of the dimerization reaction is reported as -28 kJ/mol with B3LYP functional.[27] Mora-Fronz et al.[28] reported the reaction energy for dimerization -36 kJ/mol in sodium alkaline environment with a continuum solvent model and a pure density functional theory method using double zeta basis set (BLYP/DNP) . This work with TPA^+ , the reaction energy for dimerization with MP2 approximation is -70 kJ/mol.

5.3.3 Trimerization reaction

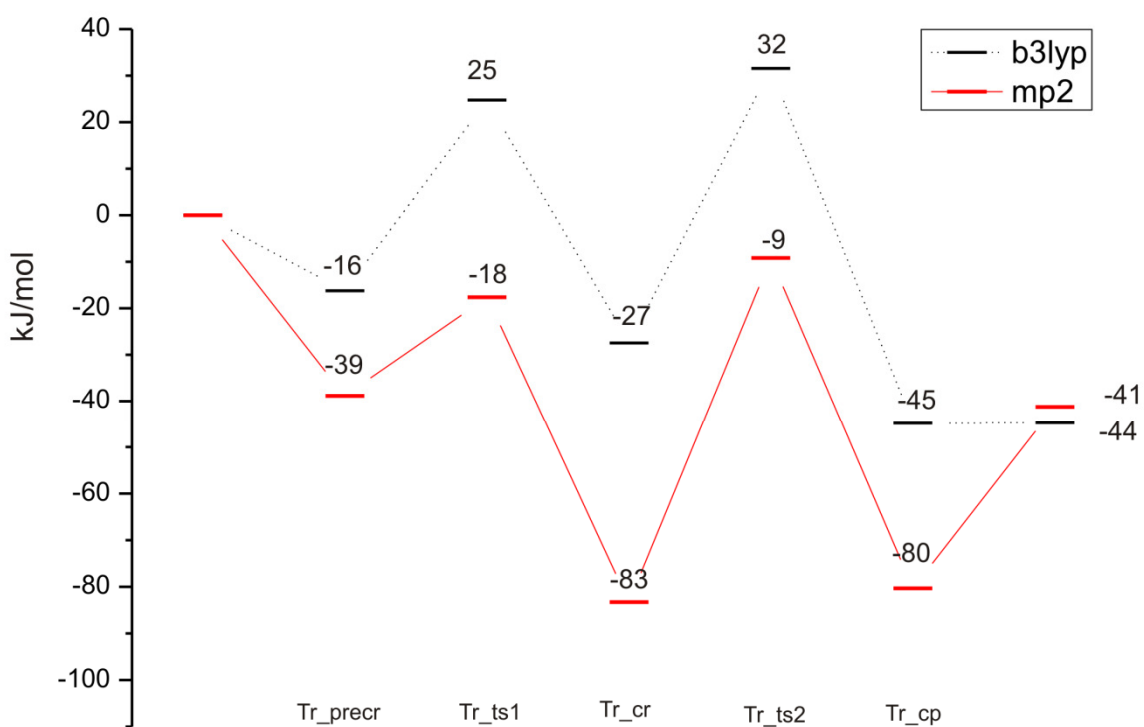


Fig 5.4. Energy profile (kJ/mol) of the trimerization reaction of silica. The reactants consist of an anionic dimer with interaction with TPA^+ and one monomer. The final products are an anionic trimer with interaction with TPA^+ (Tr_cp_pro) and water.

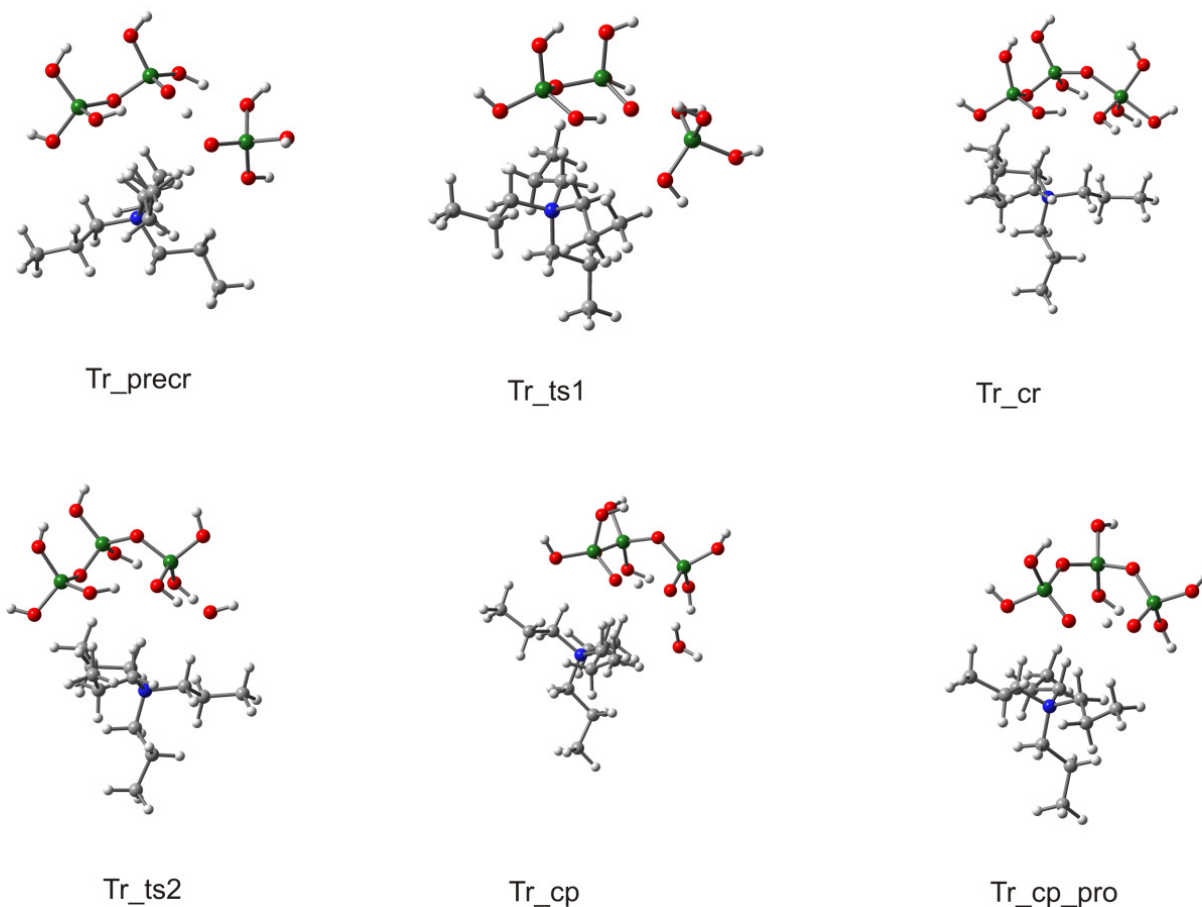


Fig 5.5. Structure of silica species for the trimerization of silica. White, red, green, blue, brown are Hydrogen, Oxygen, Silicon, Nitrogen and Carbon respectively.

The anionic pathway of trimerization is very similar to the mechanism of dimerization and is depicted in Figure 5.4 and Figure 5.5. First, the formation of a SiO-Si bond has a barrier of 21 kJ/mol. The intermediate is a five-coordinated complex with a geometry similar to the case of the dimer. The most favourable approach of the monomer is to form an almost cyclic-like structure. H-bonding controls the preferred conformation. It explains why the linear trimer has a ring-like conformation as has also been found by others works [16,20]. Second, the hydroxyl group leaves and H transfer occurs at the same time. The leaving group is a water molecule. This second step has a barrier equal to 74 kJ/mol, which is similar as the value found in the case of the dimerization reaction.

One of the main difference in the energy profile between dimerization and trimerization is the stability of five-fold intermediate. In the case of dimerization, the five-fold intermediate has the same energy as the pre-transition state. However, in the case of trimerization this five-fold silicon is more favourable than the pre-transition state 44 kJ/mol. Hydrogen bonding may provide a low energy structure of the intermediate state.

The reaction energy of trimerization with TPA^+ is -44 kJ/mol. This values is slightly lower than that in the case of Na^+ reported by Mora-Fronz et al.[28] (-16 kJ/mol). In the trimerization reaction, TPA^+ also shows an important interaction to stabilize five-silicon complex and product structure.

5.3.4. Three-ring closure reaction

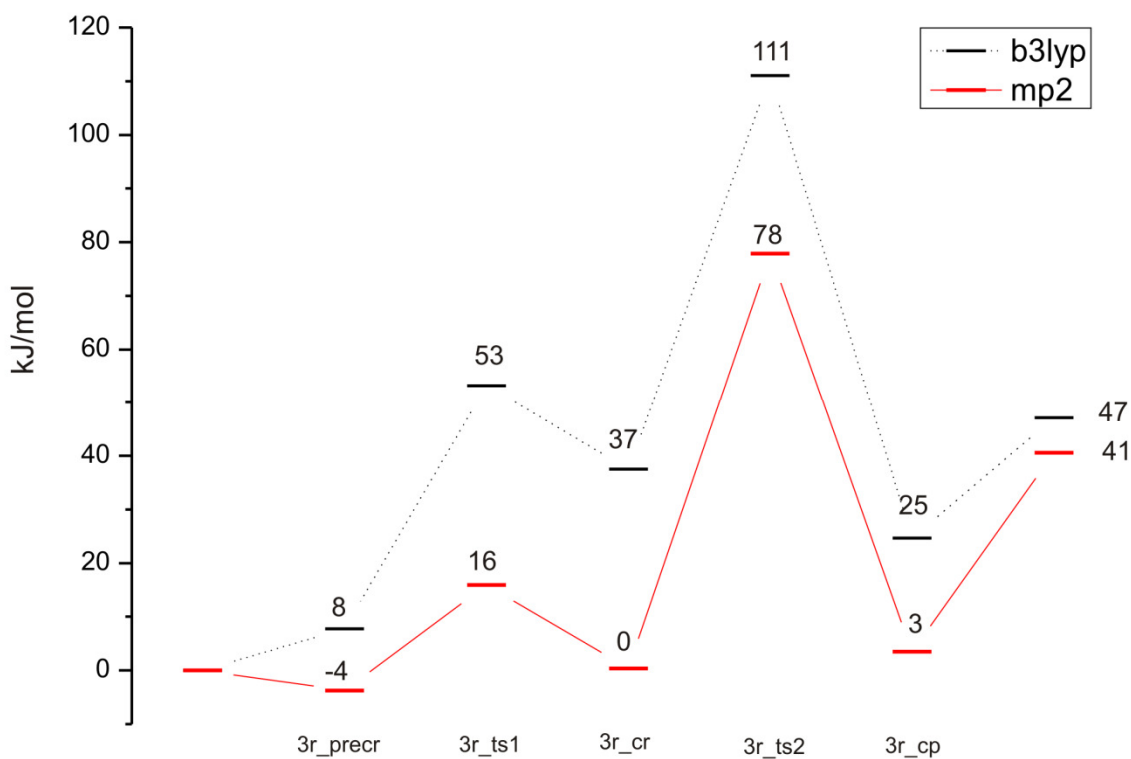


Fig 5.6. Energy profile (kJ/mol) of the 3-ring closure reaction of silica. The reactant is an anionic linear trimer with interaction with TPA^+ . The final products are an anionic 3-ring with interaction with TPA^+ (3r_cp_pro) and water.

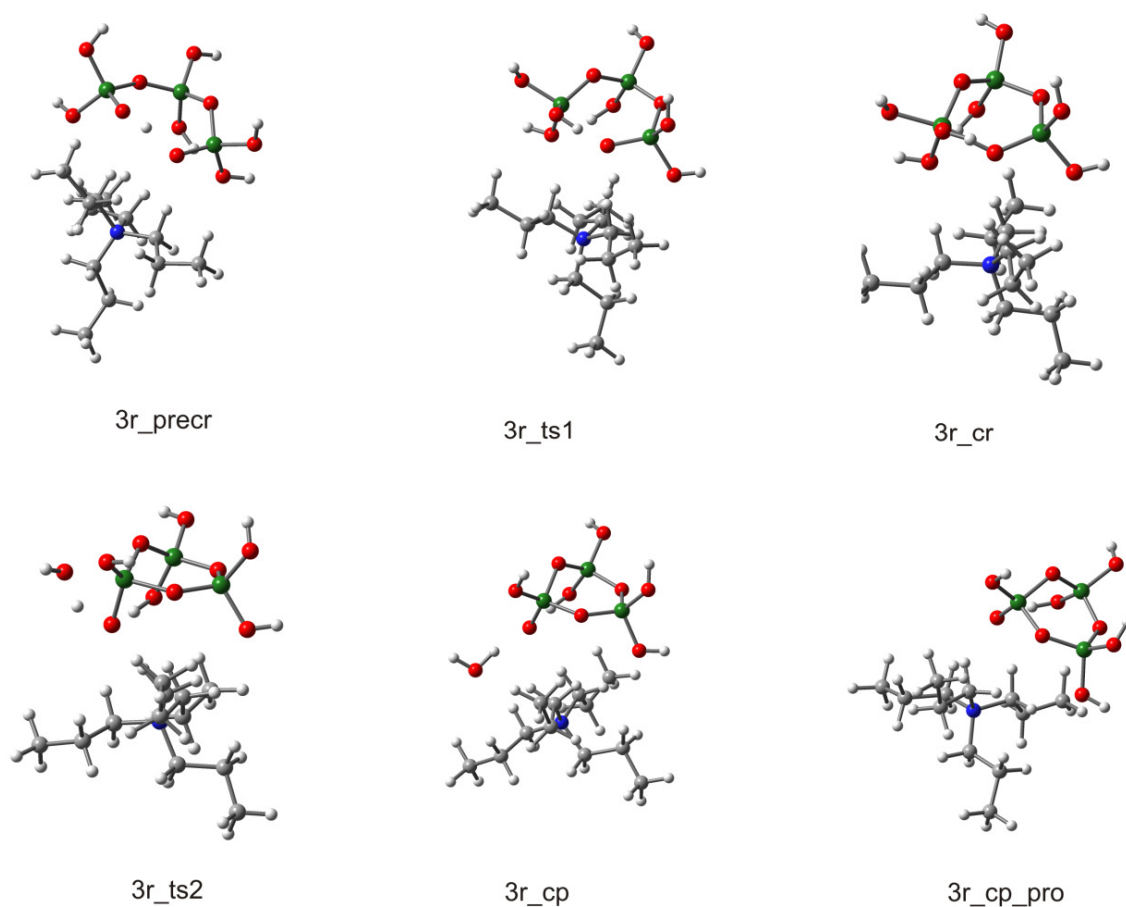


Fig 5.7. Structure of silica species for the 3-ring closure reaction of silica. White, red, green, blue, brown are Hydrogen, Oxygen, Silicon, Nitrogen and Carbon respectively.

Experimentally, the 3-ring and the double 3-ring are observed as dominant structures during the first hours of silica condensation in the presence of organic compound TPA^+ . Using mass spectroscopy, Pelsler et al. [11] reported that TPA^+ has a strong coupling with 3-ring structure. Formation of the 3-ring has been suggested to occur via an intramolecular condensation reaction.[26, 30] Calculations on the thermodynamics indicate that the 3-ring is a stable product in solution[20]. Here we study the mechanism of 3-membered ring formation via the internal condensation reaction according to the anionic mechanism.

There is an important difference with the two previously discussed anionic reactions in mechanism reaction. For ring closure, intramolecular hydrogen bridges between the hydroxyl groups of the molecules have to be broken in order to create a geometry so that internal ring

closure can actually happen. B3LYP predicts that there are unfavourable energies of a pre-transition state configuration (Fig 5.7 3r_preocr) and intermediate with five-coordinated silicon (Fig 5.7 3r_cr). Meanwhile, MP2 approximation shows that these intermediate structures have comparable stabilities with the reactant (see Fig 5.6). The activation energy for initial SiO-Si bond formation is relatively low (20 kJ/mol).

The water removal step has a similar activation barrier as for linear species. The overall barrier of 3-ring formation is 78 kJ/mol, which is similar to that of dimerization and linear trimerization. Hence, 3-ring species have a comparable kinetic rate with linear species. This observation is supported by experimental study where the signal of 3-ring structure is clearly recognised in the first hours of pre-nucleation stage.

Table 5.2. Calculated activation barriers (kJ/mol) for the condensation reactions forming silicate clusters from monomeric to 3-ring species via the anionic mechanism. For the linear oligomers, the reactants are a silicate anion and a monomer $\text{Si}(\text{OH})_4$ to form the larger silicate anion and water as products. For the internal condensations, the reactants are the silicate anion that leads to the monocharged ring and a water as products. E_{act1} is the activation barrier of SiO-Si bond formation step, E_{act2} is the activation barrier of water removal step. The overall-barrier is the difference in energy between the highest transition state and the lowest reactants or reactant complex.

Energy: MP2/6-311G(d,p) // Geometry: B3LYP/6-31+G(d,p) COSMO solvent model	With presence of TPA^+			Without TPA^+ ^[a]		
	Reaction	E_{act1}	E_{act2}	ΔE	E_{act1}	E_{act2}
$(\text{OH})_3\text{SiO}^- \longrightarrow \text{Si}-\text{O}-\text{Si}$	13	69	-70	39	79	-33
$\text{Si}-\text{O}-\text{Si} \longrightarrow \text{Si}-\text{O}-\text{Si}-\text{O}-\text{Si}$	21	74	-44	32	76	-16
$\text{Si}-\text{O}-\text{Si}-\text{O}-\text{Si} \longrightarrow \text{Si}_3\text{O}_6$	20	78	41	19	85	

[a]: The geometries was taken from our previous study at B3LYP/6-31+G(d,p) level [27] and perform a single point calculation at MP2 level.

[b]: Mora-Fronz et al.[28], BLYP/DNP including explicit Na^+ and water model.

5.4. CONCLUSIONS

In the present study, the reaction mechanisms of silica condensation were investigated using DFT and MP2 calculations. Formation of dimer, trimer and three-ring silicate oligomers has been studied in the presence of organic cation TPA⁺.

The interaction between TPA⁺ and anionic silica consist of an electrostatic part and a weak VdW part. High-level computational methods such as MP2 are essential to investigate silica systems in the presence of an organic compound.

We have portrayed the anionic mechanism which process in two steps. The first step is the formation of the SiO-Si linkage bond between two reactants. The second one is the removal of the water group from the intermediate to form a product. TPA⁺ stabilises the transition state for Si-O bond formation. The ring closure reactions occur with a comparable barriers to that of linear growth despite the unfavourable thermodynamic issue because of loss of intramolecular hydrogen bonds.

REFERENCES

1. C. J. Brinker and G. W. Scherer, *Sol-Gel Science: The Physics and Chemistry of Sol-Gel Processing* Academic Press, Boston, 1990.
2. R. K. Iler, *The Chemistry of Silica*, John Wiley & Sons New York, 1979.
3. C. S. Cundy and P. A. Cox, *Chem. Rev.*, 2003, **103**, 663-702.
4. C. T. G. Knight and S. D. Kinrade, *J. Phys. Chem. B*, 2002, **106**, 3329-3332.
5. C. E. A. Kirschhock, R. Ravishankar, F. Verspeurt, P. J. Grobet, P. A. Jacobs and J. A. Martens, *J. Phys. Chem. B* 2002, **106**, 3333.
6. A. R. Felmy, H. Cho, J. R. Rustad and M. J. Mason, *Journal of Solution Chemistry*, 2001, **30**, 509-525.
7. P. P. E. A. de Moor, T. P. M. Beelen, R. A. van Santen, L. W. Beck and M. E. Davis, *J. Phys. Chem. B*, 2000, **104**, 7600-7611.
8. P. P. E. A. de Moor, T. P. M. Beelen, R. A. van Santen, K. Tsuji and M. E. Davis, *Chem. Mater.*, 1999, **11**, 36-43.
9. C. E. A. Kirschhock, R. Ravishankar, F. Verspeurt, P. J. Grobet, P. A. Jacobs and J. A. Martens, *J. Phys. Chem. B*, 1999, **103**, 4965-4971.
10. P. Bussian., F. Sobott., B. Brutschy, W. Schrader and F. Schüter, *Angewandte Chemie*, 2000, **39**, 3901-3905.
11. S. A. Pelster, W. Schrader and F. Schuth, *J. Am. Chem. Soc.*, 2006, **128**, 4310.
12. S. L. Burkett and M. E. Davis, *Chem. Mater.* , 1995, **7**, 920.
13. S. L. Burkett and M. E. Davis, *Chem. Mater.* , 1995, **7**, 1453.
14. S. L. Burkett and M. E. Davis, *Chem. Mater.* , 1994, **98**, 4647.
15. J. D. Rimer, O. Trofymuk, R. F. Lobo, A. Navrotsky and D. G. Vlachos, *J. Phys. Chem. C*, 2008, **112**, 14754-14761.

16. J. C. G. Pereira, C. R. A. Catlow and G. D. Price, *J. Phys. Chem. A*, 1999, **103**, 3252-3267.
17. J. C. G. Pereira, C. R. A. Catlow and G. D. Price, *J. Phys. Chem. A*, 1999, **103**, 3268-3284.
18. J. C. G. Pereira, C. R. A. Catlow and G. D. Price, *Chem. Commun*, 1998, 1387.
19. J. A. Tossell, *Geochimica et Cosmochimica Acta*, 2005, **69**, 283-291.
20. M. J. Mora-Fonz, C. R. A. Catlow and D. Lewis, *Angew Chem. Int. Ed*, 2005, **44**, 3082.
21. Y. T. Xiao and A. C. Lasaga, *Geochim. Et Cosmo Acta* 1996, **60**, 2283.
22. L. J. Criscenti, J. D. Kubicki and S. L. Brantley, *J. Phys. Chem. A*, 2006, **110**, 198-206.
23. A. Pelmenschikov, J. Leszczynski and L. G. M. Pettersson, *J. Phys. Chem. A*, 2001, **105**, 9528-9532.
24. J. C. G. Pereira, C. R. A. Catlow, G. D. Price and R. M. Almeida, *J. Sol-gel Science and Technology*, 1997, **8**, 55.
25. N. Z. Rao and L. D. Gelb, *J. Phys. Chem. B*, 2004, **108**, 12418-12428.
26. J. R. B. Gomes, M. N. D. S. Cordeiro and M. Jorge, *Geochimica et Cosmochimica Acta*, 2008, **72**, 4421-4439.
27. T. T. Trinh, A. P. J. Jansen and R. A. vanSanten, *J. Phys. Chem. B*, 2006, **110**, 23099-23106.
28. M. J. Mora-Fonz, C. R. A. Catlow and D. W. Lewis, *J. Phys. Chem. C*, 2007, **111**, 18155-18158.
29. C. R. A. Catlow, D. S. Coombes, D. W. Lewis and J. C. G. Pereira, *Chem. Mater.*, 1998, **10**, 3249-3265.
30. C. L. Schaffer and K. T. Thomson, *J. Phys. Chem. C* 2008, **33**, 12653.
31. S. Caratzoulas and D. G. Vlachos, *J. Phys. Chem. B*, 2008, **112**, 7-10.
32. A. D. Becke, *Phys. Rev. A* 1988, **38**, 3098. A. D.; Becke, *J. Chem. Phys.*, 1993, **98**, 1372.; A. D. Becke, *J. Chem. Phys.*, 1993, **98**, 5648
33. J. Backer, M. Muir, A. J. and A. Scheiner, in *Chemical Applications of Density-Functional Theory*, ACS Symposium Series eds. B. B. Laird, R. B. Ross and T. Ziegler, American Chemical Society, Washington DC, 1996.
34. M. J. Frisch, G. W. Trucks, H. B. Schlegel, G. E. Scuseria, M. A. Robb, J. R. Cheeseman, J. A. Montgomery, Jr., T. Vreven, K. N. Kudin, J. C. Burant, J. M. Millam, S. S. Iyengar, J. Tomasi, V. Barone, B. Mennucci, M. Cossi, G. Scalmani, N. Rega, G. A. Petersson, H. Nakatsuji, M. Hada, M. Ehara, K. Toyota, R. Fukuda, J. Hasegawa, M. Ishida, T. Nakajima, Y. Honda, O. Kitao, H. Nakai, M. Klene, X. Li, J. E. Knox, H. P. Hratchian, J. B. Cross, V. Bakken, C. Adamo, J. Jaramillo, R. Gomperts, R. E. Stratmann, O. Yazyev, A. J. Austin, R. Cammi, C. Pomelli, J. W. Ochterski, P. Y. Ayala, K. Morokuma, G. A. Voth, P. Salvador, J. J. Dannenberg, V. G. Zakrzewski, S. Dapprich, A. D. Daniels, M. C. Strain, O. Farkas, D. K. Malick, A. D. Rabuck, K. Raghavachari, J. B. Foresman, J. V. Ortiz, Q. Cui, A. G. Baboul, S. Clifford, J. Cioslowski, B. B. Stefanov, G. Liu, A. Liashenko, P. Piskorz, I. Komaromi, R. L. Martin, D. J. Fox, T. Keith, M. A. Al-Laham, C. Y. Peng, A. Nanayakkara, M. Challacombe, P. M. W. Gill, B. Johnson, W. Chen, M. W. Wong, C. Gonzalez, and J. A. Pople, Gaussian, Inc., Wallingford CT, 2004. Gaussian 03, Revision C.02,
35. GAMESS-UK is a package of ab initio programs. See: "<http://www.cfs.dl.ac.uk/gamess-uk/index.shtml>", M.F. Guest, I. J. Bush, H.J.J. van Dam, P. Sherwood, J.M.H. Thomas, J.H. van Lenthe, R.W.A Havenith, J. Kendrick, "The GAMESS-UK electronic structure package: algorithms, developments and applications", *Molecular Physics*, Vol. **103**, No. 6-8, 20 March-20 April 2005, 719-747.
36. S. Simon, M. Duran and J. J. Dannenberg, *The Journal of Chemical Physics*, 1996, **105**, 11024-11031.

CHAPTER 6

Silica Condensation Influenced By Organic Template

The free energy of the oligomerization reaction of silica, the initial steps of silica formation in contact with tetrapropylammonium (tetramethylammonium TMA^+ and tetrapropylammonium TPA^+) cation has been studied by quantum chemical techniques. The solvent effect is included using the COSMO model. The energy of formation of various linear, branched and ring oligomers (up to double 4-ring) was investigated. This chapter shows that the TPA^+ stabilizes selectively particular silicate oligomers, while TMA^+ is specially favors the formation of 4-ring and double 4-ring.

6.1. INTRODUCTION

Various experimental techniques can be used to reveal the structural information about species in solution and nucleation processes. During the first hours of sol-gel reactions, various silicate oligomers are formed in solution. They can be dimers, trimers, tetramers, 3-rings, 4-rings, double 3-rings, double 4-rings or other larger oligomer. The dominant species depends sensitively on reaction conditions, solvent used and presence or absence of structure directing agent (SDA).[9,10] Pelster et al.[11,15-17] were able to track the evolution of different silica species undergoing condensation reactions in aqueous solutions. Using electrospray mass spectrometry (ESI MS) in conjunction with three different reactor systems, they were able to follow the growth of silica oligomers in solution. They found that the double 4-ring is the main product when using TMA^+ , while double 3-ring is dominant when using TEA^+ [15,16] Burkett et al.[12–14] showed that the use of different ammonium salts as templating agents lead to different products. They also identified the cubic octamer, prismatic hexamer, and cyclic-trimer as the predominate products when using TMA^+ , TEA^+ , and TPA^+ respectively. Recently, Rimer et al.[18] studied silica nanoparticle formation using microcalorimetry to measure the heats of reaction evolved from the addition of tetraethylorthosilicate (TEOS) to basic aqueous solutions of monovalent cations. They observed that Na^+ , TMA^+ and TBA^+ behave similarly, while changes in the magnitude of enthalpy for TPA^+ solutions are 4 times larger. Hence, TPA^+ strongly affects the enthalpy of nanoparticle formation. It is known that solutions of Na^+ , TMA^+ , and TBA^+ hydroxides do not lead to silicalite-1 formation, while those of TPA^+ do selectively generate the MFI framework type of silicalite-1.

Theoretical modeling of zeolite synthesis has proven to be a challenging task. Many different approaches have been used to date, using both quantum chemical and classical molecular mechanics techniques. Many electronic structure calculations [19-31] have been performed to reveal information about the mechanism of the elementary reaction step in the pre-nucleation stage. A study on the energies of the dimerization reaction of mono-silicic acid was reported by Tossel [22]. Using the COSMO solvent model, the author studied the free energy of reaction changes by varying temperature and dielectric constants of the solvent. The author found that the condensation reaction is more favorable at high temperature than at room temperature. Free energies of the silica condensation reaction have been recently presented by Mora-Fonz et al.

[23, 31]. The authors found that the formation of the small ring fragment is thermodynamically favorable in high pH media. At different pH of solution, the silica condensation reaction follows a different mechanism and has a different activation barrier [27, 30]. It is generally accepted that the reaction occurs in high pH solution according to an anionic mechanism. It is more favorable since its activation barrier is lower [30, 31].

Catlow et al. [32] have carried out MD simulations of silica precursors in contact with a structure directing agent. They found that long range electrostatic interactions are of crucial importance.

However, there is still a glaring lack of insight into the exact role of the template molecules during the pre-nucleation stages of zeolite synthesis. Organic compound provide an electrostatic stabilization to silicate structures [31, 34] but the contribution of weak Van-der-Waals (VdW) interaction can also be important. Our simulations in chapter 5 have shown that TPA⁺ stabilizes the transition state of SiO-Si bond formation and kinetically favors the condensation reaction. It is also important to extend this direction to investigate the thermodynamic properties of the larger system in the presence various organic templates.

Here we compare free energies of condensation reactions in the presence of TMA⁺ or TPA⁺. The MP2 approximation is applied in order to evaluate the VdW interaction between the organic template and the anionic silica fragment.

6.2. COMPUTATIONAL DETAILS

All calculations were performed using the TURBOMOLE program package [35]. The global optimizations of the cluster structures were carried out at the DFT level with the B3LYP exchange-correlation functional and split valence plus polarization (def2-SVP) basis sets [36]. The B3LYP [37] method has been reported to provide excellent descriptions of various reaction profiles and particularly of geometries and vibrational properties of various molecules [38]. Single-point MP2 calculations were performed for the DFT-optimized structures using the resolution of the identity approximation,[39] and def2-TZVPP[40] basis sets. In all calculation such as optimization, single point energy and frequency analysis, the solvent effect is included using the COSMO model in TURBOMOLE.

The silica condensation reaction is more favorable in a high pH media with an anionic mechanism [23,30,31]. In this chapter, our models only address the anionic silicate in the presence of one organic compound.

The initial geometry guess of silicate was taken from our previous simulation in the gas phase [30]. We initially studied several interaction configuration between the template and silicate structure using a quick optimization with a semi-empirical method using the Spartan package [42]. After this quick optimization step, the most stable structure was chosen for further evaluation with DFT and MP2 method as described above.

6.3. RESULT AND DISCUSSION.

Typically silicate synthesis takes place in high pH media (ca. 10-14)[1,2]. The mechanism of silica condensation can follow through three routes: neutral, anionic (base catalyzed) or cationic (acid catalyzed). At high pH condition, the anionic pathway is the favorable route. In our simulations, the silicic acid $\text{Si}(\text{OH})_4$ molecule is the building unit to make silicate oligomers. The oligomerization process consists of step by step addition of one silicic acid to the negatively charged oligomer [30]. We do not consider the coupling of two oligomers to form a larger linear or branched one. To investigate the interaction of organic template with the silica, we used the model of one positively charged TAA⁺ and one negatively charged silicate oligomer. The total charge of the system is neutral. In this section we will discuss the formation of various linear, branched, ring oligomer from dimer up to double 4-ring species. The free energy and the entropy of reaction will also be analyzed.

6.3.1 Formation of linear and branched oligomer

The DFT optimized structures of the template – silicate complex are shown in Figure 6.1-6.5. According to our previous anionic mechanism [30], the position of the negative charge of silicate molecule is initially located at the end of the oligomer chain. After the optimization procedure, this position can move to the middle of the chain through an internal hydrogen transfer.

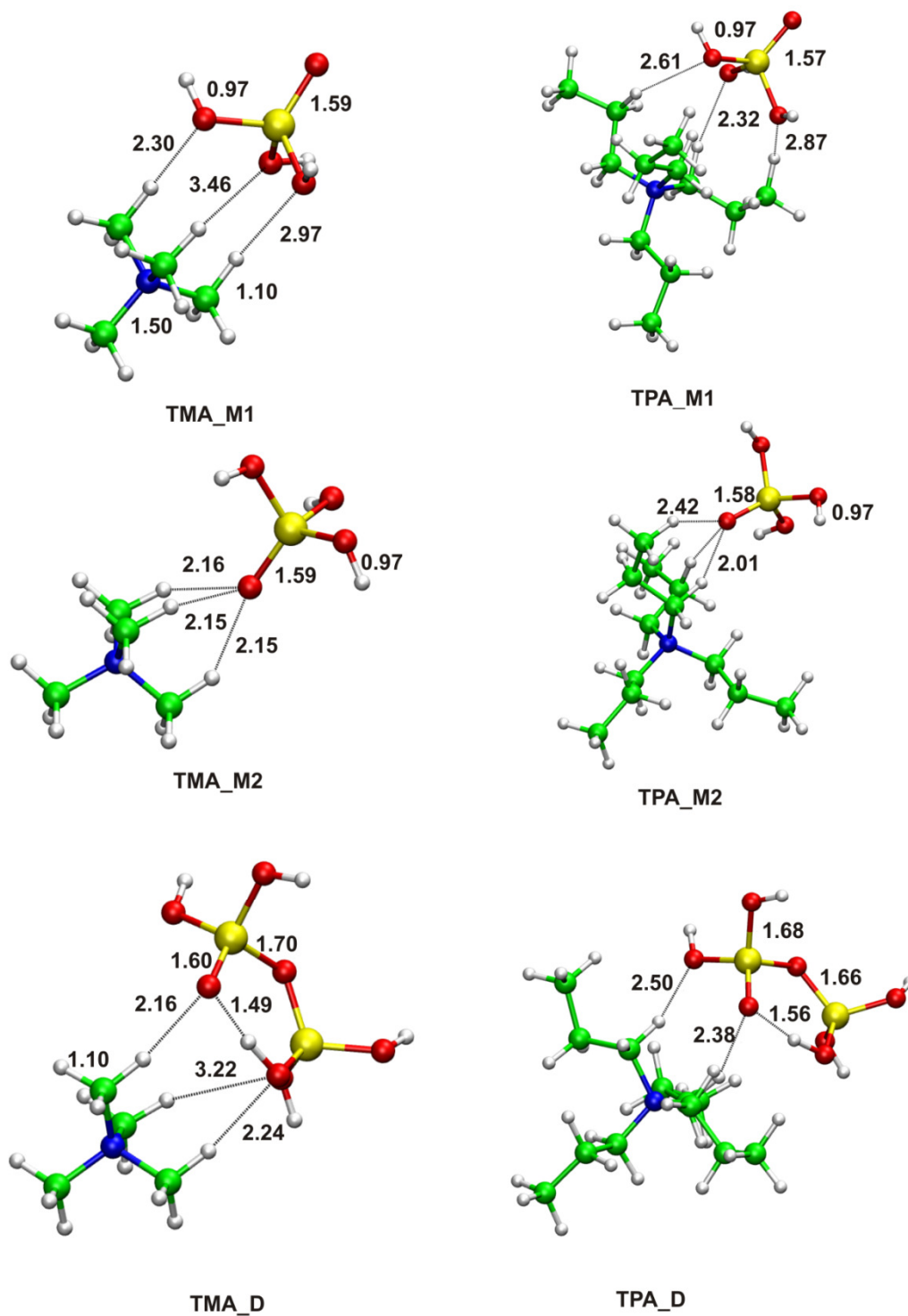


Figure 6.1 Optimized structures of monomer (M1,M2) and dimer(D) in contact with TMA⁺, TPA⁺ respectively. Distance is in Angstrom

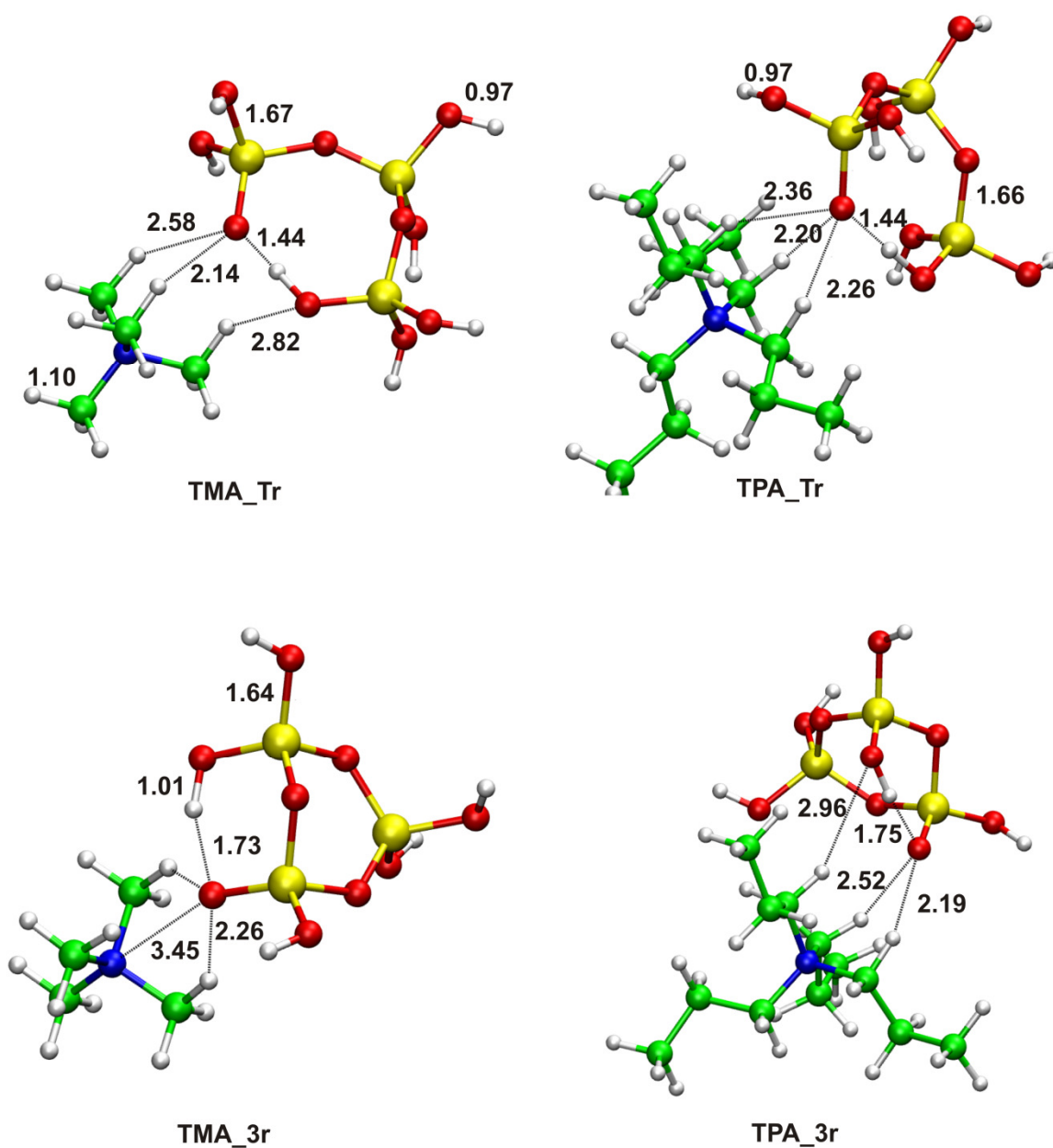


Figure 6.2. Optimized structures of linear trimer (Tr) and 3-ring (3r) in contact with TMA⁺, TPA⁺ respectively. Distance is in Angstrom

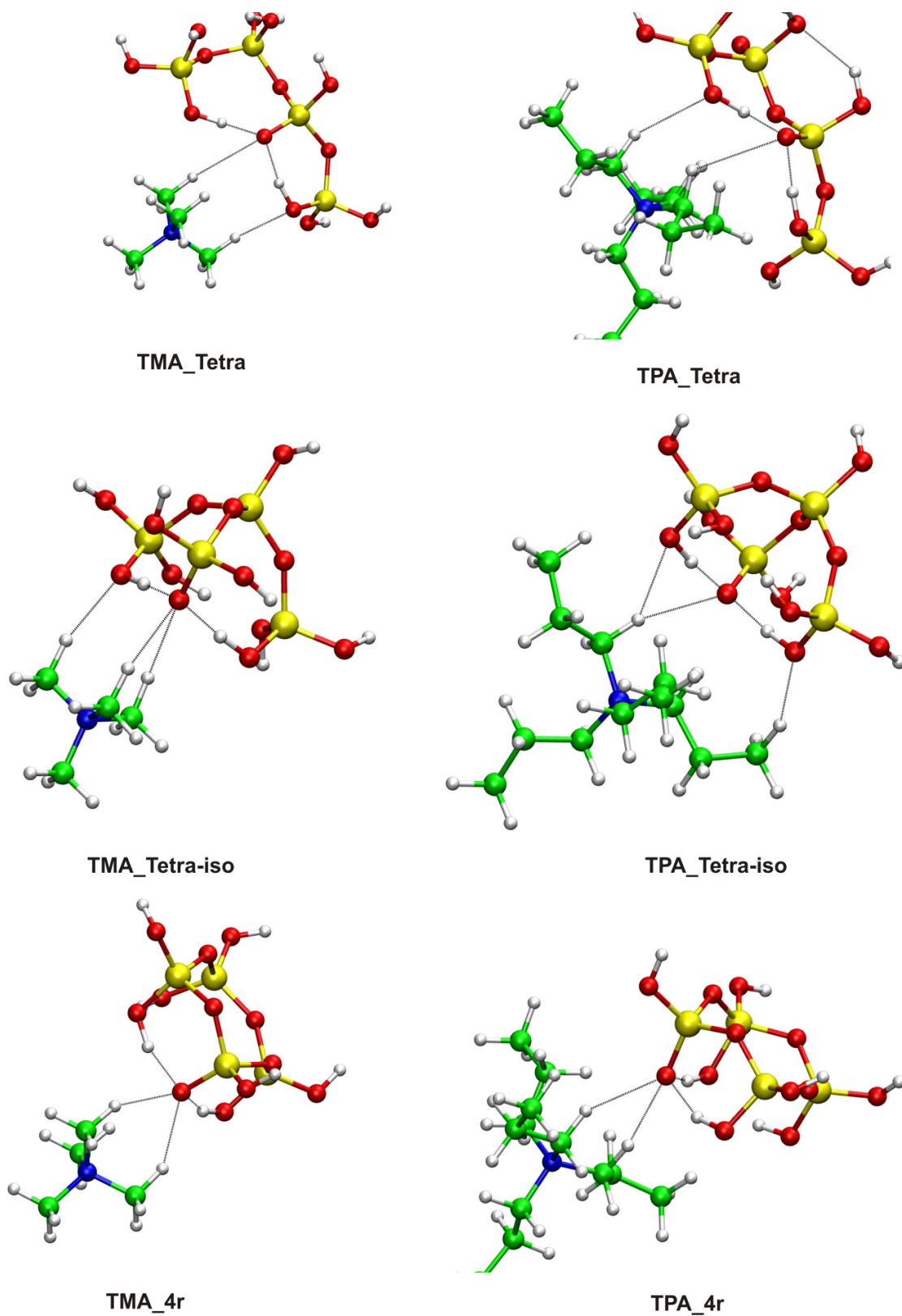


Figure 6.3. Optimized structures of linear tetramer (Tetra), branched tetramer (Tetra-iso) and 4-ring (4r) silicate oligomers in contact with TMA⁺, TPA⁺ respectively .

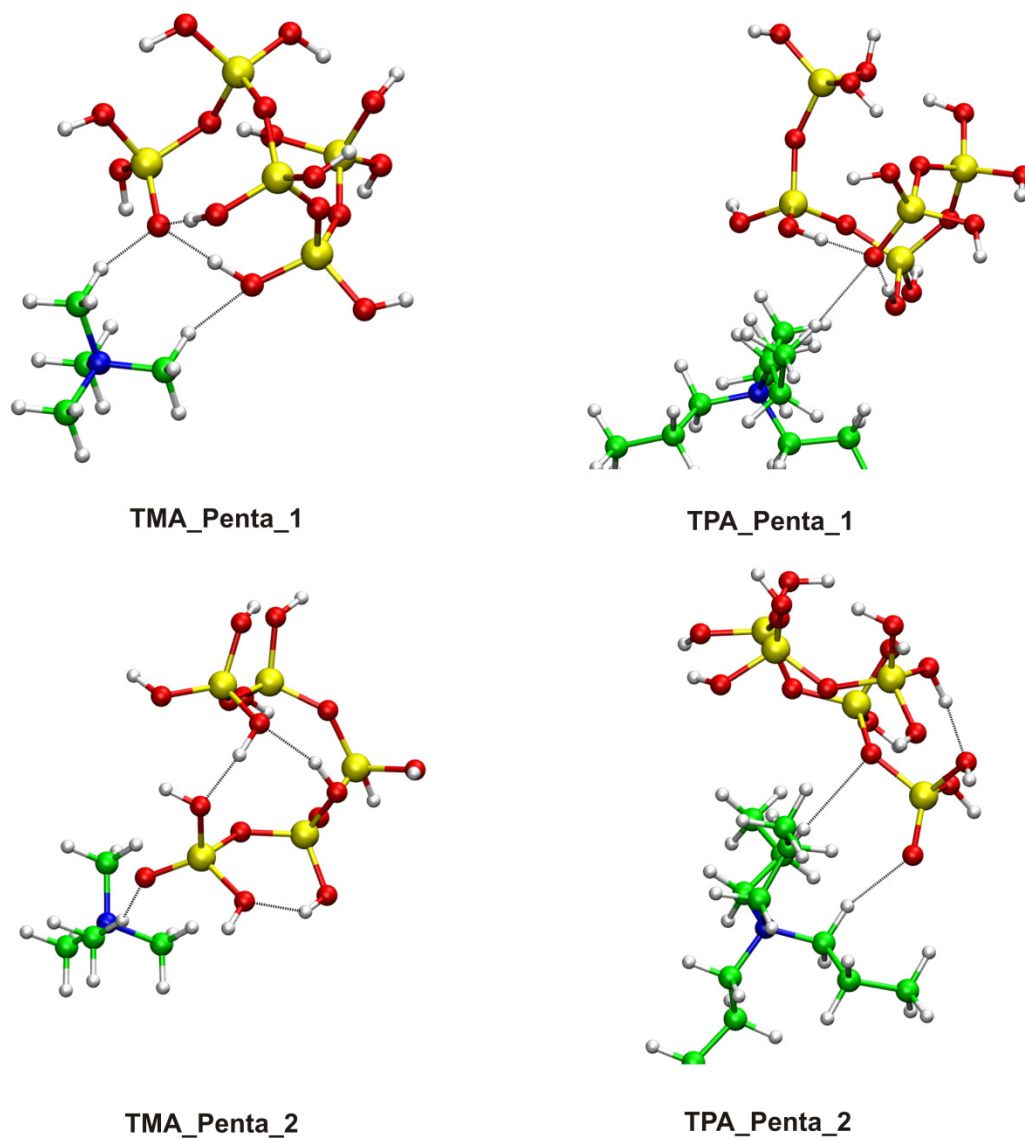


Figure 6.4: Optimized structures of linear pentamer zigzag conformer (Penta_1) and ring-like conformer (Penta_2) in contact with TMA⁺, TPA⁺ respectively.

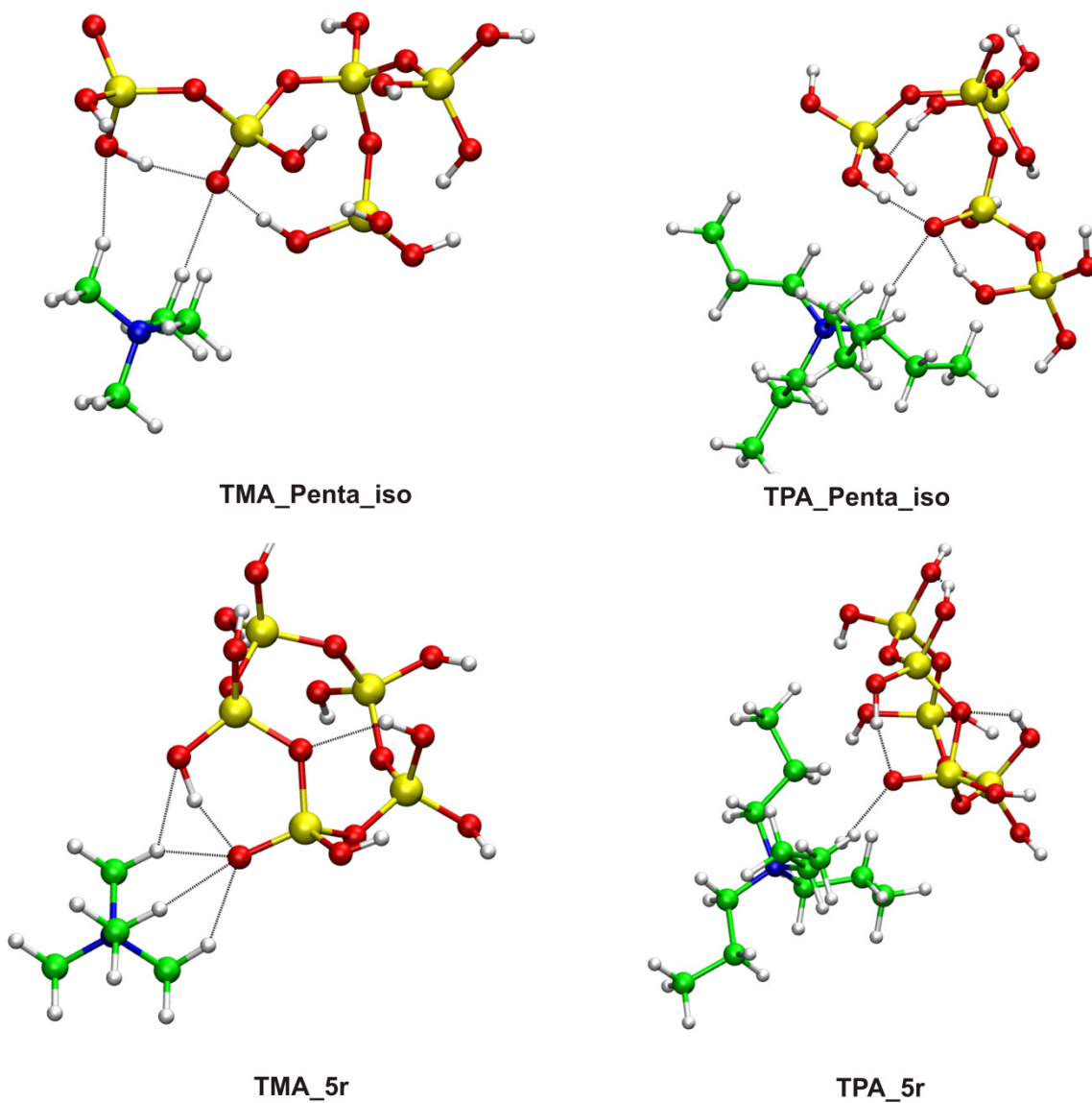


Figure 6.5: Optimized structures of branched pentamer (Penta_iso) and 5-ring (5r) silicate oligomers in contact with TMA⁺, TPA⁺ respectively.

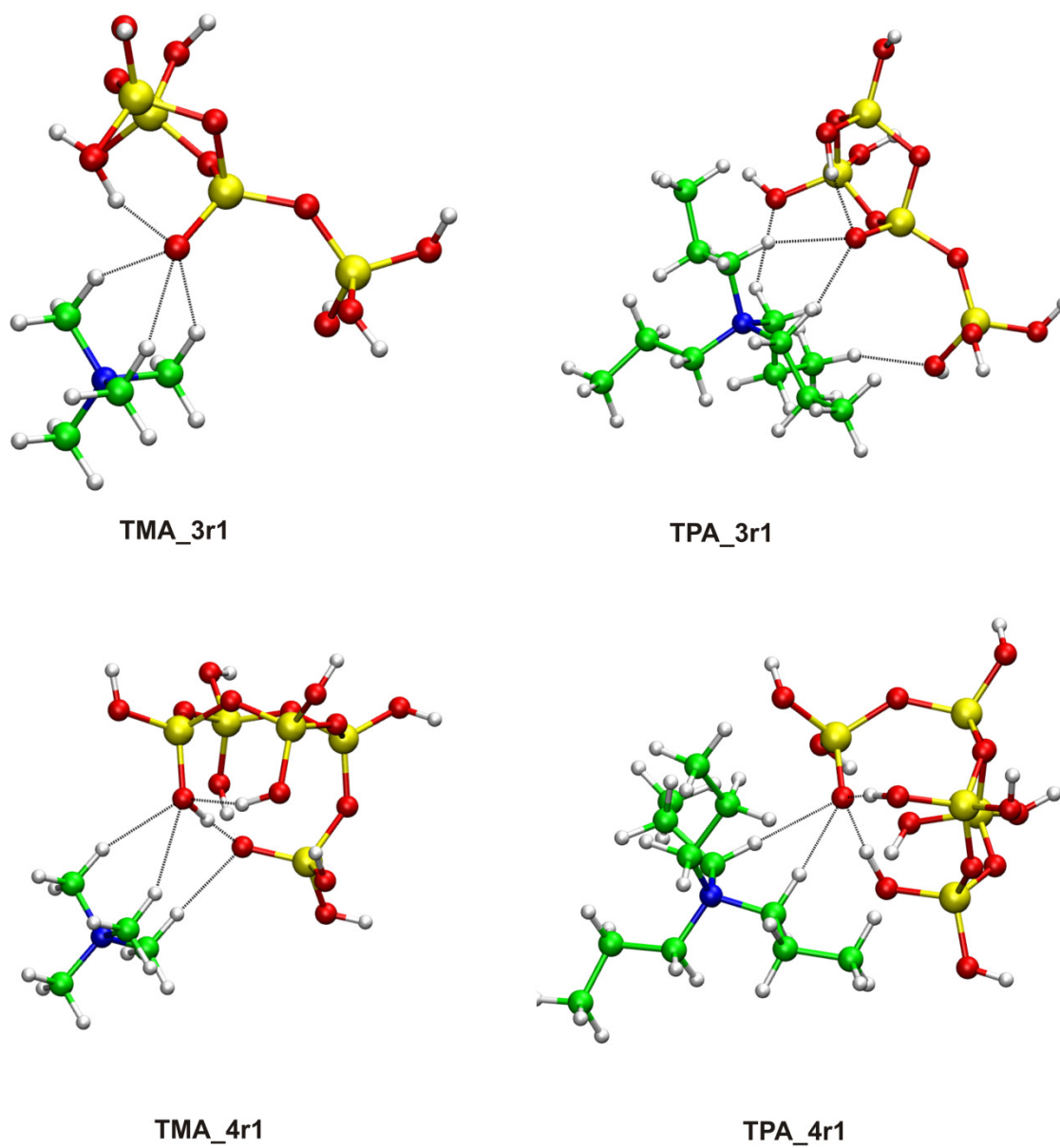


Figure 6.6: Optimized structures of 3-ring fragment (3r1) and 4-ring fragment (4r1)silicate oligomers in contact with TMA⁺, TPA⁺ respectively.

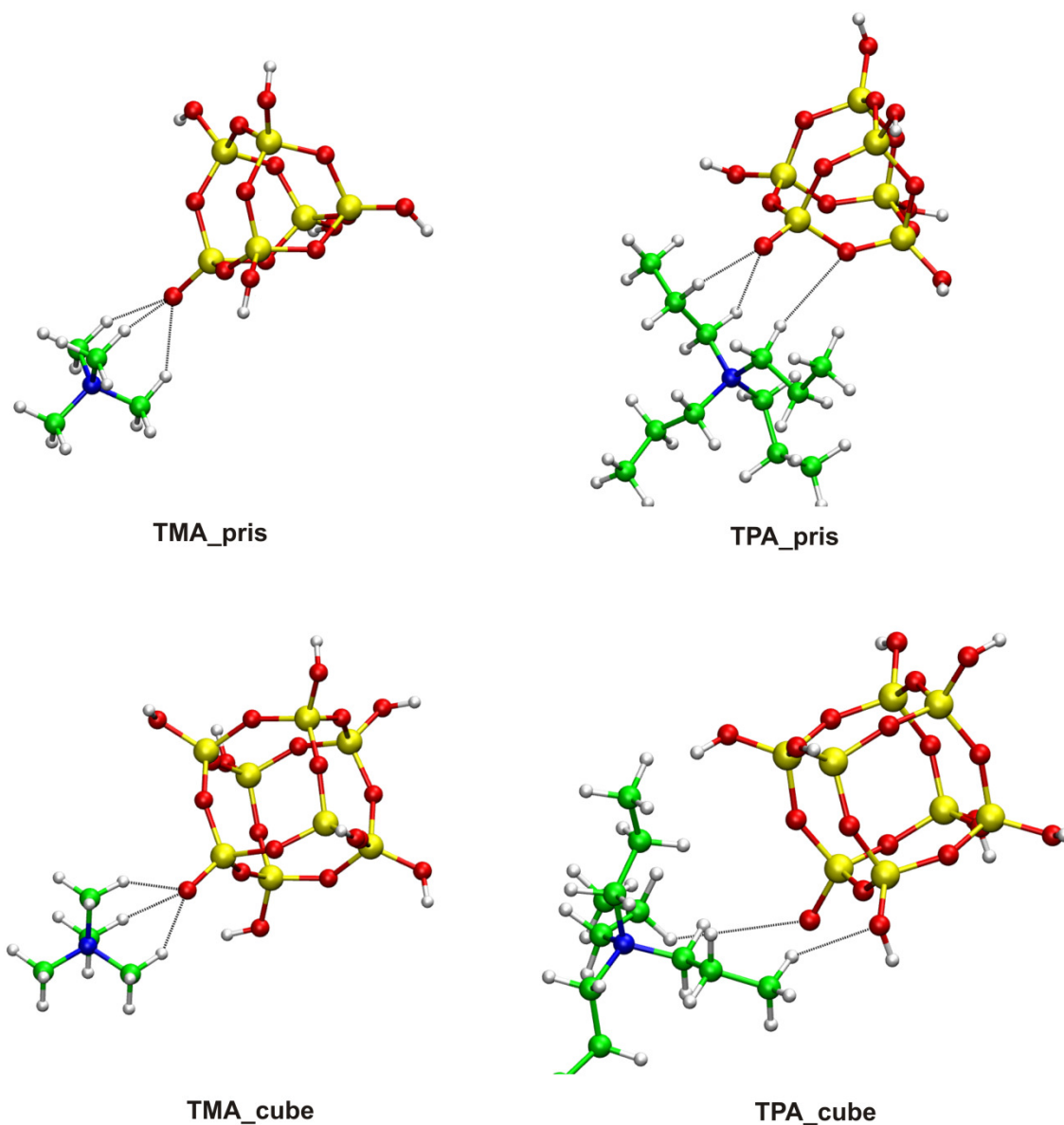


Figure 6.7: Optimized structures of double 3-ring (pris) and double 4-ring (cube) silicate oligomers in contact with TMA^+ , TPA^+ respectively.

There are two coupling possibilities between the organic template and anionic monomeric silicates. These geometries are shown in Figure 6.1 (structure TAA.M1 and TAA.M2). The difference is that the oxygen coordination and the charge of oxygen in contact with template. We considered the distance of free oxygen atom (negative charged) of silicate and the nitrogen atom (positive charged) of organic template. That distance is far in the TAA.M1 structure, but it is close in the TAA.M2. In the gas phase, the TAA.M2 structure is much more stable than

TAA.M1 since the electrostatic interaction is more important when the distance is shorter. We calculated that in the gas phase TMA.M2 is more stable than TMA.M1 -42 kJ/mol. When the COSMO solvation is included in the calculation, the energy difference between TAA.M1 and TAA.M2 is estimated only -3 kJ/mol. This implies that the relative stabilities of silicate species is also dependant on the solvation energy. In our studies, we take the TAA.M2 as the reference state to compute the free energy for dimerization reaction.

Table 6.1: Free energy ΔG (kJ/mol) and entropy ΔS (J/mol/K) of the formation of linear and branched silica calculated with RI-MP2/TZVPP at 298K.

Reaction	ΔG (kJ/mol)		ΔS (J/mol/K)		ΔG (kJ/mol)	ΔG (kJ/mol)
	TPA ⁺	TMA ⁺	TPA ⁺	TMA ⁺	Ref[31]	Ref[23]
					With Na ⁺	Without
					counterion	counterion
TAA.M+M -> TAA.D + H ₂ O	-83	-9	-42	-46	-33	-28
TAA.D+M -> TAA.Tr + H ₂ O	-26	-2	-37	-43	-16	-30
TAA.Tr+M -> TAA.Tetra + H ₂ O	-31	4	-53	-41	-10	-50
TAA.Tetra+M -> TAA.Penta + H ₂ O	-33	-16	-32	-67		-74
TAA.Tr+M -> TAA.Iso-Tetra + H ₂ O	-58	-15	-18	-10		
TAA.Tetra+M -> TAA.Iso-Penta + H ₂ O	-25	2	-35	-41		

The dimerization reaction is essential to silica chemistry. There are number of a computational studies for the energy of this reaction. Using DFT/TNP, Catlow et al. [32] reported a gas-phase dimerization free energy of -9.2 kJ/mol, while Tosell [22], using G2/COSMO, reported a value of +8.8 kJ/mol in the gas phase. Earlier, we reported a value of +9kJ/mol for the neutral dimerization and -28 kJ/mol for the reaction of a monomer with a deprotonated monomer, both using B3LYP/6-31G(d,p) with COSMO solvation[30]. Mora-Fronz et al. [31] using explicit water model and Na⁺ as a counter ion reported a value of -33 kJ/mol. However, the interaction with the organic compound has so far not been studied. We found that in the presence of TMA⁺ and TPA⁺, the free energy of reaction behaves very differently. The dimerization reaction is thermodynamically highly favorable in the presence of TPA⁺. The free energy in the case of TPA⁺ and TMA⁺ are -83 kJ/mol and -9 kJ/mol, respectively. This is due to the differences of the interaction energies of template and the dimer.

The larger TPA⁺ stabilizes the dimer much more than the smaller TMA⁺. TPA⁺ has a longer side chains with three carbon atom, while TMA⁺ has chain with only one carbon atom. The longer hydrocarbon chains provide the larger Van-der-Waals interaction between the template and silicate. We estimate the interaction energies between the dimer-TPA⁺ and dimer-TMA⁺ to be -25 kJ/mol and -8 kJ/mol, respectively. The template does not affect the entropy of reaction. In the both case of TPA⁺ and TMA⁺, the entropy of the dimerization reaction is ~ 45 J/mol/K.

The free energies of trimerization in the case of TPA⁺ and TMA⁺ are -28 kJ/mol and -2 kJ/mol, respectively. Compared with the calculated value of Mora-Fronz et al.[31] in presence of Na⁺ (-16 kJ/mol), TPA⁺ is more favorable for this reaction.

The energetic properties of the formation reaction of linear tetramer and pentamer are reported in Table 6.1. We again observe the stabilizing role of TPA⁺ over TMA⁺ in the condensation reaction. The free energies of formation of linear tetramer and linear pentamer in the case of TPA⁺ are comparable (around -30 kJ/mol). But in the case of TMA⁺, formation of linear tetramer (4kJ/mol) is less favorable as the formation of linear pentamer (-16 kJ/mol).

The creation of branched tetramer and branched pentamer are thermodynamically exothermic. The free energies of these reactions are reported in Table 6.1. TPA⁺ favors the formation of branched tetramer more than that of the linear tetramer. The formation of branched pentamer and the linear pentamer have comparable energies in the presence of TPA⁺. Now in the presence of TMA⁺, the formation of branched tetramer and linear pentamer are more favorable than that of linear tetramer and branched pentamer.

It is interesting to note that the formation of higher oligomers is thermodynamically not significantly more favorable than formation of the small oligomers as reported before [20-31]. In previous studies, the stabilities of silicate was only controlled by the internal hydrogen bonds. The inclusion of counter ion such as organic compounds appears to be essential.

The entropies of the condensation reaction are negative. The entropic properties do not depend on the kind of organic compound that the silicate is in contact with. The change in entropy in the case of TPA⁺ and TMA⁺ is very similar. It means that these small silicates have a similar conformation for all of the organic compounds.

6.3.3 Formation of single and double ring structure

Experimental studies clearly show that the ring structure is very important in the early stage of zeolite synthesis. More interestingly, the ring size depends on an organic template compound. The use of different TAA⁺ can lead to a different ring species, for example the main product when using TMA⁺, TEA⁺, TPA⁺ is double-4-ring (D4R), 4 ring, double 3-ring (D3R) respectively [11-17]. In this section we will try to estimate the energetic properties of the ring closure process.

Formation of single ring fragment

Table 6.2: Free energy ΔG (kJ/mol) and entropy ΔS (J/mol.K) of the formation of ring silica from the linear oligomer. Value calculated with RI-MP2/TZVPP at 298K.

Reaction	ΔG (kJ/mol)		ΔS (J/mol.K)		ΔG (kJ/mol) Without counterion ^[23]
	TPA ⁺	TMA ⁺	TPA ⁺	TMA ⁺	
TAA.Tr -> TAA.3-ring + H ₂ O	-11	-19	142	175	-21
TAA.Tetra -> TAA.4-ring + H ₂ O	-22	-44	111	157	-44
TAA.Penta1 (zigzag) -> TAA.5-ring + H ₂ O	18	-2	127	184	/
TAA.Penta2 (cyclic) -> TAA.5-ring + H ₂ O	-52	-74	124	131	-53

The free energies of the formation of 3-ring and 4-ring from the linear trimer and tetramer are shown in Table 6.2. Both TPA⁺ and TMA⁺ support the formation of 3-ring and 4-ring system. The formation of linear and branched oligomer mentioned in the above section has a negative change in entropy. Meanwhile, the ring closure reaction has a positive entropy. Entropy changes are the main driving force for these reactions. This due to the fact that the reaction releases one water molecule as a product. In Figure 6.2 and Figure 6.3, it is shown that the linear trimer and linear tetramer already have a cyclic-like conformation controlled by the internal hydrogen bonds. They are expected to close the ring easily and have a little entropy change. Based on the difference in free energies of reaction, we predict that in the case of TPA⁺, the ratio of 4-ring to 3-ring is not as high as in the case of TMA⁺. TMA⁺ favors 4-ring formation, because the linear tetramer is not very stable like in the case of TPA⁺. One expects that with TMA⁺, the 4-ring

might be the most dominant species while with TPA^+ , the 4-ring will have a relative low concentration. This observation is in good agreement with experimental work. It was found that the 4-ring is dominant when using TMA^+ in some first hours of zeolite synthesis at low concentration[15-17].

In both cases that TPA^+ and TMA^+ are use, 4-ring is always more stable than the 3-ring oligomer. This implies that the 4-ring is the thermodynamic stable product and will appear in the final structure of zeolite. We also calculated the energy of formation of the 5-ring structure from the linear pentamer. The reactant linear pentamer can have several conformation have the different internal hydrogen bonds. In this paper we only consider two conformations, one has a zigzag shape and the other has a cyclic shape (Figure 6.4). The zigzag conformer is more stable than the cyclic shape conformer by about 70 kJ/mol because there are more internal hydrogen bonds in the zigzag than in cyclic isomer. The zigzag conformer of linear pentamer has not been reported in earlier simulations [20,23,30]. In order to make a five ring from linear pentamer, the linear one should change into a new conformation which is cyclic-like [20,23]. We expect that in water solution the external hydrogen bonds between water and silicate can compensate internal hydrogen bonds and can reduce the energy gap between these two conformers.

Table 6.3: Free energy $\Delta G(\text{kJ/mol})$ and entropy $\Delta S (\text{J/mol.K})$ of the formation of 3-ring and 4-ring fragment. Value calculated with RI-MP2/TZVPP at 298K.

Reaction	$\Delta G(\text{kJ/mol})$		$\Delta S (\text{J/mol.K})$		$\Delta G(\text{kJ/mol})$ Without counter ion. ^[23]
	TPA^+	TMA^+	TPA^+	TMA^+	
TAA.Tetra -> TAA.3ring-1 + H ₂ O	11	17	146	195	/
TAA.iso-Tetra -> TAA.3ring-1 + H ₂ O	39	-1	111	164	/
TAA.Penta1 -> TAA.4ring-1 + H ₂ O	-53	-56	138	165	-21
TAA.Iso-Penta -> TAA.4ring-1 + H ₂ O	-61	-74	141	139	/

Another possibility to form a 3-ring and 4-ring fragment is the closure reaction of the position 1,3 or 1,4 of a higher oligomer. The structures of the product are depicted in Figure 6. Table 3 reports the free energies and entropies of reactions. In the presence of TPA⁺ or TMA⁺, the 3-ring fragment is not favorable as the 4-ring fragment. Although the formation of 3-ring and 4-ring fragments have favorable entropy but 3-ring internally constrained and not as stable as 4-ring. This observation is also supported by the absence of 3-ring silica structures in the final zeolite framework.

Formation of double ring silicate

Table 6.4: Free energy ΔG (kJ/mol) and entropy ΔS (J/mol.K) of the formation of double 3-ring and double 4-ring silica. Value calculated with RI-MP2/TZVPP at 298K.

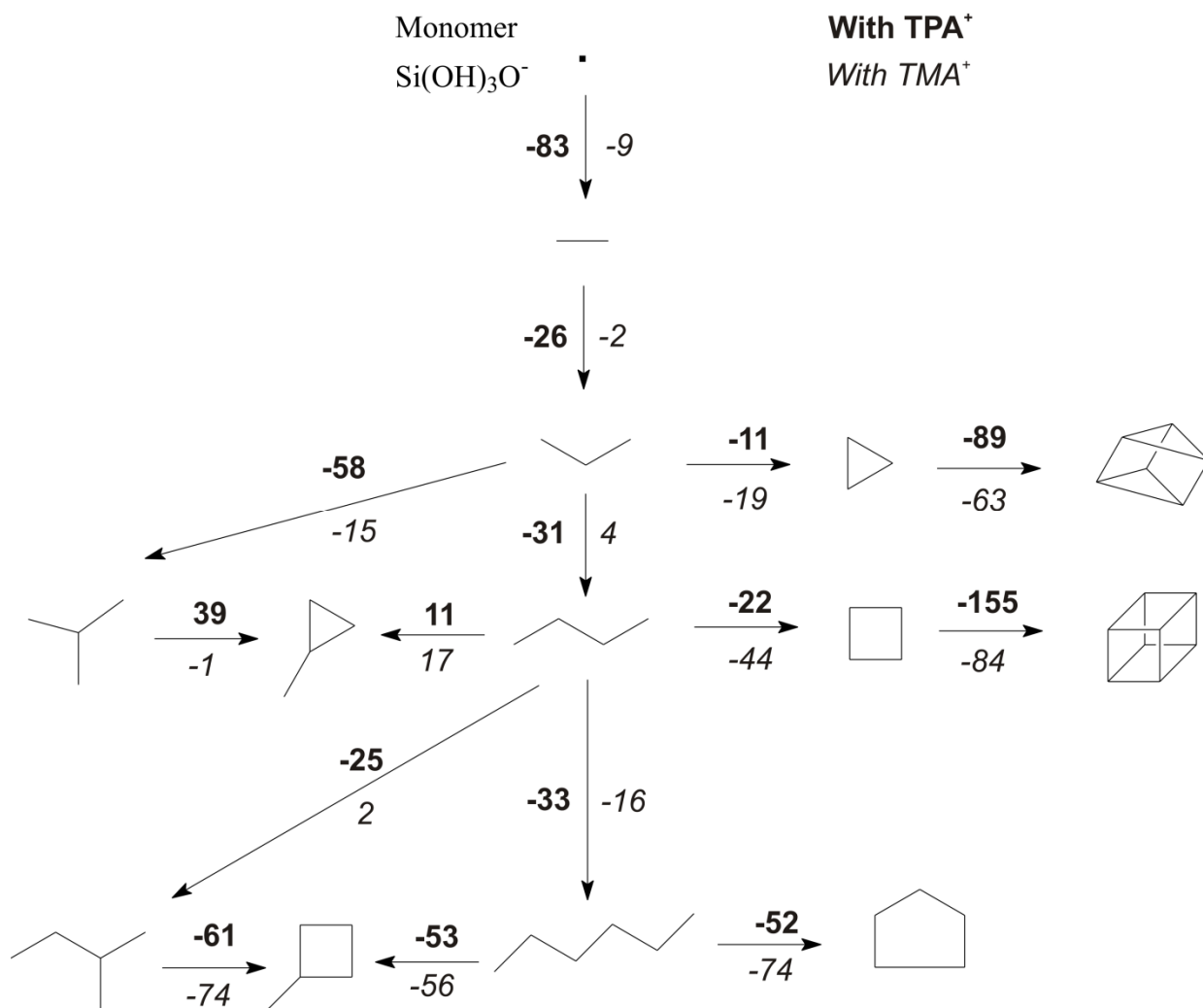
Reaction	ΔG (kJ/mol)		ΔS (J/mol.K)	
	TPA ⁺	TMA ⁺	TPA ⁺	TMA ⁺
TAA.3-ring + 3-ring -> TAA.D3R + 3H ₂ O	-89	-63	189	195
TAA.4-ring + 4-ring -> TAA.D4R + 4H ₂ O	-155	-84	432	368

The existence of the prismatic hexamer and cubic octamer of silicate synthesized with organic template was confirmed by experimental studies [16-18]. There may be two possible ways to form the double ring system from a single 3-ring or single 4-ring oligomers. The first route is to gradually add the monomer into the single ring one by one, the other way is through a condensation reaction of two single rings to produce a double ring. In this chapter, we calculated the formation of these double rings as mentioned in the latter case. In our model, one single ring in contact with TAA⁺ reacts with another free single ring to form a double ring in contact with TAA⁺ and release water molecules.

Table 6.4 shows that the formation of the D3R and D4R is thermodynamically favorable. This observation is consistent with experimental studies of Pelsler et al. [16,17]. They found that when using TMA⁺ as the template, the dominant species observed was D4R. Condensation reaction to

form D4R gains more energy than that reaction to form D3R. The entropy of these reactions is very favorable. The role of TAA⁺ is not important for the entropy change. The entropy of reaction to form D3R is around 190 J/mol/K. This value is much smaller than the entropy of reaction to form D4R (~ 400 J/mol/K).

A summary of all calculated free energies of the reactions starting with monomer up to the double 4-ring oligomer is presented in Scheme 6.1. TPA⁺ stabilizes the formation of oligomer more than TMA⁺. Formation of 4-ring from linear oligomer is more favorable with TMA⁺. This observation is consistent with the experimental reports [16-18]. From that single ring, condensation reactions leading to prismatic and cubic cages are very favorable in the presence of TPA⁺ as well as TMA⁺. It is interesting to note that the formation of 3-ring fragment from higher oligomer via a 1,3 internal ring closure reaction is thermodynamically unfavorable. Meanwhile the formation of 4-ring fragments from higher oligomer is favorable. This agrees with the experimental observation that no 3-ring building blocks are present in the final structure of zeolite framework. However, higher rings such as 4-ring and 5-ring fragments are commonly obtained.



Scheme 6.1. Free energy ΔG (kJ/mol) of the condensation reaction calculated at 298.15K for silicate clusters from monomer to D4R species with the presence of organic template. Optimization with B3LYP/SVP/COSMO and single point with RI-MP2/TZVPP/COSMO were used. The values in bold and italic format are for the interaction with TPA⁺ and TMA⁺, respectively. For linear and branched oligomer formation the values are for the reaction of a silicate species with a monomeric species to give water as a product. Internal condensation reactions form the ring structures and water molecule as the products.

6.4. CONCLUSIONS

In the present study, the reaction mechanisms of silica condensation were investigated using DFT and MP2 calculations. Formation of various silicate oligomer from dimer to double 4-ring has been studied in the presence of organic cation such as TMA⁺ and TPA⁺.

The interaction between TPA^+ and anionic silica consist of an electrostatic part and a weak Van-der-Waals energy part. High-level computational methods such as RI-MP2 are essential to investigate silica systems in the presence of an organic compound.

The results show that TAA^+ , especially TPA^+ , can enhance the condensation reaction of silica. The role of organic compound in zeolite synthesis is not only important for the formation of nanoparticle but also very crucial to the stabilities of silicate oligomer in the early stage of the synthesis reaction.

The TPA^+ favors the formation of linear small oligomer such as dimer and trimer. Condensation reactions in the presence of TPA^+ gain more energy than with TMA^+ or the alkali counter ion (e.g Na^+). This is due to the favorable interaction between product and TPA^+ . It is mainly relates to the difference in the Van-der-Waals interaction energies between template and oligomers.

The formation of linear and branched higher oligomer is thermodynamically favorable. The branched oligomer has a strong interaction with TPA^+ . Entropy change is the driving force of the ring closure reaction. The ring formation is favorable even at room temperature. The 4-ring fragment tends to be more stable than the 3-ring fragment.

REFERENCES

1. C. J. Brinker and G. W. Scherer, *Sol-Gel Science: The Physics and Chemistry of Sol-Gel Processing*, Academic Press, Boston, 1990.
2. R. K. Iler, *The Chemistry of Silica*, John Wiley & Sons New York, 1979.
3. C. S. Cundy and P. A. Cox, *Chem. Rev.*, 2003, **103**, 663-702.
4. C. T. G. Knight and S. D. Kinrade, *J. Phys. Chem. B*, 2002, **106**, 3329-3332.
5. C. E. A. Kirschhock, R. Ravishankar, F. Verspeurt, P. J. Grobet, P. A. Jacobs and J. A. Martens, *J. Phys. Chem. B* 2002, **106**, 3333.
6. A. R. Felmy, H. Cho, J. R. Rustad and M. J. Mason, *Journal of Solution Chemistry*, 2001, **30**, 509-525.
7. P. P. E. A. de Moor, T. P. M. Beelen, R. A. van Santen, L. W. Beck and M. E. Davis, *J. Phys. Chem. B*, 2000, **104**, 7600-7611.
8. P. P. E. A. de Moor, T. P. M. Beelen, R. A. van Santen, K. Tsuji and M. E. Davis, *Chem. Mater.*, 1999, **11**, 36-43.
9. C. E. A. Kirschhock, R. Ravishankar, F. Verspeurt, P. J. Grobet, P. A. Jacobs and J. A. Martens, *J. Phys. Chem. B*, 1999, **103**, 4965-4971.
10. P. Bussian., F. Sobott., B. Brutschy, W. Schrader and F. Schüter, *Angewandte Chemie*, 2000, **39**,

- 3901-3905.
11. S. A. Pelster, W. Schrader and F. Schuth, *J. Am. Chem. Soc.*, 2006, **128**, 4310.
 12. S. L. Burkett and M. E. Davis, *Chem. Mater.*, 1995, **7**, 920.
 13. S. L. Burkett and M. E. Davis, *Chem. Mater.*, 1995, **7**, 1453.
 14. S. L. Burkett and M. E. Davis, *Chem. Mater.*, 1994, **98**, 4647.
 15. J. D. Rimer, O. Trofymlyuk, R. F. Lobo, A. Navrotsky and D. G. Vlachos, *J. Phys. Chem. C*, 2008, **112**, 14754-14761.
 16. S. A. Pelster, B. Weimann, B. B. Schaack, W. Schrader, F. Schüth, *Angew. Chem. Int. Ed.* 2007, **46**, 6674
 17. S. A. Pelster, F. Schüth, W. Schrader, *Anal. Chem.* 2007, **79**, 6005.
 18. B. B. Schaack, W. Schrader, F. Schüth, *Angew. Chem. Int. Ed.* 2008, **47**, 9092
 19. J. C. G. Pereira, C. R. A. Catlow and G. D. Price, *J. Phys. Chem. A*, 1999, **103**, 3252-3267.
 20. J. C. G. Pereira, C. R. A. Catlow and G. D. Price, *J. Phys. Chem. A*, 1999, **103**, 3268-3284.
 21. J. C. G. Pereira, C. R. A. Catlow and G. D. Price, *Chem. Commun*, 1998, 1387.
 22. J. A. Tossell, *Geochimica et Cosmochimica Acta*, 2005, **69**, 283-291.
 23. M. J. Mora-Fonz, C. R. A. Catlow and D. Lewis, *Angew Chem. Int. Ed.*, 2005, **44**, 3082.
 24. Y. T. Xiao and A. C. Lasaga, *Geochim. Et Cosmo Acta* 1996, **60**, 2283.
 25. L. J. Criscenti, J. D. Kubicki and S. L. Brantley, *J. Phys. Chem. A*, 2006, **110**, 198-206.
 26. A. Pelmenschikov, J. Leszczynski and L. G. M. Pettersson, *J. Phys. Chem. A*, 2001, **105**, 9528-9532.
 27. J. C. G. Pereira, C. R. A. Catlow, G. D. Price and R. M. Almeida, *J. Sol-gel Science and Technology*, 1997, **8**, 55.
 28. N. Z. Rao and L. D. Gelb, *J. Phys. Chem. B*, 2004, **108**, 12418-12428.
 29. J. R. B. Gomes, M. N. D. S. Cordeiro and M. Jorge, *Geochimica et Cosmochimica Acta*, 2008, **72**, 4421-4439.
 30. T. T. Trinh, A. P. J. Jansen and R. A. vanSanten, *J. Phys. Chem. B*, 2006, **110**, 23099-23106.
 31. M. J. Mora-Fonz, C. R. A. Catlow and D. W. Lewis, *J. Phys. Chem. C*, 2007, **111**, 18155-18158.
 32. C. R. A. Catlow, D. S. Coombes, D. W. Lewis and J. C. G. Pereira, *Chem. Mater.*, 1998, **10**, 3249-3265.
 33. C. L. Schaffer and K. T. Thomson, *J. Phys. Chem. C* 2008, **33**, 12653.
 34. S. Caratzoulas and D. G. Vlachos, *J. Phys. Chem. B*, 2008, **112**, 7-10.
 35. TURBOMOLE V5.10 2008, a development of University of Karlsruhe and Forschungszentrum Karlsruhe GmbH, 1989-2007, TURBOMOLE GmbH, since 2007; available from <http://www.turbomole.com>.
 36. A. D. Becke, *Phys. Rev. A* 1988, **38**, 3098. A. D.; Becke, *J. Chem. Phys.*, 1993, **98**, 1372.; A. D. Becke, *J. Chem. Phys.*, 1993, **98**, 5648
 37. J. Backer, M. Muir, A. J. and A. Scheiner, in *Chemical Applications of Density-Functional Theory, ACS Symposium Series* eds. B. B. Laird, R. B. Ross and T. Ziegler, American Chemical Society, Washington DC, 1996.
 38. RI-MP2: Optimized Auxiliary Basis Sets and Demonstration of Efficiency. F. Weigend, M. Häser, H. Patzelt and R. Ahlrichs; *Chem. Phys. Letters* **294**, 143 (1998).
 39. S. Simon, M. Duran and J. J. Dannenberg, *The Journal of Chemical Physics*, 1996, **105**, 11024.
 40. Fully Optimized Contracted Gaussian Basis Sets for Atoms Li to Kr. A. Schäfer, H. Horn and R. Ahlrichs; *J. Chem. Phys.* **97**, 2571 (1992).
 41. F. Weigend, M. Häser, H. Patzelt and R. Ahlrichs; *Chem. Phys. Letters* **294**, 143 (1998).
 42. Spartan'08 chemistry tools for education and industry available from <http://www.wavefun.com>

SUMMARY

The classical syntheses of zeolitic materials are based on silicates or alkoxy silanes in alkaline solutions, often with organic additives that act as structure-directing agents (SDA). The SDA are thought to be mainly responsible for the formation of a specific zeolite structures. However, this thesis shows that the silicate-template interactions also are important to be initial condensation reaction take place in the prenucleation stage. At this point it is also still under discussion whether growth proceeds by a monomer addition sequence or the assembly of preformed building blocks. In this thesis, the essential chemical properties of the silica condensation process such as the role of water, hydrogen bonding, counter ion effect, interaction with template have been addressed.

The mechanism of the silica condensation reaction of small oligomer from dimer to pentamer in gas phase was studied in chapter 2. In this chapter, the reaction mechanism of silica condensation was investigated using DFT calculations for various structures of silicate oligomers. There are two different reaction paths for the condensation reaction: one reaction path proceeds via neutral species and the other occurs via the anionic species. An anionic mechanism that occurs in two steps. The first step is the formation of the SiO-Si linkage bond between two reactants. The second one is the removal of the water group from the intermediate to form a product. It infers that the water removal is the most difficult step in reaction pathway. Based on the calculated activation barriers of silicate formation, the anionic pathway is kinetically preferred over the neutral one. Thus, the polymerization of silicate species mainly concerns the anionic species. The ring closure reactions occur with high barriers because of loss of intramolecular hydrogen bonds. The decrease of the overall activation barrier for the formation of higher linear and branched molecules is ascribed to more favorable hydrogen bonding effects for these cases. The importance of inter- and intramolecular hydrogen bonding to the relative activation barriers of SiO-Si bond formation was found.

In chapter 3, it was argued that it is essential to include explicitly water molecules in silica condensation and sol-gel chemistry computational studies. The rate limiting step is not the water removal step as in the gas phase simulation in chapter 2. The overall barrier is mostly depends on the first barrier of the SiO-Si bond formation. The activation barrier of the water removal step

depends on the mechanism of water assisted internal or external proton transfer, independent from the size of oligomer. The kinetic and thermodynamic trends of formation of higher oligomers from dimer silica are found to be quite different between explicit solvent simulations and gas phase simulation. The gas phase model in chapter 2 proposes that the linear and branched higher silica structures are more favorable than the 3-ring and 4-ring. In contrast, this study in solution observed that 3-ring formation is more favorable than the formation of higher branched and ring silica oligomers. As a consequence, the 3-ring silica structure will be a dominant species during the first stage of pre-nucleation process in pure silica condensation. This is in good agreement with experimental studies of the early stage of zeolite synthesis. Water molecules are also essential to assist proton transfer and form stabilization hydrogen bond.

The counter ion (Li^+ and NH_4^+) effect to the silica condensation reaction was investigated in chapter 4. It was also shown that the activation barrier of the water removal step depends only on the water assisted, which is independent of the size of oligomer. The overall barrier mostly depends on the initial barrier of the SiO-Si bond formation. The position of cation has a strong effect on the barrier height of this step. When close to the reactive center of the dimerization reaction, Li^+ does not change strongly the activation barrier, meanwhile NH_4^+ increase significantly the activation barrier. The relative rates of formation of the higher oligomers from dimer silica are found to be quite different between Li^+ and NH_4^+ case. The presence of Li^+ favors the linear and branched higher silica structures over the 3-ring structures. In contrast, with NH_4^+ in solution it has been observed that 3-ring formation is more favorable than the formation of higher branched silica oligomers. The positive charge of counter ion decreases most significantly the rates of SiO-Si bond formation in the dimer. For the first step of the dimerization reaction, the hydrogen bonding effects are more important than the electrostatic interaction. In consecutive oligomerization reaction steps, the cation has a weak effect on activation barrier.

The importance of organic templates is well known for zeolite synthesis. Chapter 5 presents the catalytic role of template in the formation of the initial silicate structure. Formation of dimer, trimer and three-ring silicate oligomers has been studied in the presence of organic cation tetrapropylammonium TPA^+ . The interaction between TPA^+ and anionic silica consist of an electrostatic part and a weak VdW part. TPA^+ stabilises the transition state for Si-O bond

formation. The ring closure reactions occur with comparable barriers to that for linear growth despite the unfavorable thermodynamics for ring closure reaction due to the loss of intramolecular hydrogen bonds.

Chapter 6 reports an extensive investigation on the effect of the template on the relative stabilities of higher oligomers than could be considered in chapter 5. Various silicate structures from dimer to double 4-ring, related to initial stage of zeolite synthesis, have been studied in the presence of organic cations such as tetramethylammonium TMA^+ and tetrapropylammonium TPA^+ . The results show that organic template, especially TPA^+ , stabilizes silicate oligomers. As we found before, the TPA^+ favors the formation of linear small oligomer such as dimer and trimer. Condensation reactions in the presence of TPA^+ gain more energy than with TMA^+ or the alkali counter ion (e.g. Na^+). This is due to the favorable interaction between product and TPA^+ . It mainly relates to the difference in the Van-der-Waals interaction energies between template and oligomers. For both templates, the 4-ring fragment tends to be more stable than the 3-ring fragment. The unique figure of TMA^+ is the higher stabilization of the 4-ring structures compared to the other oligomers. For TPA^+ these differences are much less. This observation is consistent with experimental results.

This thesis contributes to the understanding of the prenanoparticle oligomerization process that occurs initially in zeolite synthesis. Several factors control the chemical reactivity of silica condensation in solution at this early stage (e.g. hydrogen bonding, water rearrangement, electrostatic effect, Van-der-Waals interaction). The internal and external hydrogen bonding is crucially related the geometry of small silicate oligomers. The electrostatic interaction between that alkaline counter ion and reactive region of condensation reaction increase the activation barrier of silica condensation reaction. It has been shown that the organic template enhances the OSi-O bonding of small oligomer as well as the stabilities of higher oligomers. The Van-der-Waals interaction between the template and silicate structure is more important when the size of oligomer is larger. This implies that the organic templates not only act as the generally accepted role of structure directing agents to the nanoparticle formation but also have an important role in the earlier stage of oligomerization.

TÓM TẮT

Quá trình tổng hợp vật liệu zeolite (một loại chất xúc tác được sử dụng rộng rãi trong quá trình xử lý dầu mỏ) được tổng hợp từ silicate hoặc alkylsilane trong môi trường kiềm. Thông thường sự tổng hợp này được thực hiện với một chất hữu cơ được gọi là chất định hướng cấu trúc (structure directing agents: SDA). Các chất SDA này được cho rằng phụ trách việc tạo thành các cấu trúc khác nhau của zeolite. Trong luận văn này đã cho thấy các chất này còn có vai trò quan trọng trong các quá trình phản ứng đầu tiên, lúc mới tạo thành các phân tử ban đầu của quá trình tạo zeolite. Hiện nay vẫn còn sự tranh luận xung quanh quá trình hình thành zeolite thông qua việc tạo thành từ từ bằng các phân tử monomer của silicate hay là thông qua sự kết hợp của các khối đại phân tử. Trong luận văn này, các tính chất hóa học căn bản của quá trình phản ứng trùng ngưng silica và các ảnh hưởng đến phản ứng như vai trò của nước, của liên kết hydrogen, của các ion và của các hợp chất hữu cơ sẽ được đề cập đến.

Cơ chế của phản ứng trùng ngưng silica của những phân tử đơn giản nhất, từ dimer cho tới pentamer ở trong pha khí đã được tính toán bằng phương pháp hàm mật độ (DFT) ở trong chương 2. Có hai cơ chế khác nhau: một là cơ chế thông qua các phân tử trung hòa (neutral) điện tích, hai là cơ chế thông qua các phân tử mang điện tích âm (anionic). Cơ chế thứ hai có hai giai đoạn, giai đoạn đầu là tạo liên kết SiO-Si, giai đoạn thứ hai là tách bỏ nước. Cơ chế này là cơ chế tối ưu hơn và năng lượng và động hóa học. Các phản ứng đóng vòng xảy ra với hàng rào năng lượng cao vì sự mất các liên kết hydrogen ở bên trong. Chương này chỉ ra tầm quan trọng của liên kết hydrogen ở trong và ở ngoài đối với hàng rào năng lượng của phản ứng.

Ở chương 3, việc thêm các phân tử nước là rất cần thiết đối với việc nghiên cứu phản ứng. Nó ảnh hưởng rất lớn đến sự bền vững và hàng rào năng lượng của phản ứng. Lúc này, giai đoạn quyết định động học không phải là bước tách nước như ở trong chương 2 mà phụ thuộc vào bước đầu tiên là tạo liên kết SiO-Si. Hàng rào năng lượng của quá trình tách nước phụ thuộc vào cơ chế phản ứng và không phụ thuộc vào kích cỡ của silica oligomer. Khi quá trình được nước xúc tác sẽ đi theo một cơ chế khác và có hàng rào năng lượng nhỏ hơn. Ở chương 2, ta thấy sự tạo các oligomer thẳng và nhánh được ưu đãi hơn các dạng vòng 3, vòng 4. Nhưng ở chương này với sự có mặt của nước, ta thấy dạng vòng 3 được ưu đãi hơn và điều này rất phù hợp với các kết quả thực nghiệm.

Nghiên cứu sự có mặt của các ion đối (Li^+ và NH_4^+) được trình bày ở chương 4. Cũng giống như chương 3, quá trình tách nước được quyết định bởi các phân tử nước có mặt xung quanh chứ không phụ thuộc vào kích thước của các oligomer. Hàng rào năng lượng của cả phản ứng chủ yếu phụ thuộc vào quá trình tạo liên kết SiO-Si. Vị trí của các ion có sự ảnh hưởng quan trọng tới phản ứng, nhất là đối với phản ứng dimer hóa thì NH_4^+ làm tăng rất nhiều hàng rào năng lượng, trong khi Li^+ thì lại không làm tăng năng lượng. Điện tích dương của các ion là giảm đi khả năng phản ứng của các quá trình trùng ngưng silica.

Sự quan trọng của các hợp chất hữu cơ đến quá trình tổng hợp zeolite đã được biết đến từ lâu. Ở trong chương 5, tôi trình bày vai trò xúc tác của chất hữu cơ tetrapropylammonium (TPA) đến cơ chế và năng lượng của phản ứng. Sự liên kết giữa TPA và silica gồm có sự liên kết tĩnh điện và liên kết Van der Waals. TPA làm bền hơn trạng thái chuyển tiếp của quá trình tạo liên kết SiO-Si và làm giảm hàng rào năng lượng của quá trình này.

Ở chương 6 là sự mở rộng nghiên cứu ở chương 5 với hợp chất hữu cơ khác là tetramethylammonium (TMA) và TPA. Các phân tử được silica từ đơn giản nhất là dimer tới phức tạp là đôi vòng 4 được tính toán năng lượng phản ứng và độ bền tương đối. TMA làm bền hơn vòng 4 so với các cấu trúc khác của silicate. Với sự có mặt của TPA thì các cấu trúc vòng, thẳng, nhánh của silica có độ bền tương đương với nhau. Quan sát này cũng phù hợp với những kết quả thực nghiệm

Tóm lại luận văn này đã đóng góp vào sự hiểu biết thêm về phản ứng trùng ngưng silica xảy ra trong quá trình tổng hợp zeolite ở những giai đoạn đầu tiên. Có nhiều yếu tố ảnh hưởng tới phản ứng như liên kết hydrogen, tương tác tĩnh điện, tương tác Van der Waals, kết cấu của mạng phân tử nước. Nghiên cứu cũng chỉ ra rằng các chất hữu cơ trong quá trình tổng hợp zeolite không những có vai trò chủ yếu trong việc hình thành các khối phân tử lớn mà còn có vai trò quan trọng trong việc hình thành những phân tử oligomer ban đầu.

LIST OF PUBLICATIONS

1. Trinh, T.T; Jansen, A.P.J; van Santen, R.A. *Mechanism of Oligomerization Reaction of Silica*, J. Phys. Chem. B **2006** *110*, 23099. (Chapter 2)
2. Trinh, T.T; Jansen, A.P.J; van Santen, R.A; Meijer, E.J. *Role of Water in Silica Oligomerization*. J. Phys. Chem. C. **2009** *113*, 2647 (Chapter 3)
3. Trinh, T.T; Jansen, A.P.J; van Santen, R.A; Meijer, E.J. *The role of water in silicate oligomerization reaction*. Phys. Chem. Chem. Phys **2009**, DOI: 10.1039/b819817a (Chapter 3)
4. Trinh, T.T; Jansen, A.P.J; van Santen, R.A; VandeVondele, J; Meijer, E.J. *Effect of Counter Ions on The Silica Oligomerization Reaction*, ChemPhysChem **2009**, accepted (Chapter 4)
5. Trinh, T.T; Jansen, A.P.J; Meijer, E.J.; van Santen, R.A. *Catalytic role of Tetrapropylammonium in silica oligomerization reaction*, in preparation (Chapter 5)
6. Trinh, T.T; Jansen, A.P.J; de Bruin, B; Meijer, E.J.; van Santen, R.A. *Silica Condensation Influenced By An Organic Template*, J. Phys. Chem. C. Submitted (Chapter 6).
7. Trinh, T.T; Jansen, A.P.J; van Santen, R.A; Meijer, E.J; van Duin, A. *Reactive force field molecular dynamic simulation of silica oligomerization*, in preparation

Acknowledgments

I would like to express my deepest gratitude to Prof. Rutger van Santen for giving me the opportunity to work in his research group. I'm very grateful for his knowledge, patience, scientific guidance, help and enthusiasm. Rutger, thank you for the numerous suggestions and discussion. I would also extend my gratitude to my initial supervisor Dr. Tonek Jansen for encouraging me to overcome the scientific problem and for the language correction in manuscript writing.

Special thanks to Dr. Evert Jan Meijer (University of Amsterdam) who gave me a lot of help and instruction every time I went to Amsterdam. Ever Jan, I'm very grateful for your academic writing that save our publication time and for introducing me to Joost VandeVondele (University of Zurich). Joost, thank you very much for your valuable technical training and fruitful discussion.

I would like to thank the members and ex-members of the theory group, Chrétien, Peter, Joost, Cristina, Willy, Bouke, Ojwang, Evgeny, Pieter, Ionel, Sharan, Bartek, Luis, Olus, Shu- Xia, Xue-Qing for the nice scientific discussions in the lunch meeting, for creating friendly atmosphere in the 4th floor. Special thanks Joost and Bouke, as system administrators, their responses were always helpful and in the right time. Bouke and Nicole, I love that Halloween party with your hilarious costume. My special thanks to Cristina, who was always a good friend to talk with. Cristina, thanks so much for your financial help when I first came to Tu/e and your card really touched me.

I am grateful to all SKA members for their cooperation, helpful discussions, leisure activities, kindness and friendship. Elize and Marion are acknowledged for their help and patience in administrative questions. I also extend my gratitude to all the people who were not mentioned above but supported me during my time in SKA.

I would like to thank all my professors in chemistry department of HoChiMinh city University of Natural Sciences, Vietnam who brought me into the real world of chemistry. Special thanks to Thầy Bùi Thọ Thanh, Thầy Hà Thúc Huy and Cô Huỳnh Thị Kiều Xuân for their care, patience, scientific tuition and French teaching.

I would like to express my deep appreciation to all Vietnamese friends in the Netherlands for their beside-being, friendship and support. My special thanks to anh Hóa, anh Vượng, anh Mẫn for their valuable help when I just arrived in Eindhoven. I am grateful to all other Vietnamese friends for a home-feel atmosphere that we have had through wonderful parties, football game, and other enjoyable pursuits. There are many people that I can not mention all here, some most thankful are such as anh Thanh chị Huệ, chị Vân Anh anh Kim, anh Phương chị Trang, Thùy, Thanh, Trường, Quỳnh, Tuấn, Hằng, Bi, Phú, Hiền, anh Hòa, anh Long,....

Last but definitely not least, the most sincere gratefulness to my family. I'm greatly indebted to my parent, no word can express what I want to say. My grateful thanks to my younger brother and my fiancée who provide me endlessly moral support, encouragement and love.

Eindhoven, 2009

Trịnh Thành Thuật

CURRICULUM VITAE

Thuat T. Trinh was born on the 20th of January 1982 in Hanoi, Vietnam. After his graduation from high school in 1999, he started his bachelor at Ho Chi Minh National University of Science, Vietnam with the major of Physical Chemistry-Theory Chemistry. In 2002, he joined the Laboratory of Theoretical Chemistry at his university as a research assistant, where his first scientific passion began with quantum chemical calculations, qualitative structure reactive relationship (QSAR) and genetic algorithm. In 2003 he won a scholarship for his master degree at Ecole Nationale Supérieure des Ingénieurs en Arts Chimiques Et Technologique Institut National Polytechnique de Toulouse, France. His master thesis was on the quantum calculations of oxidation reaction in alloys aluminum-platinum. In October 2004, he joined the theory group at the Eindhoven University of Technology for his PhD research on the simulation of zeolite synthesis process.

“Success is not final, failure is not fatal; it is the courage to continue that counts.”

(Winston Churchill)